DSPACE

https://dspace.org/

The geology and structural influences on copper mineralisation, distribution and spatial occurrence in the Lubambe copper deposit, Central African Copperbelt, Zambia

Taruvinga, Tapiwa

2022

https://hdl.handle.net/10539/37058

Downloaded from a DSpace repository. https://dspace.org/

WITS UNIVERSITY

MSc Economic Geology Research Project

School of Geosciences

The geology and structural influences on copper mineralisation, distribution and spatial occurrence in the Lubambe copper deposit, Central African Copperbelt, Zambia.

By

Tapiwa Taruvinga (2347086)

DECLARATION

I, **TAPIWA TARUVINGA**, declare that this dissertation is my own work. It has not been submitted before for any degree or examination in any other University or tertiary institution. This is submitted as partial fulfilment of the Degree of Master of Science in Economic Geology at the University of Witwatersrand of South Africa.

Signature of the candidate…….

Date…02/11/2022…….

DEDICATION

I wish to dedicate this Research Project to my three children Tinotenda, Thandeka-Erin and Tatenda-Nicole. I would not have done this program if it was not for all of you. I have set the bar for you to surpass when your time comes. I shall continue working hard, loving and sacrificing for you.

ACKNOWLEDGEMENTS

I would like to thank the Almighty God for giving me the gift of life to enable me to start and complete my MSc studies.

Much appreciation goes to my family, particularly my wife (Tendai Ndumo Taruvinga) and children for supporting me and allowing me time to study.

It is a pleasure to thank Bulemin Resources management, Andrew Nkambule (MHSRIP), Khanyisile Nkambule and David Legong for the time, material, financial and moral support rendered during the course of my studies.

I wish to thank Lubambe Copper Mine of Zambia Limited management and the exploration department for allowing me to use their geological data and providing me with core samples for my project.

Am also grateful to Professor Paul Nex and Desmond Subramani for their supervision, encouragement and support throughout the course work and research project.

Many thanks to the Wits University School of Geoscience Laboratory team for cutting my samples and making thin sections to aid my research project.

Lastly, I would like to thank my fellow classmates for all the cooperation and study time we shared.

ABSTRACT

The genetic relationship between copper mineralisation, stratigraphy and basin architecture in the Central African Copper Belt is very important as it plays a critical role in controlling and localising mineralisation. Evidence from basinal geometrical studies in most Zambian Copper Belt deposits suggests that major thrust faults and folded structures were developed during the Lufilian orogeny, which involved inversion of basement structures during periods of compression. The Konkola Dome and the Kirila Bombwe anticline are examples of major basement units where re-activation of extensional faults resulted in the generation of major structures later used as channel ways by copper-bearing fluids. The presence of undeformed sulphides often hosted within structures shows that deformation predates mineralisation and critically played a major role in preparing the ground and structures for mineralisation.

An integration and re-interpretation of geophysical and geological data in the Lubambe Mining Area has resulted in a significantly improved understanding of the geology of the area and potential controls on ore distribution. Despite limited subsurface information from the geophysical datasets, the exercise has provided significant confidence to detailed mapping of poorly exposed parts of the area. Interpretation outcomes from this mapping and geophysical (aeromagnetic and gravity) suggest that the distribution of major folds reflects an early extensional, basement architecture which is thought to be key to ore deposit formation in the Lubambe License Area. Additionally, geological modelling of the Lubambe-Konkola Area has shown that a relationship potentially exists between ore distribution, fold axes and stratigraphic thickness trends. Specifically, the model suggests that both copper grades and Ore Shale 1 Member thickness trends are controlled by NE-trending growth faults which can be traced to the eastern-side of the property. There is modest correlation between the traces of faults interpreted from geophysical surveys and the occurrence of structures seen in drill core in the selected holes which provides evidence of faults during and immediately after sedimentation. This suggests that the depocentres were fault-bounded basin into which mineralising fluids flowed to deposit ores in the OS1 Member.

Copper ore within the Lubambe License Area includes very fine-grained chalcopyrite and chalcocite with some bornite, malachite, chrysocolla and limonite staining. Hypogene copper mineralisation in the Lubambe license area occurs as disseminated and along bedding planes adopting similar grain sizes as the host rock. This is accompanied by secondary copper minerals and iron oxides filling veins, fractures and joints.

The Ore Shale 1 Member within the Lubambe License area thickens towards the southeast and can be correlated to the regional structure. Copper grades in the rich zones can be correlated with two small sub-basins in the East and South limbs and another around the Extension Area. Significant structural control on copper distribution can be observed on copper grade distribution maps superimposed on structural maps showing major and intermediate structural features. There are significant concentrations of chalcocite near surface and also down dip in the East and South Limbs and the Extension Area. Chalcopyrite is widely distributed except near surface. Bornite is concentrated in the centre of the East Limb. Malachite and chrysocolla are well correlated with Acid Soluble copper and are found mainly near surface. Evidence also suggests that metal concentration and upgrading of the ore deposit was influenced by macro and meso-scale structural features during supergene processes as highly mineralised areas were coinciding with faulted and folds zones.

A spatial relationship between the distribution of mineralisation and sedimentary architecture has been demonstrated to show a strong correlation in the Lubambe License Area. This interpretation is consistent with ore genesis models of sedimentary-hosted copper deposits.

TABLE OF CONTENTS

DECLARATION i
DEDICATION ii
ACKNOWLEDGEMENTS iii
ABSTRACT iv
LIST OF FIGURES viii
LIST OF TABLES xi
ABBREVIATIONS AND ACRONYMS xii
CHAPTER 1 1
1.1 GENERAL INTRODUCTION 1
1.2 REGIONAL GEOLOGICAL SETTING 1
1.3 LUBAMBE LOCAL GEOLOGY 3
1.4 LUBAMBE AREA STRATIGRAPHY 5
1.5 MINERALISATION WITHIN THE LUBAMBE COPPER DEPOSITS 7
1.6 MINERALISATION MODEL FOR LUBAMBE COPPER DEPOSITS 7
1.7 MINING ACTIVITIES AT LUBAMBE COPPER MINE 8
1.8 PROBLEM STATEMENT 10
1.9 RESEARCH MAIN OBJECTIVE 10
1.9.1 SPECIFIC OBJECTIVES 10
1.10 JUSTIFICATION OF STUDY 111
1.11 METHODOLOGY 11
CHAPTER 2 12
2.1 INTRODUCTION 12
2.2 REGIONAL TECTONIC AND STRUCTURAL SETTING 12
2.3 TECTONIC DOMAINS 13
2.4 DEFORMATION 14
2.5 BACKGROUND TO THE LUBAMBE COPPER MINE 15
2.6 EXPLORATION HISTORY 16
2.7 REGIONAL GEOPHYSICAL EXPLORATION IN THE LUBAMBE LICENSE AREA 17
2.7.1 AIRBORNE ELECTROMAGNETICS 18
2.7.2 AIRBORNE RADIOMETRIC 19
2.7.3 GRAVITY SURVEYING 19
2.8 MINING OPERATIONS AT LUBAMBE COPPER MINE 19
2.9 LUBAMBE EXTENSION AREA – BROWNFIELD EXPLORATION 20
CHAPTER 3 23

3.1 INTRODUCTION 23
3.1.1 Surface Mapping of Outcrops 23
3.1.2 Core Logging 23
3.1.3 Petrography 24
3.1.4 GIS and Orebody Modelling 24
3.1.5 Geochemical Assay Results Analysis from core 24
3.1.5.1 Summary of Core Handling, Preparation and Analysis Procedures 25
CHAPTER 4 26
4.1 INTRODUCTION 26
4.2 SURFACE MAPPING OF OUTCROPS 26
4.2.1 KAFUFYA FORMATION OUTCROPS 27
4.2.1.1 Sandstones 27
4.2.1.2 Arkose 27
4.2.3 SUMMARY OF MAPPING RESULTS 30
4.3 CORE LOGGING 32
4.3.1 BASEMENT COMPLEX 33
4.3.2 LOWER ROAN GROUP 33
4.3.2.1 Kafufya Formation 33
4.3.2.2 Nchanga Formation 34
4.3.2.3 Shale with Grit Formation 40
4.3.3 UPPER ROAN GROUP 41
4.3.3.1 Chingola Dolomite (CHD) Formation 41
4.3.3.2 The Breccia Complex Formation 43
4.3.4 MWASHIA GROUP 44
4.3.4.1 Mwashia Formation 44
4.3.5 LOWER KUNDELUNGU GROUP 46
4.3.5.1 Grand Conglomerate Formation 46
4.3.5.2 Kakontwe Limestone Formation 47
4.3.5.3 Shales and Dolomites 48
4.3.6 CORE LOGGING RESULTS 48
4.4 GEOLOGICAL MODELLING 50
4.4.1 STRATIGRAPHIC MODELLING 50
4.4.2 OREBODY ELEVATION VARIATION IN THE KONKOLA - LUBAMBE AREA 52
4.4.3 MINERALISATION MODELLING 53
4.5 PETROGRAPHY 55
4.5.1 MICRO-PETROGRAPHIC ANALYSIS 56

4.5.1.1 TT017 Petrography....56
4.5.1.2 TT018 Petrography....57
4.5.1.3 TT019 Petrography....60
4.5.1.4 TT020 Petrography....62
4.5.1.5 TT021 Petrography....64
4.5.1.6 TT022 Petrography....66
4.5.1.7 TT023 Petrography....68
4.5.1.8 TT024 Petrography....70
4.6 COPPER-BEARING MINERALS SPATIAL DISTRIBUTION IN THE LUBAMBE AREA....72
4.6.1 DATA COLLECTION PROCEDURE....72
4.6.1.1 Chalcopyrite....73
4.6.1.2 Chalcocite....74
4.6.1.3 Bornite....75
4.6.1.4 Pyrite....76
4.6.1.5 Limonite....77
4.6.2 TOTAL COPPER DISTRIBUTION IN THE LUBAMBE AREA....78
4.6.3 TRUE THICKNESS MODEL....80
4.6.4 ACID-SOLUBLE COPPER OXIDES....81
CHAPTER 5....83
5.1 INTRODUCTION....83
5.2 RELATIONSHIP BETWEEN STRUCTURES AND MINERALISATION WITHIN THE PROJECT AREA....83
5.2.1 Field Mapping....87
5.2.2 Petrography....87
5.2.3 Copper-bearing Mineral Elements Distribution....88
5.2.4 Oxide Copper Mineral Distribution....88
5.3 PROSPECTIVITY POTENTIAL OF THE PROJECT AREA....89
CHAPTER 6....92
6.1 CONCLUSIONS....92
6.2 RECOMMENDATIONS....93
REFERENCES....97
APPENDIX 1....101

LIST OF FIGURES

CHAPTER 1

Figure 1-1: Geology of Central Africa displaying the major copper deposits in Zambia and the DRC (modified from Barra et al., 2005). The study area is outlined in red. 1
Figure 1-2: Simplified geological map of the Central African Copperbelt, showing the distribution of the main deposits and their ore types together with the location of the Lubambe Copper deposit (modified from Selley et al., 2005). 2
Figure 1-3: Geological map of the Lubambe and Konkola areas showing the stratigraphic distribution and the extent of known copper resources between Konkola and Musoshi (modified from Hitzman et al., 2012). 4
Figure 1-4: Simplified stratigraphic column of the Lubambe license area (modified from Simposya and Hart, 2008). 6
Figure 1-5: Showing the mineralisation model adopted in the Greater Konkola basin. Basinal brines (in purple) circulating and leaching out metals then depositing them in shales (After Selley et al., 2005). 7
Figure 1-6: Showing the Lubambe orebody model from mining and exploration data (Mwelwa, 2020) 8
Figure 1-7: Geological map of the Lubambe area showing the location of the Lubambe Copper Mine No. 2 Shaft location and 2012 estimated Cu resource figures relative to other deposits in the Greater Konkola basin (modified from Hitzman et al., 2012). 9

CHAPTER 2

Figure 2-1: Geological maps showing the tectonic setting of the Central African Copper Belt (After Porada (1989)). 12
Figure 2-2: Tectonic domains of the Lufilian Fold Belt (a) Location of the Central African Copperbelt in the Lufilian fold belt (b) Lufilian fold belt location in Zambia and tectonic domains (c) Schematic sections of the Lufilian Fold Belt showing different tectonic domains (Selley et al., 2005). 14
Figure 2-3: Plan showing locations of Lubambe Copper Mine (East Limb and South Limb), Extension Area and Kawiri Areas within license 7061-HQ-LML. 15
Figure 2-4: Showing Lubambe discovery, production and ownership over time (Stacey, 2020)..... 16
Figure 2-5: Google image showing the Lubambe License Area and the Kawiri basins targeted for geophysical exploration. 17
Figure 2-6: Magnetic and EM Images and Interpretations from the 2011 Fugro Airborne Survey (Carey and Cevallos, 2012). 18
Figure 2-7: Showing picture of No.2 Shaft (2011) at Lubambe Mine which provides access to the South Limb. 20
Figure 2-8: Location map showing the extent of the Extension Area (pink polygon) (Stacey, 2020). 21
Figure 2-9: Cross section showing the orebody profile from the Lubambe Mine Area to Konkola Copper Mine (Stacey, 2020). 21
Figure 2-10: Lubambe Extension Area project benchmark in respect to other world class undeveloped copper discoveries (adopted from Stacey, 2020). 22

CHAPTER 3

Figure 3-1: Showing photos taken during the re-logging of core at Lubambe Copper Mine (a) marking lithological contacts (b) structural data collection using an IQ logger. 23

CHAPTER 4

Figure 4-1: Plan showing the mapped portions within the Lubambe Mining License Area. 26
Figure 4-2: Photo showing a planar cross-bedded Kafufya Formation sandstone outcrop. Location: 581887E / 8640159N. 27

Figure 4-3: Photo showing bedded and weathered gently dipping Kafufya Formation arkose outcrop. Location: 581877E / 8640273N.. 28
Figure 4-4: Photo showing a Kafufya Formation conglomerate outcrop undergoing selective weathering. Quartz resisting weathering formed a rough surface. Location: 579410E / 8639448N.. 29
Figure 4-5: Photos showing Konkola Dome granite outcrop(a) porphyritic feldspathic clasts exposed after weathering (b) Pink subhedral coarse feldspathic phenocrysts outstanding in a granitic outcrop.. 29
Figure 4-6: Revised geological map of the Lubambe mining license area showing the revised map based on compiled mapping and geophysical data interpretation (modified from Woodhead, 2006). 30
Figure 4-7: Photo showing the Kafufya Formation dominated by vuggy and leached sandstones, arkoses and conglomerates from borehole KN191A.. 33
Figure 4-8: Photo showing the OS1 (shales and siltstones) / Kafufya Formation (Footwall Conglomerate) contact from borehole KN129. (Cu% grades labelled in orange). 34
Figure 4-9: Photo showing mineralised OS1 unit from borehole KN191A with upper assay and lithological contact coinciding. (Cu% grades labelled in orange).. 35
Figure 4-10: Photos showing mineralised core samples in OS1 Member (a) Massive chalcocite mineralisation from borehole KN192; (b) malachite filling vugs in borehole KN44; (c) blebby and bedding-parallel chalcocite from borehole KN101B.. 36
Figure 4-11: Photo showing OS2 Member (greyish interbedded arkose and sandstones) and OS3 Member (Lower Pink Arkose Marker) from borehole KN190. 37
Figure 4-12: Photo showing interbedded sequences of the OS4 Member (Shale with Arkose) from borehole KN120. 38
Figure 4-13: Photo showing Dolomitic Shale unit (at the bottom) with folded and slump structures grading to shales within the OS5 Member of borehole KN191A.. 39
Figure 4-14: Photos showing mineralised core samples from the OS5 Member of borehole KN194D1 (a) strong blebby bornite mineralisation along folded bedding in shales and blebby chalcopyrite disseminations in dolomite; (b) chalcopyrite mineralisation parallel to bedding and lamination planes in shales. 39
Figure 4-15: Photo showing the bedded pebbly arkosic conglomerate of the Konkola Member in borehole KN120. 40
Figure 4-16: Photo showing the Shale with Grit (SWG) Member in borehole KN190. Gritty beds thicknesses increasing with depth. 41
Figure 4-17: Photo showing greenish argillaceous shales and siltstones with white gritty spots of the Chingola Dolomite Formation in borehole KN191A. 42
Figure 4-18: Photo showing the highly oxidised and silicified dolomites of the Chingola Dolomite Formation in borehole KN191A. 42
Figure 4-19: Photo showing a clast supported crackled breccia and matrix supported polylithic conglomeratic breccia in borehole KN191A.. 43
Figure 4-20: Photo showing brecciated meta-gabbros (amphibolite dyke) in borehole KN116.. 44
Figure 4-21: Photo showing laminated / banded shales with carbonate veins parallel to bedding and biotite porphyroblasts within the Mwashia Formation in borehole KN110. 44
Figure 4-22: Photo showing dolomitic siltstones unit with phlogopite spots within the Mwashia Formation in borehole KN191A. 45
Figure 4-23: Photo showing crackled mudstones and shales with scapolite spots, borehole KN190. 45
Figure 4-24: Photo showing shales with irregular carbonate veins, borehole KN121B. 46
Figure 4-25: Photo showing the Grand Conglomerate Formation with some polylithic clasts in a shaly matrix, borehole KN192. 47
Figure 4-26: Photo showing the Kakontwe Formation from borehole KN192 comprising calcite rich limestones and dolomites. 48
Figure 4-27: Simplified stratigraphic log of the Lubambe Area based on the core logging carried out (modified from Arthurs et al., 2009).. 49
Figure 4-28: Plan showing collar positions of the drilling carried out in the Lubambe license area up to 2018. (Green circles show re-logged drill holes validated for modelling in this study). 51
Figure 4-29: Image showing Geological / Stratigraphic Model of the Lubambe Area. 52

Figure 4-30: Section showing the orebody elevation profile from Konkola to Lubambe based on drilling (image along the line A-B). Orebody is shown by the continuous surface in the image.. 53
Figure 4-31: Cross section showing the stratiform nature of mineralisation within the Lubambe license area. (Litho-stratigraphic unit OS1 mineralised zone (red) at the bottom) (modified after Mwelwa, 2020).. 53
Figure 4-32: Image showing modelled mineralised envelope based on drill hole intersections in the Lubambe License Area. 54
Figure 4-33: Map showing collar locations of drill holes from which samples for micro-petrographic analysis were taken.. 55
Figure 4-34: Photo showing TT017 hand specimen. 56
Figure 4-35: Photomicrograph showing TT017 image under XPL. 57
Figure 4-36: Photomicrograph showing TT017 image under Reflected Light. 57
Figure 4-37: Photo showing TT018 hand specimen. 58
Figure 4-38: Photomicrograph showing TT018 image under XPL. 58
Figure 4-39: Photomicrograph showing TT018 image under reflected light. 59
Figure 4-40: Photo showing TT019 hand specimen. 60
Figure 4-41: Photomicrograph showing TT019 image under XPL. 60
Figure 4-42: Photomicrograph showing TT019 image under reflected light. 61
Figure 4-43: Photo showing TT020 hand specimen. 62
Figure 4-44: Photomicrograph showing TT020 image under XPL. 63
Figure 4-45: Photomicrograph showing TT020 image under reflected light. 64
Figure 4-46: Photo showing TT021 hand specimen. 64
Figure 4-47: Photomicrograph showing TT021 image under XPL. 65
Figure 4-48: Photomicrograph showing TT021 image under reflected light. 66
Figure 4-49: Photo showing TT022 hand specimen. 66
Figure 4-50: Photomicrograph showing TT022 image under XPL. 67
Figure 4-51: Photomicrograph showing TT022 image under reflected light. 68
Figure 4-52: Photo showing TT023 hand specimen. 68
Figure 4-53: Photomicrograph showing TT023 image under XPL. 69
Figure 4-54: Photomicrograph showing TT023 image under reflected light. 70
Figure 4-55: Photo showing TT024 hand specimen. 70
Figure 4-56: Photomicrograph showing TT024 image under XPL. 71
Figure 4-57: Photomicrograph showing TT024 image under reflected light. 71
Figure 4-58: Plan showing chalcopyrite distribution in the Lubambe Area as visually estimated in drill core. ... 73
Figure 4-59: Plan showing chalcocite distribution in the Lubambe Area as visually estimated in drill core. 74
Figure 4-60: Plan showing bornite distribution in the Lubambe Area as visually estimated in drill core. 75
Figure 4-61: Plan showing pyrite distribution in the Lubambe Area as visually estimated in drill core. 76
Figure 4-62: Plan showing limonite distribution in the Lubambe Area as visually estimated in drill core. 77
Figure 4-63: Plan showing Total Copper distribution in the Lubambe area. 79
Figure 4-64: Illustration showing total copper distribution of drill hole traces KN114 and KN120. 79
Figure 4-65: Plan showing the OS1 true thickness distribution plot of mineralised envelopes in the Lubambe area. 80
Figure 4-66: Plan showing oxidation ratios (OX_RAT) within the Lubambe area. 81

CHAPTER 5

Figure 5-1: Map showing structural interpretation of the Lubambe Aeromagnetic data. (after Woodhead, 2006). 83
Figure 5-2: Map showing the Konkola-Lubambe geology and the interpreted structural framework of the project area (based on interpretation by Woodhead, 2006).. 85
Figure 5-3: Illustration showing the Total Cu x Thickness spatial distribution in the Lubambe project area. 86

Figure 5-4: Illustration showing targets A and B recommended for further exploration in the Lubambe License Area. 90
Figure 5-5: Illustration showing target C recommended for further exploration in the Lubambe License Area. 91

CHAPTER 6

Figure 6-1: Plan showing intersections underneath the Lubengele Tailings Storage Facility (boundary shaded in blue) from the Lubambe 2019 – 2020 drilling. 94
Figure 6-2: Showing plotted assay results for OS5 and OS1 intersections from borehole KN192. 95
Figure 6-3: Showing plotted assay results for OS5 and OS1 intersections from borehole KN194. 95

LIST OF TABLES

Table 1: Summary information of selected samples for petrography within the Lubambe license area..... 55
Table 2: Example of numerical values derived from text in the ACQUIRE database..... 72

ABBREVIATIONS AND ACRONYMS

ARM	African Rainbow Minerals
ASCu	Acid-soluble Copper
CACB	Central African Copper Belt
CCB	Congolese Copperbelt
CHD	Chingola Dolomites Formation
DRC	Democratic Republic of Congo
EMRC	Energy Mineral Resources Capital
GCON	Grand Conglomerate
KCM	Konkola Copper Mine
LCM	Lubambe Copper Mine
LTSF	Lubengele Tailings Storage Facility
OS	Ore Shale
OX_RAT	Oxidation Ratio
PPL	Plane Polarised Light
SWG	Shale with Grit Member
TCu	Total Copper
TDEM	Time Domain Electromagnetics
XPL	Crossed Polarised Light
ZCB	Zambian Copper Belt
ZCCM	Zambia Consolidated Copper Mines

CHAPTER 1

INTRODUCTION

1.1 GENERAL INTRODUCTION

The Lubambe copper deposit lies within the Central African Copperbelt (CACB) which is one of the largest sediment-hosted stratiform Cu–Co deposits in the world, extending from Zambia in the east through to the southwestern part of the Democratic Republic of Congo (DRC) (Woodhead, 2006; Hitzman et al., 2012). The CACB comprises two main parts, the Congolese Copperbelt (CCB), also known as the Katangan Copperbelt, which comprises deposits located north of the DRC – Zambia border and the Zambian Copperbelt (ZCB) with deposits lying on the Zambian side (Figure 1-1). It hosts more than 200 Million tonnes (Mt) Copper (Cu) and >8 Mt Cobalt (Co), which represents half of the world's mineable cobalt reserves (Cox et al., 2007; Lydall and Auchterlonie, 2011). In addition to the world's highest-grade accumulation of sedimentary rock-hosted copper and cobalt, this region is host to rich polymetallic mineralisation that includes significant deposits of zinc, lead, gold, silver, nickel, and uranium (Kirkham, 1989).

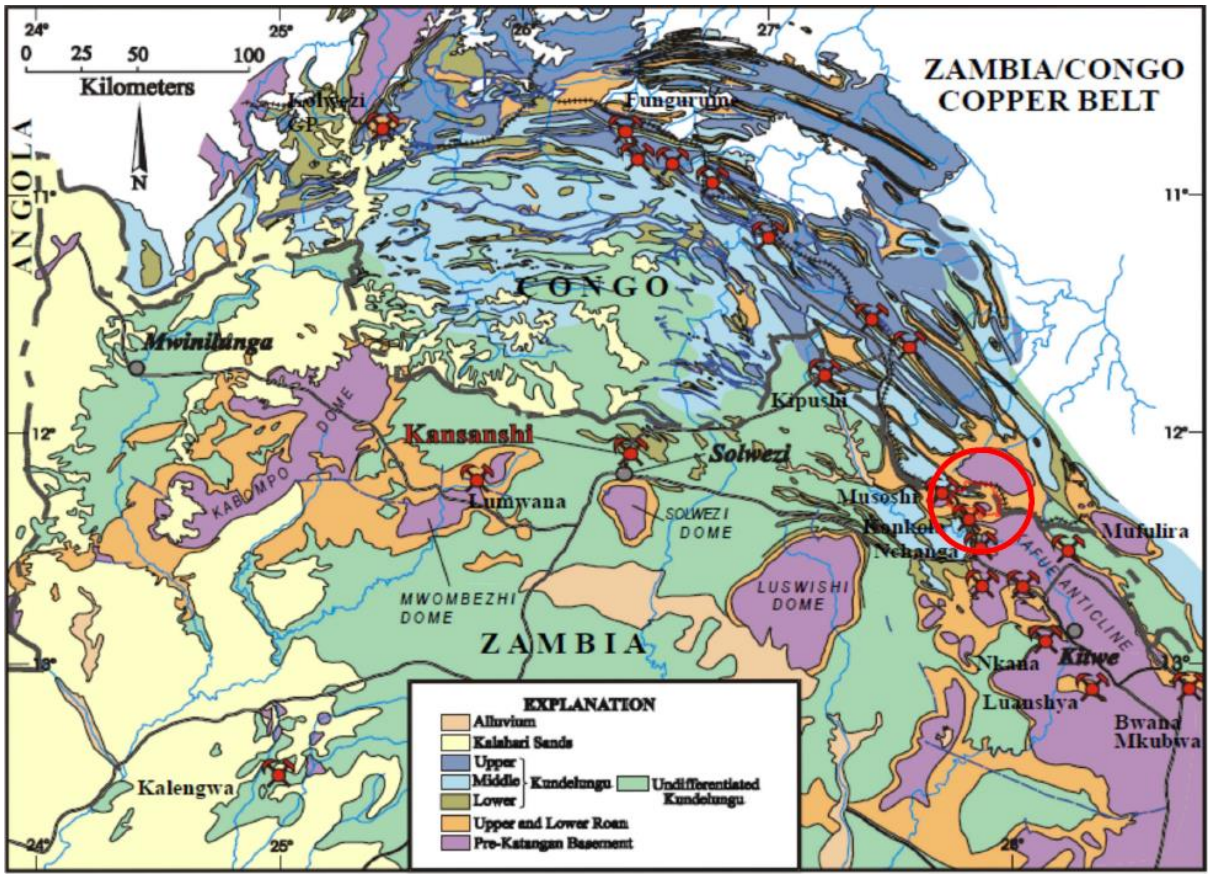

Figure 1-1: Geology of Central Africa displaying the major copper deposits in Zambia and the DRC (modified from Barra et al., 2004). The study area is outlined in red.

1.2 REGIONAL GEOLOGICAL SETTING

The CACB lies within the Lufilian Fold Belt, which formed during the Lufilian orogeny between the Neoproterozoic and the early Palaeozoic (Key et al., 2001). The Lufilian Arc was primarily formed as the result of basin closure and inversion by collision of the Kalahari and Congo cratons (Cosi et al.,

1992; Selley et al., 2005) and has a convex/arcuate shape extending approximately 850 km from Zambia through DRC, Angola and back into the northwestern part of Zambia (Cailteux and Kampunzu 1995). It is bounded by several structural provinces; the Bangweulu Block to the northeast, the Irumide Belt in the east, the Zambezi Belt in the south, and the Kibaran Belt in the north (Jackson et al., 2003).

The Lubambe copper deposit is located on the northwestern part of the ZCB and is one of the many major copper and cobalt (Cu +/-Co) deposits occurring within the CACB (Figure 1-2). Bull et al. (2011) notes the ZCB as representing an autochthonous "Zambian-type" deposit within the late Proterozoic Lufilian Arc fold-thrust belt.

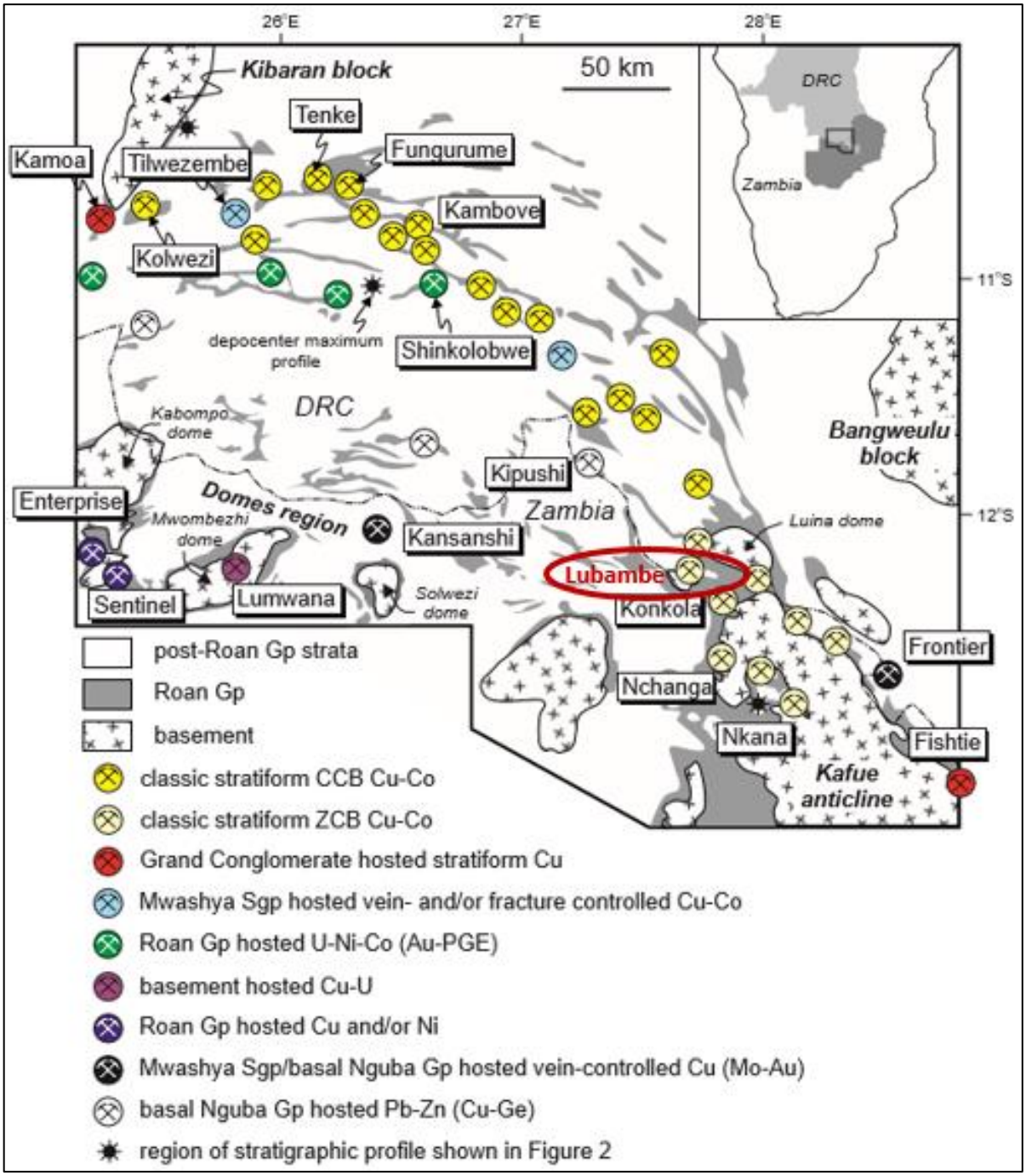

Figure 1-2: Simplified geological map of the Central African Copperbelt, showing the distribution of the main deposits and their ore types together with the location of the Lubambe Copper deposit (modified from Selley et al. (2005)).

An understanding of the regional stratigraphic and structural setting has been a critical tool for exploration, mining and resource evaluation (Selley et al., 2005). Several copper deposits in the ZCB have demonstrated a strong correlation and spatial relationship between grade distribution and sedimentary architecture (Bull et al., 2011). This is mainly based on the understanding that syn-sedimentary normal faults play a key role in controlling sediment deposition and accumulation patterns in a basin and subsequently copper mineralisation. Basin architecture or geometry in the form of basement domes or 'palaeo-highs' are interpreted to reflect footwall blocks of early extensional faults whilst thickness variation of the basal sandstone-dominated (syn-rift) strata provide material that was leached or stripped of mineral elements that precipitated at redox boundaries (Theron, 2013). The basin geometry and thickness variation and nature of the basal succession have been identified as some of the key features related to ore distribution (Hitzman et al., 2012). Selley et al. (2005) attribute present-day fold patterns to reactivation of faults, a feature deemed important in terms of supergene alteration and structural modification of the orebody.

The Lubambe copper deposit differs from other copper deposits in the ZCB in that no basement has been intersected through drilling so there is very little information about the thickness variations of the footwall strata whereas in other ZCB deposits, footwall units can generally be linked to formational stratal pinch-outs against "palaeo-highs" representing the basement. In the Lubambe deposit, orebodies can be at extreme depths (e.g., >1600 m) whilst overlying a very thick footwall sequence, thereby making the 'drill-to-basement' approach as applied in other ZCB deposits difficult and costly. Modelling of potential-field geophysical data (gravity, magnetics and EM) has been used to estimate the 'depth-to-basement' and/or constrain the larger structural patterns but there is still no certainty about the depth of basement (Reid, 2020).

1.3 LUBAMBE LOCAL GEOLOGY

The geology of the southeast flank of the Lufilian Arc comprises a series of basins and domes formed by a combination of Lufilian tectonics and the buttressing effect of the pre-existing basement geomorphology (Key et al., 2001; Theron, 2013). The rocks of the Katanga Supergroup, the host to the Cu-Co mineralisation, are draped around the domes ('basement highs') and infill the basins (Bull et al., 2011). The Katanga Supergroup rocks in the Lubambe area rise in the south and north against the Kirila Bombwe and Konkola domes respectively (Figure 1-3). The area between the two domes consists of irregular, but flat-lying, Katangan strata, which host the Konkola Deep and the Lubambe orebodies.

The Lubambe orebodies are located on the western flank of a basin-like embayment of prospective Roan Group strata that lies between a series of basement domes or inliers comprising the Konkola dome in the northwest, the Kirila Bombwe anticline in the southeast and the Luina Dome to the northeast (Figure 1-3). The greater Konkola basin (red in Figure 1-3) is host to a resource of about 700 Mt @ 2.8 % Total Copper (TCu) (Hitzman et al., 2012). The mineralisation extends around the eastern perimeter of the Konkola dome to Musoshi Mine in the DRC (Figure 1-3). The Musoshi Mine orebody is currently being mined by SODIMICO Pvt Ltd of the DRC.

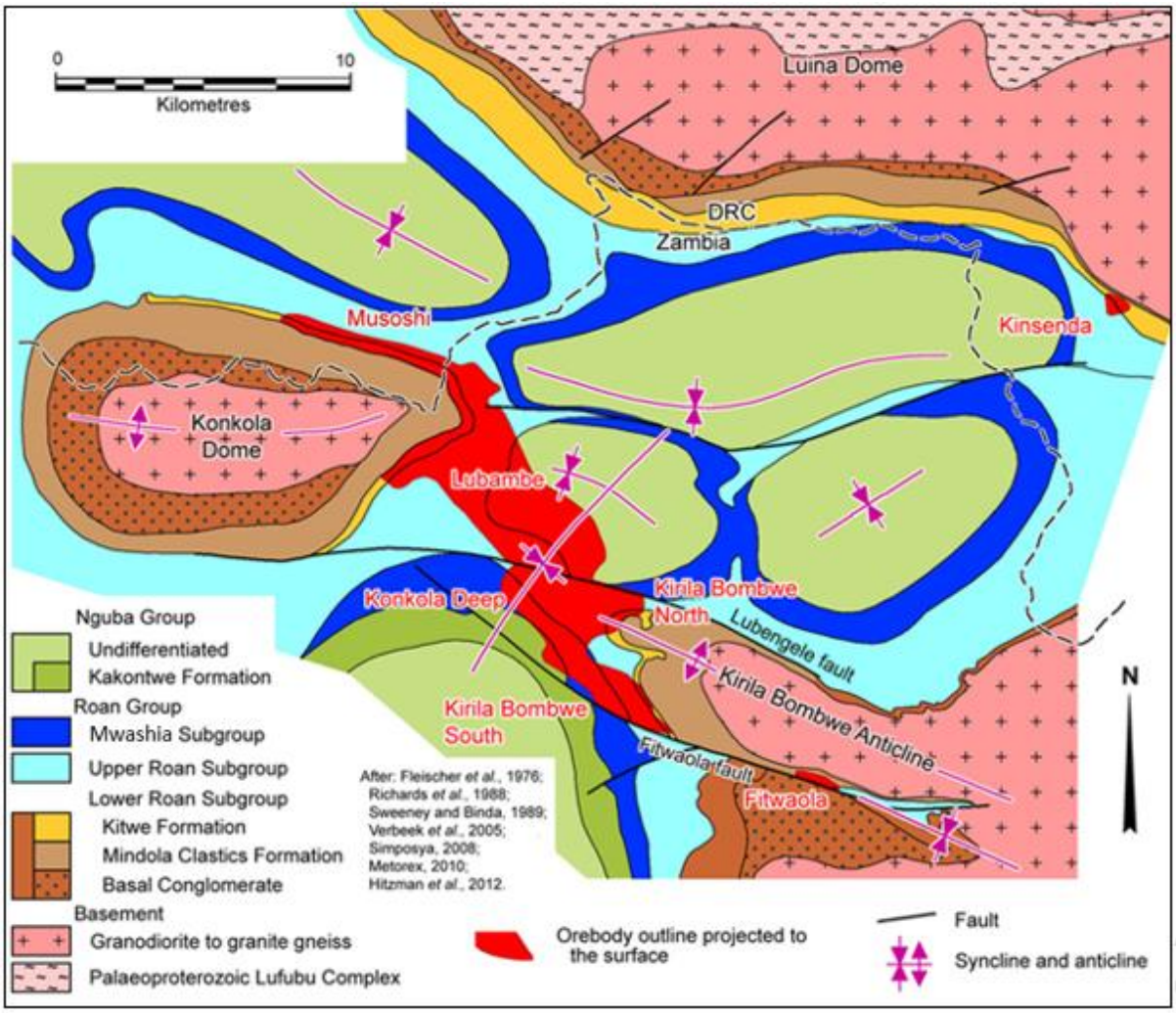

Figure 1-3: Geological map of the Lubambe and Konkola areas showing the stratigraphic distribution and the extent of known copper resources between Konkola and Musoshi (modified from Hitzman et al., 2012).

Since outcrop is scarce, the stratigraphy and structure of the basins hosting the Lubambe deposits are largely based on historic trenching and drilling, and more recently, on interpretations of airborne geophysical data (Woodhead, 2006; Carey and Cevallos, 2012). The basement domes and anticlines that flank the Kawiri basin comprise an undifferentiated assemblage of granite, gneiss and schist that ranges from Palaeoproterozoic (~1880 Ma) to Neoproterozoic (>880 Ma) in age (Kampunzu and Cailteux, 1999, Wendorff, 2005). The Kirila Bombwe anticline in the southeast includes a distinctive porphyritic granite, with large, orbicular microcline phenocrysts, known as the Muliashi Porphyry, dated at (1882 ± 23 Ma) (Wendorff, 2005).

1.4 LUBAMBE AREA STRATIGRAPHY

The stratigraphy of the Lubambe area comprises an undifferentiated basement which is unconformably overlain by the Katangan Supergroup (Figure 1-4), a weakly metamorphosed succession of Neoproterozoic sedimentary rocks (Anglovaal Mining, 1999a). The basement is overlain by the basal Roan Group, which comprises a clastic-dominated succession (the Lower Roan Subgroup) overlain by carbonates, evaporites and breccias (the Upper Roan Subgroup) (Mendelsohn, 1989). The units of the Roan Group display stratigraphic geometries considered typical of extensional rift basins, with thickness and facies changes and sharp lateral pinch-outs controlled by palaeo-topography (Annels, 1974; Selley et al, 2005). The depositional environment of the basal units is generally interpreted as fluvial, becoming progressively shallow-marine to evaporitic in nature (Selley et al., 2005). This trend is characterised by a transition from several discrete sub-basins to a larger, amalgamated basin and a change from subaerial (oxidized) to shallow-marine (reduced) strata. The majority of the ore in the ZCB occurs at this transition (a redox boundary), namely in a regionally persistent horizon of laminated, shales/siltstone (±10 m thick) known as the 'Ore Shale 1' (Hitzman et al., 2012).

The 'post-rift', middle to upper parts of the Roan Group is dominated by a carbonate-evaporite sequence that includes a stratabound, polylithic breccia complex interpreted to be formed by evaporite dissolution and halokinesis (salt tectonics) (Saintilan et al., 2018). Gabbro bodies (~765-735 Ma (Rainaud et al., 2005) occur as discontinuous lenses interpreted as fragmented sills whilst the Mwashia Formation units (Figure 1-4) that immediately overlie the breccia complex are characterised by unconformable relationships and sharp thickness variations. Broad, open synclines separated by tight to overturned anticlines are a characteristic feature of the region, probably a combined result of evaporite dissolution (i.e., withdrawal basins), and subsequent inversion (Selley et al., 2005).

The Roan Group is overlain by an upper siltstone-shale succession called the Mwashia Group (Mendelsohn (1961)). The latter occurs in a series of three juxtaposed synclines that occupy the centre of the Konkola and Kawiri basins (Figure 1-3). The younger Nguba Formation is locally preserved in the synclinal cores and comprises a thin but regionally persistent horizon of diamictite of interpreted glaciogenic origin (the Grand Conglomerate) ((Binda and Van Eden (1972)), which is in turn overlain by successions of Kakontwe limestones, shales and dolomites of the Upper Kundelungu succession (Figure 1-4).

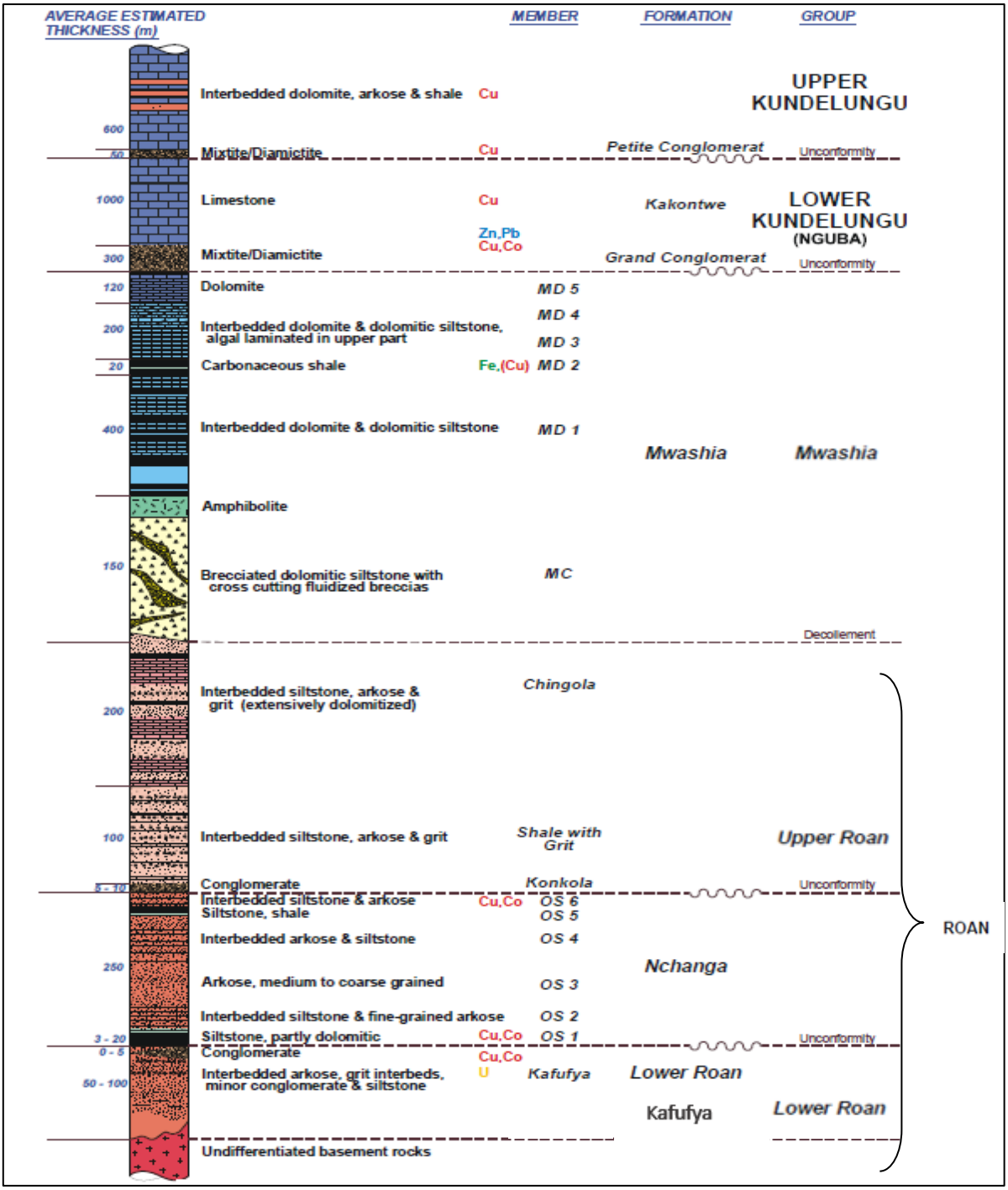

Figure 1-4: Simplified stratigraphic column of the Lubambe license area (modified from Simposya and Hart, 2008).

In contrast to elsewhere in the ZCB, the footwall succession in the Lubambe-Konkola area is anomalously thick (a maximum of 1650 m is recorded at Konkola Copper Mine (KCM)), while the hangingwall succession is relatively coarse-grained and arenaceous. Such features are interpreted to indicate a proximal position with respect to a major basin-bounding structure that potentially controls the sedimentary transition into the CCB to the north (Selley et al., 2005). The latter is characterised by a marked change in lithofacies architecture and orebody host rocks (Selley et al., 2005).

1.5 MINERALISATION WITHIN THE LUBAMBE COPPER DEPOSITS

The OS1 Member is the lowermost redox boundary in the Lubambe project area and comprises of siltstones composed of 45% K-feldspar, 35% quartz, 10% white mica, 5% dolomite and 5% subordinate rutile, tourmaline and zircon (Mwelwa, 2020). The true thickness of the OS1 Member varies from 2 to 15 m. This member abruptly overlies the Kafufya Formation, which dominantly comprises conglomerates, sandstones and arkoses and is the principal host to mineralisation (Sutton and Maynard, 2005). It is a fine-grained partially dolomitised siltstone, with thin white dolomitic interbeds and occasional thin sandy lenses that are preferentially oxidised and leached (Simposya and Hart, 2008). Mineralisation assumes the grain size of the host rock and occurs as finely disseminated sulphides, in some cases as coarser grains along bedding planes and cleavage, thin veinlets, lenticles and stringers. Mineralisation mainly comprises chalcopyrite, chalcocite, bornite, digenite, covellite, pyrite and carrollite in approximate order of abundance. A large proportion of the non-sulphide (oxide) copper minerals occur along fractures and veins (Sutton and Maynard, 2005).

The OS1 mineralisation also extends into the footwall with significant copper oxides being observed. Malachite, pseudo-malachite, chrysocolla, cuprite and azurite are the most common copper oxides present (Simposya and Hart, 2008; Arthurs et al., 2009).

1.6 MINERALISATION MODEL FOR LUBAMBE COPPER DEPOSITS

The mineralisation model for the Greater Konkola basin (which covers the Lubambe Copper deposits) involves deep-seated basin marginal faults reactivated during Lufilian deformation controlling oxidised fluid movement (Broughton, 2014). Mineralisation occurs through interaction of the oxidised (Cu-bearing) fluids with a reduced stratigraphic horizon, e.g., shales, hydrocarbons, etc. (Figure 1-5) (Broughton, 2014; Bull et al., 2011). Red beds are also leached of their metal content by circulating convectional cells. Faults within the basin become channel ways for movement of basinal brines, leaching and subsequently precipitating metal ions (Broughton, 2014; Cox, 2003). High-grades of copper and cobalt in the stratiform ores are attributed to the sedimentary depositional environment (including alkali lakes, playas and sabkhas) (Saintilan et al., 2018; Tembo et al., 1999).

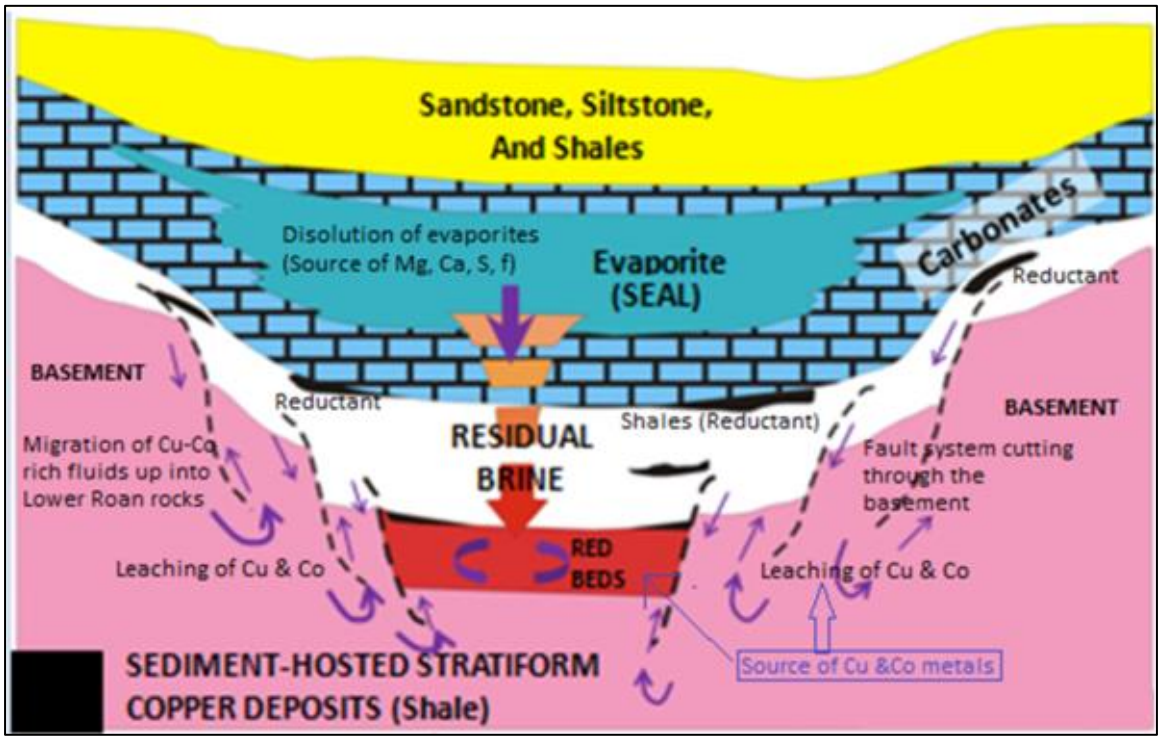

Figure 1-5: Mineralisation model adopted in the Greater Konkola basin. Basinal brines (in purple) circulate and leach out metals and then depositing them in shales (after Selley et al., 2005).

After deposition of the Katangan sequence and before lithification, the evaporites acted as a seal and source of the salinity in the brines that were circulating (indicated by purple arrows in Figure 1-5). As the fluids leached the metals, convection cells were generated due to higher temperatures in the basement and red beds, and the brines with contained metals rose up through the stratigraphy, encountered the redox boundary and precipitated metals (Theron, 2013). Continuous circulation of the brines resulted in continuous enrichment of the shale and arenite units just above the redox boundary (Theron, 2013). The basement and the walls of the basement confined this process whilst the thick sequence of the Katanga units, particularly the thick evaporitic unit, acted as the seal (Torremans et al., 2013).

1.7 MINING ACTIVITIES AT LUBAMBE COPPER MINE

Lubambe Copper Mine Limited (LCM) lies in the northern part of the Mining License 7061-HQ-LML area and covers approximately 240 square kilometres. Copper mineralisation is largely hosted within the OS1 Member. This member is the Copper Belt orebody equivalent and abruptly overlies the Kafufya Formation, which is the equivalence of the Mindola Clastics Formation in the Copperbelt stratigraphy. The Lubambe deposit is subdivided into three (3) major orebodies, that is, the East Limb, the South Limb and the Extension Area orebodies (Figure 1-6). Recent drilling carried out between 2019 and 2020 has proven orebody continuity on the eastern side of the Extension Area. The orebodies define the major high-grade zones in the license area.

Mineralisation in the East and South Limbs (Figure 1-6), extends down dip from approximately 150 m below surface to approximately 1650 m. The Lubambe orebody is a flat orebody with a dip ranging from 5° to 55° in the shallow dipping area. The orebody dip in the existing operation ranges from 15˚ to 70˚ and has a true thickness ranging from 5 to 14 m. Because of varying dips, different mining techniques are utilised at Lubambe Copper Mine, that is, sub-level open stoping (dip >55˚), Longitudinal Room and Pillar (dip ranging from 30˚ to 55˚) and Cut and Fill (dip <30˚) (Mwelwa, 2020).

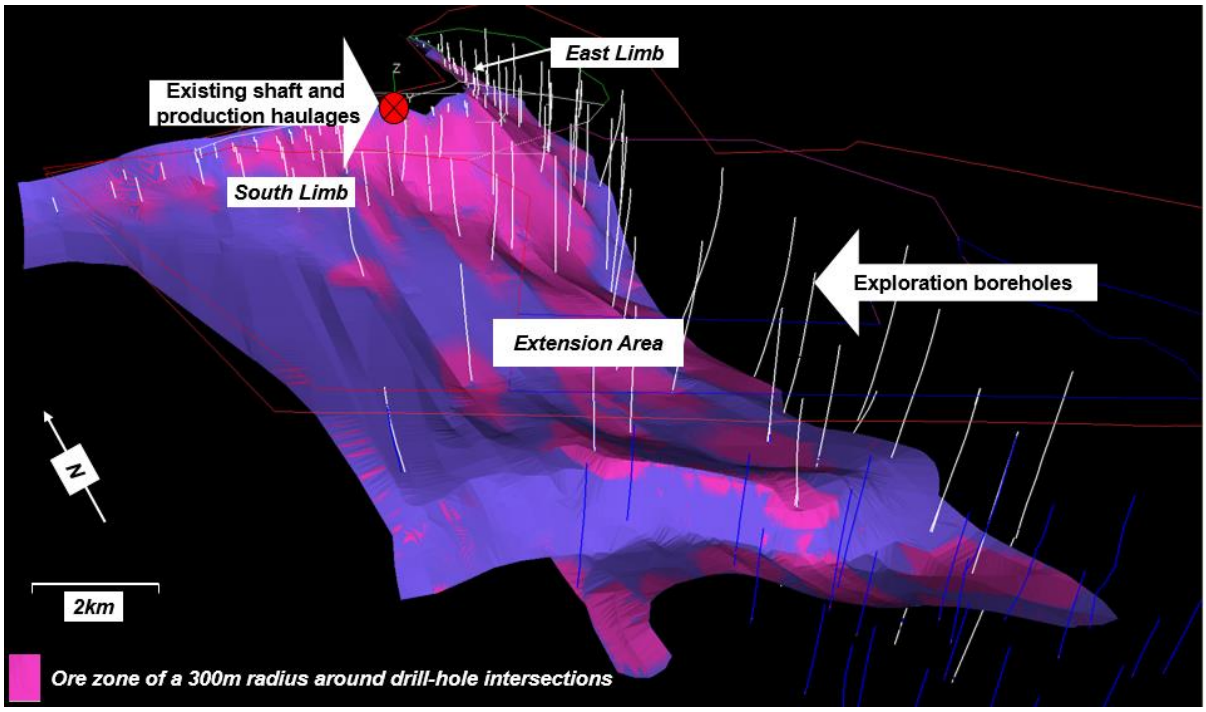

Figure 1-6: Showing the Lubambe orebody model from mining and exploration data (Mwelwa, 2020).

The East Limb is on the northeastern side of the Konkola Dome, the South Limb on the southeastern side of the dome and the Extension Area comprise of merged orebodies (East Limb and South Limb) extending to the southeastern margin of the project area (Figure 1-7). The orebody sub-outcrops at approximately 40 m below surface in the northwest of the lease area, where the Konkola Dome forms a basement high. From the sub-outcrops, the orebody slopes to the east and to the south where the depth of the orebody reaches 1650 m. The orebody differs from other copperbelt deposits in that it is less steeply dipping and narrower than the deposits currently being mined (Condor Consulting, 2014). Mining operations are centred on the old No. 2 shaft (Figure 1-6 and 1-7), which accesses the South Limb, together with two new declines to access the East Limb. The mine is designed to exploit the northern portion of the 'Greater Konkola Ore body', which extends from Konkola Mine in the south, to the Musoshi Mine in the north within the DRC (Figure 1-7).

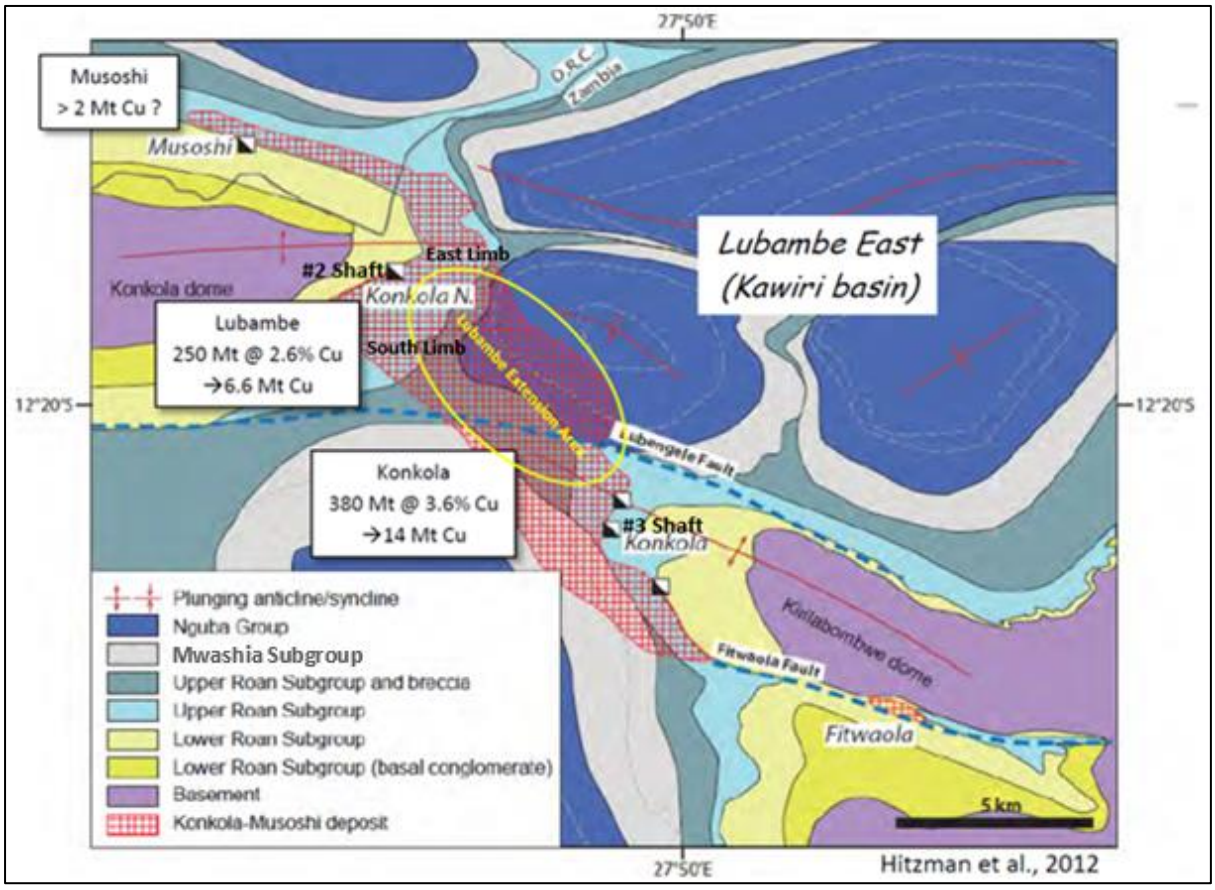

Figure 1-7: Geological map of the Lubambe area showing the location of the Lubambe Copper Mine No. 2 Shaft location and 2012 estimated Cu resource figures relative to other deposits in the Greater Konkola basin (modified from Hitzman et al., 2012)

Production commenced in 2014, and is expected to ramp up to approximately 2 million tonnes of ore per annum containing approximately 52,000 tonnes of recoverable copper in concentrate by 2022.

1.8 PROBLEM STATEMENT

The Lubambe copper deposit is a classic copperbelt style, stratiform, shale-hosted, copper orebody. Mineralisation within the project area is characterised by metals derived from pre-Katangan granitic basement, subsequent carbonate replacement of sulphates to form sulphide mineralisation in the Lower Roan Group (Nchanga Formation), and secondary mineralisation associated with reworked sedimentary strata in oxides and micas within the hanging wall sequence (Arthurs et al., 2009). Most of the copper occurrences in the project area are associated with mineralising fluids that migrated along growth faults at the basin margins to form stratiform deposits in the shale members of the Lower Roan Group, which is at the base of the Katangan Supergroup (Figure 1-5). It has been suggested that these growth faults were later reactivated as thrusts during basin inversion in the Lufilian Orogeny (Bull et al., 2011).

Mineralisation in the Lubambe copper deposit is hosted within the OS1 Member which represents the lowermost redox boundary in the Lubambe area. The OS1 Member comprises mostly shales and siltstones that unconformably overlie the conglomerates, sandstones and arkoses of the Kafufya Formation. Selley at al. (2005) notes that the OS1 is a result of a sudden transgressive event that happened in the Konkola basin after initial rifting. The OS1 Member generally dips steeply towards the east and south from the Konkola dome with orebody depth ranging from 200 - 1650 m. Three major mineralised envelopes (high-grade ore zones) have been confirmed within the license area and these are named the East Limb, which is on the northeast side of the Konkola Dome, the South Limb on the southeast side of the Konkola Dome and the Extension Area which extends to the southeast margins of the project area. All these three mineralised ore zones have shown different kinds of oxide and sulphide mineralisation, concentrations and distributions at various levels (Reid, 2020).

Although the Lubambe copper deposit has been investigated several times, there is still inadequate understanding of the influences on ore distribution and spatial occurrence at a local scale with many areas of concern remaining largely unstudied. Persistent questions about how mineralisation is related to lithology and structure and the effects of these on ore distribution, concentration and spatial occurrence are not well answered. There is a need to undertake a geological, geochemical and geophysical assessment of the Lubambe property with a view of understanding controls, distribution and spatial occurrences of mineralisation in order to assist ongoing mining, mine planning, resource delineation, exploration targeting and mineral processing.

1.9 RESEARCH MAIN OBJECTIVE

The main aim of this study is to determine the geological and structural influences on copper mineralisation and how they affect copper distribution and spatial occurrence in the Lubambe copper deposit.

1.9.1 SPECIFIC OBJECTIVES

The following specific objectives help to achieve the main objective of the study:

- To understand the mineralogy and distribution of Cu and grades within the Lubambe orebody.
- To determine the major structures controlling mineralisation in the Lubambe copper deposit.

1.10 JUSTIFICATION OF STUDY

The relationship between lithology and structure requires an evaluation at a detailed scale, for the purpose of understanding mineralisation trends, styles and controls which are critical components for grade prediction, improved mining (methods and planning), ore processing, recovery and brownfields exploration, but also to provide direct support for exploration elsewhere in the basin. A study of the lithological and structural influences to mineralisation and distribution is expected to help understand the copper-bearing fluid migration within the Konkola and Kawiri basins. Immediate outcomes at the regional-scale within the property include the identification of exploration targets to increase the resource/reserve base for the life of mine. The study also presents an opportunity to research and understand the local, regional and structural geology and structures better, thereby adding more valuable content to the Lubambe geological database.

1.11 METHODOLOGY

A number of techniques have been used to achieve the set of objectives in the study and they include;

- Core logging of surface drill holes for a better understanding of how mineralisation relates to geological formations, structures and alteration patterns.
- Surface mapping of outcrops, sub-outcrops and structural features to determine the local stratigraphic position(s) in relation to the Katangan stratigraphy. Mapping also provides an indication of bedding of the main stratigraphic units' orientation.
- Geological modelling, plan and cross-sectional plotting to show the stratigraphic lithological layering, structural features, grade distribution and variation in the study area.
- Petrographic analysis of the rock samples to document mineralogical, structural and textural features of the ore-hosting lithologies. This requires micro-petrographic studies to identify the minerals, alterations, estimate grain sizes, modal abundances and make textural interpretations.
- Geochemical analysis on core samples to determine the whole-rock major and trace element compositions which will give a determination of the distribution of copper in the project area.

CHAPTER 2

LITERATURE REVIEW

2.1 INTRODUCTION

This chapter provides background information about the project area from the time of deposit discovery to current mining and exploration activities. The information is based on available literature, research documents, historical data and records to give a better understanding of the project area from a regional scale to a local scale. Geological, geochemical and geophysical data generated by previous workers is also summarised.

2.2 REGIONAL TECTONIC AND STRUCTURAL SETTING

The Lufilian Arc (Figure 2-1), represents a Neoproterozoic to Lower Palaeozoic Pan-African orogenic belt that is underlain by a fault bounded crustal block between the Congo Craton in the north and the Kalahari Craton in the south (Kampunzu and Cailteux, 1999). The curved shape of the belt is attributed to thrusting of the Kalahari Craton onto the Congo-Tanzania Craton during Pan-African collision/rift closure (Kampunzu et al., 2009; Key et al., 2001). The belt also comprises major sinistral translation and severely deformed sedimentary strata and igneous/metamorphic basement units (Figure 2-1, Cailteux and Kampunzu 1995; Barra et al., 2005).

Previous studies have identified sheared fabrics in the basement inliers and interpreted the basement domes to have been thrust into the overlying Katangan Supergroup (Key et al., 2001). The Lufilian Arc is also associated with major copper-cobalt deposits, which are hosted within the Katanga Supergroup (Wendorff, 2005).

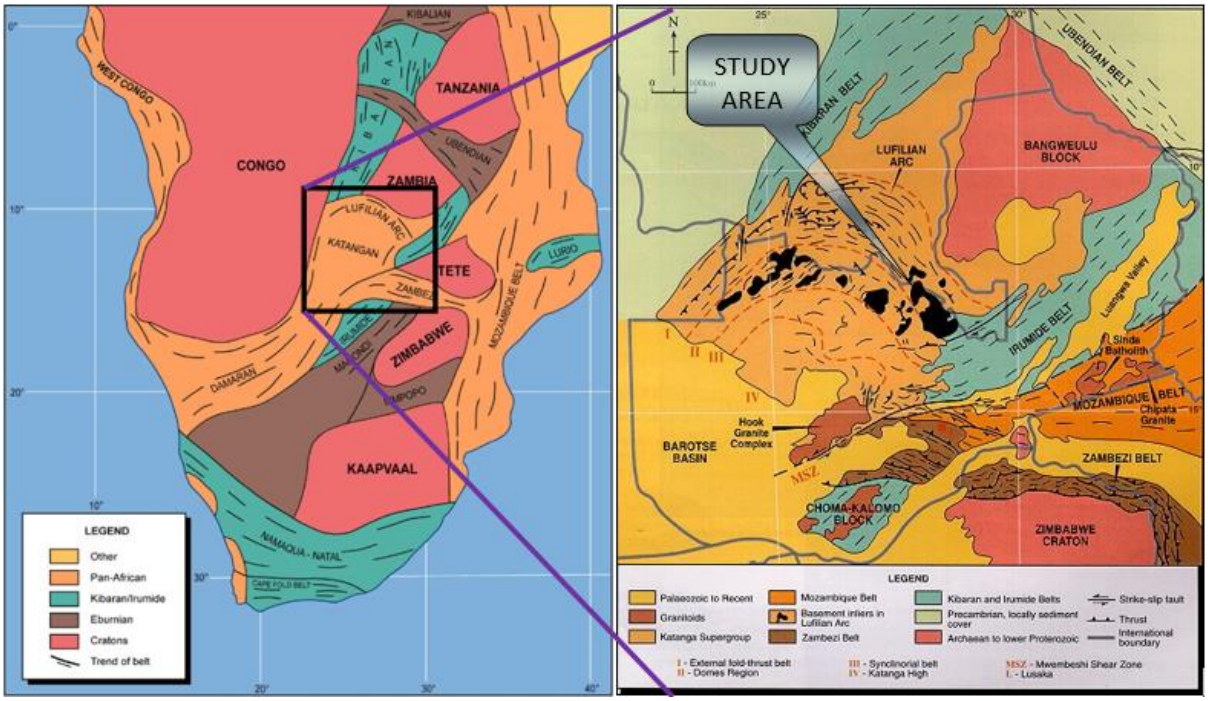

Figure 2-1: Geological maps showing the tectonic setting of the Central African Copper Belt (modified after Porada (1989)).

The Zambian Copper Belt has been affected by three major tectonic phases from early rifting to basin inversion (Rainaud et al. 2005). Sedimentation of the Katangan Supergroup and subsequent copper belt mineralisation was limited to fault-controlled basins associated with extension, that were later

inverted during the Lufilian Orogeny when compressive deformation produced complex fold patterns across the Lufilian Arc (Porada and Berhorst, 2000).

Katangan Sequence sediments were deposited in an intra-continental rift which was later closed during the Lufilian orogeny which is a period characterised by folding and thrusting (Kampunzu, and Cailteux, 1999). At a regional scale, the Greater Konkola basin is located in the central part of the CACB and on the outer margins of the ZCB. The Lower Roan Group which are the first sediments after rifting, primarily consists of continental-sourced arkose and shale, and the mineralised Ore Shale 1 Member (within the Nchanga Formation) (Roberts et al, 2005). The marine Upper Roan Group is characterised by carbonates and siltstones, while the overlying Mwashia Formation contains shallow marine siliciclastic and breccia units (Bull et al, 2011). A major decollement has been mapped at the base of the Mwashia Formation (Bull et al, 2011). The overlying Kundelungu Formation typically contains shale, carbonate, and a few basal conglomerate units that separate the upper and lower sequences (Mendelsohn, 1989; Wendorff and Key, 2009).

Throughout the ZCB, the dominant structural grains are northwest trending, representing the largest and most laterally continuous structures observed (Key et al., 2001). In the project area, this is very apparent from structural interpretation of Landsat TM imagery, aerial photography and airborne magnetic coverage.

2.3 TECTONIC DOMAINS

Several tectonic domains have been mapped within the Lufilian Arc and these comprise four structural domains (Figure 2-2), namely, the External Fold and Thrust Belt, the Domes Region, the Synclinorial Belt and the Katanga High (Key et al., 2001). The External Fold and Thrust Belt region host most deposits of the CACB whilst some deposits in the ZCB occur adjacent to the eastern-most basement inlier of the Domes Region (Selley et al. 2005).

The External Fold and Thrust Belt (Figure 2-2b, c) occurs mostly in the northern DRC and consists of repeated upper Katangan stratigraphy (Key et al., 2001; Selley et al., 2005). The repetition of Katanga Group rocks reflects the northward thrusting of lower Katangan units, which conceal the Basement Supergroup (Kampunzu and Cailteux, 1999).

The Domes Region (Figure 2-2b, c) is the second domain from the north and mostly characterised by outcropping Basement Supergroup rocks forming ‘domes’ and are surrounded by Katangan metasediments (Selley et al., 2005). Daly et al. (1984) interprets the antiformal stacks within Domes Region units as due to thick-skinned deformational processes.

A thrust contact (Figure 2-2c) separates the Synclinorial Belt from the Domes Region (Cosi et al., 1992; Selley et al., 2005). The Synclinorial Belt mostly comprises former deep-water sedimentary packages. The Lufilian orogeny at ~530 Ma is attributed for the decoupling along evaporitic horizons between the Domes Region and the Synclinorial Belt (Hanson et al., 1994). This resulted in north-directed transport of rocks from the Katanga High and the Synclinorial Belt for several kilometres (Selley et al., 2005).

The uplifted Basement Supergroup rocks make the Katangan High (Figure 2c), which is covered by thin former deeper water sedimentary packages. During the Lufilian orogeny, the Katanga High is suggested to have acted as a ramp overriding plate. Intrusions of 570-530 Ma granites affected the Katanga High (Daly, 1986; Hanson et al., 1993; Selley et al., 2005).

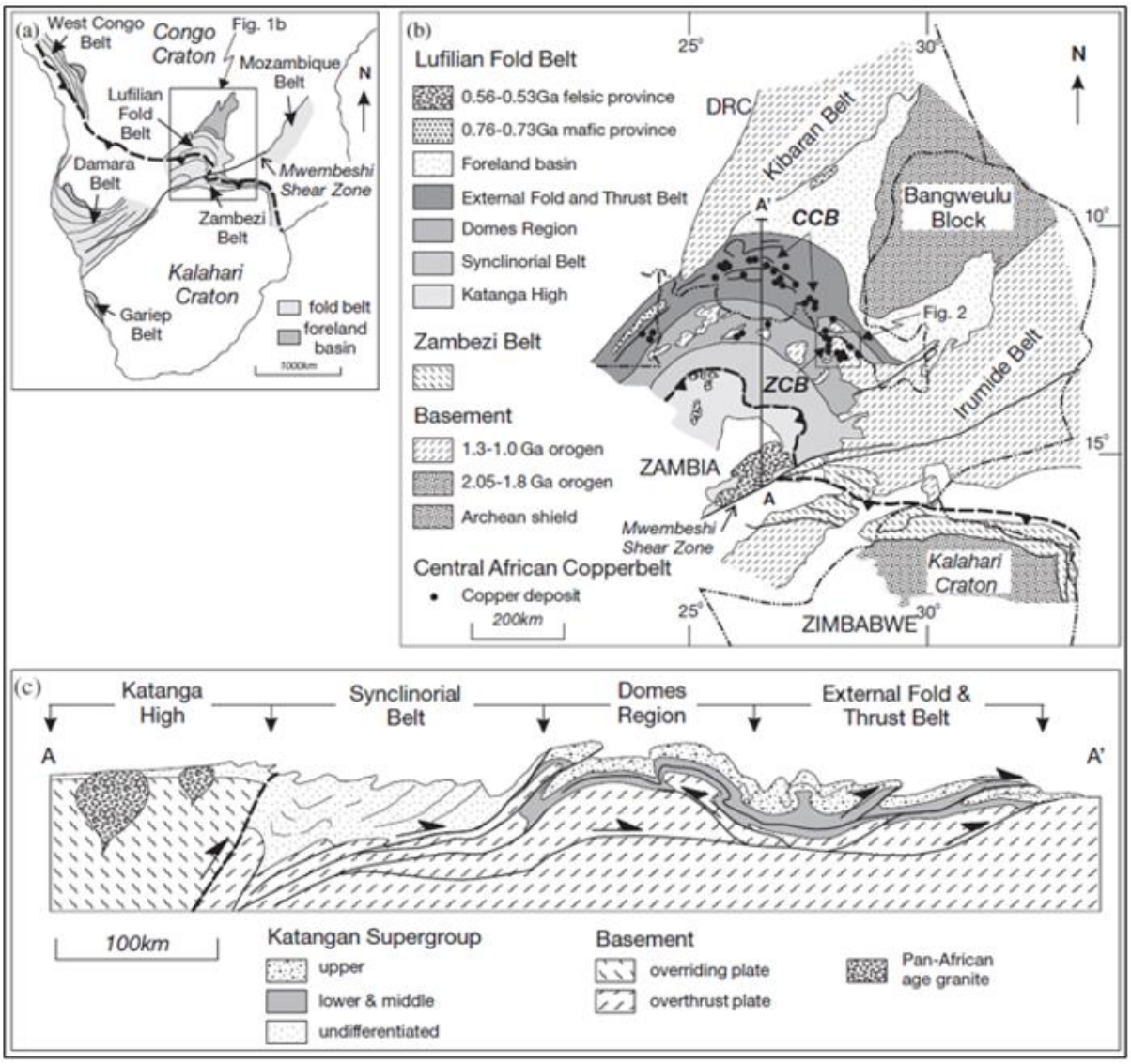

Figure 2-2: Tectonic domains of the Lufilian Fold Belt (a) Location of the Central African Copperbelt in the Lufilian fold belt (b) Lufilian fold belt location in Zambia and tectonic domains (c) Schematic section of the Lufilian Fold Belt showing different tectonic domains (Selley et al., 2005).

2.4 DEFORMATION

The Lufilian Arc has been affected by several deformation events, including crustal shortening along shallow shear zones, hydrothermal fluid flow along reactivated faults and mylonitic belts, and open folding (Cosi et al., 1992). The various phases of deformation comprise northward folding and thrusting (Kolwezi phase - D1), sinistral translation (Mwonezi phase - D2), and the Chilatembo phase - D3, with younger structures formed transverse to the main trends within the Lufilian Arc (Kampunzu and Cailteux, 1999).

The Kolwezian phase (D1) (~800 - 710 Ma) is observed throughout the Lufilian Arc characterised by northward-trending upright and overturned folds associated with folding and thrusting (Kampunzu and Cailteux, 1999). This deformation event of folding and thin-skinned thrusting formed repeated allochthonous sheets which are correlated with the main deformation in the Zambezi belt (Ngoyu et al, 1991). The early formation of the NW-SE trend of the Lufilian Arc is attributed to be a result of the D1 phase (Kampunzu and Cailteux, 1999).

The 690 Ma - 540 Ma Monwezi phase (D2) deformational event is responsible for the arcuate shape of the Lufilian Arc. This was mainly due to the effects of strike-slip faulting and the clockwise rotation of crustal blocks which occurred during this deformational event (Kampunzu and Cailteux, 1999. Open north-trending antiforms were formed after folding of the basement and basal footwall formations of the Katanga Supergroups in the central west of the Lufilian Arc (Key et al., 2001).

The last deformation phase of the Lufilian orogeny is called the Chilatembo phase (D3) which is marked by folded structures transverse to the trends of the Lufilian arc (Kampunzu and Cailteux, 1999). The D3 phase has an age younger than 540 Ma (Kampunzu and Cailteux, 1999) and is characterised by N-S and E-W striking faults cross-cutting large open folds with hinges trending between NNE-SSW and ENE-WSW (Kampunzu and Cailteux, 1999).

2.5 BACKGROUND TO THE LUBAMBE COPPER MINE

The Lubambe Copper Mine is owned as a joint venture between Energy Mineral Resources Capital (EMR Capital) with 80% shareholding and Zambia Consolidated Copper Mines (ZCCM) with 20% shareholding. It is situated within "the Greater Konkola Orebody" which combines Nchanga Copper Mine and Konkola Copper Mine, Lubambe Copper Mine and Extension Area and the Musoshi Mine in the DRC. The Greater Konkola Orebody is situated at the northwestern margin of the ZCB and stretches into the DRC within the CACB (Figure 1-7). The mine is part of a large-scale License area 7061-HQ-LML that covers approximately 250 km² previously known as the Konkola North deposit during exploration before being renamed Lubambe Copper Mine by the current owners. Current mining is exploiting the East Limb and the South Limb orebodies whilst a prefeasibility study is being finalised for the Extension Area resource (Figure 2-3). The remainder of the property is referred to as the Lubambe East Area but locally called the Kawiri Area (Figure 2-3).

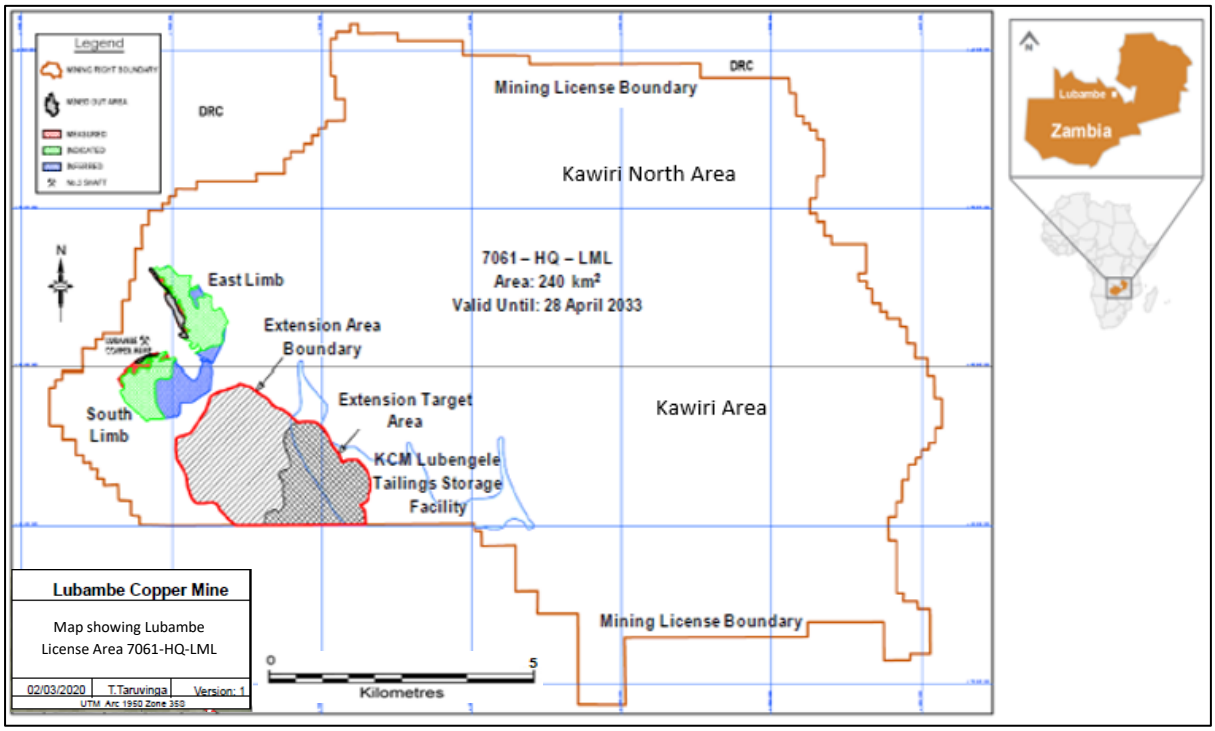

Figure 2-3: Plan showing locations of Lubambe Copper Mine (East Limb and South Limb), Extension Area and Kawiri Areas within license 7061-HQ-LML.

2.6 EXPLORATION HISTORY

The Lubambe-Kawiri area (License area 7061-HQ-LML) has a long history of copper exploration. Work was initially conducted by Anglo American, ZCCM, Anglovaal and its subsidiaries / successors, namely Konnoco, TEAL Exploration and Mining, African Rainbow Minerals (ARM) and more recently Lubambe Copper Mine (Carey and Cevallos, 2012). Copper was first discovered in the area in 1924 and limited production occurred between 1957 and 1962 from an underground operation known as Konkola (North) No.2 Shaft which is part of a semi-continuous orebody extending from Konkola in the southeast to Musoshi (in the DRC) in the northwest (Arthurs, et al., 2009). Early exploration consisted of geological mapping, soil geochemical surveys and several programs of widely-spaced diamond and reverse circulation drilling. In addition to resource evaluation, drill holes were sited at regular intervals along the southern, western and northern edges of the Kawiri basin (AMEC, 2014).

Between the late-1990s and 2009, Konnoco and ARM/TEAL conducted infill drilling at Konkola North (47,690 m) and completed several ground and airborne geophysical surveys. These included a regional aeromagnetic survey (400 m line spacing) covering all of the Kawiri area, a high-resolution Heli-borne magnetic survey (50 m line-spacing) covering the southwestern parts, a reconnaissance ground gravity survey also covering the southwestern parts and finally, a high-resolution HeliTEM electromagnetic, magnetic and radiometric survey over the entire license area. A reflection seismic test survey was also completed but failed to yield useful data due to sub-optimal acquisition parametres. Other work included diamond drilling to test conceptual targets in the southeast (Kawiri South) and central part of the Kawiri basin and a program of reverse circulation drilling to test historic geochemical anomalies.

In 2009, VALE Zambia Pvt Ltd partnered with African Rainbow Minerals (ARM) and ZCCM to develop the property and renamed the project the Lubambe Copper Mine. EMR Capital took over the project under a joint venture with ZCCM. To date, the project has focused largely on mining the East Limb and South Limb at Lubambe Copper Mine as well as Extension Area resource evaluation and development.

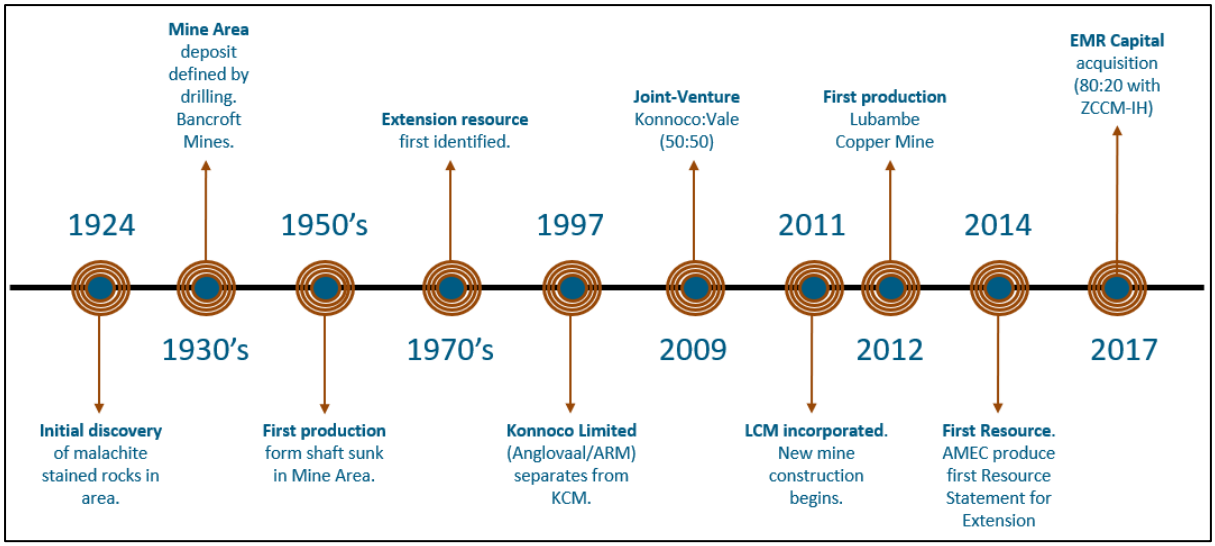

Figure 2-4: Diagram showing the Lubambe discovery, production and ownership over time (Stacey, 2020).

2.7 REGIONAL GEOPHYSICAL EXPLORATION IN THE LUBAMBE LICENSE AREA

Most of the Lubambe Copper Mine mining and exploration activities are concentrated in the South Limb, East Limb and Extension Area of the Lubambe orebody which are all situated in the Konkola Basin. The Konkola Basin is considered prospective for Ore Shale mineralisation and is yet to be thoroughly explored. The remaining regions of license 7061 – HQ – LML contain the Kawiri North and Kawiri South Basins (Figure 2-5). In the early 1990s, the available data for the Kawiri North and Kawiri South Basins was considered insufficient for exploration targeting hence a geophysical program was developed which incorporated Airborne Gravity Gradiometer, TEMPEST Time Domain Electromagnetics (TDEM), radiometrics and magnetics (Carey and Cevallos, 2012). The combined geophysics greatly assisted in the understanding of the structural framework, development of exploration targets and siting of the proposed deep, large diameter dewatering bore holes in the Extension Area.

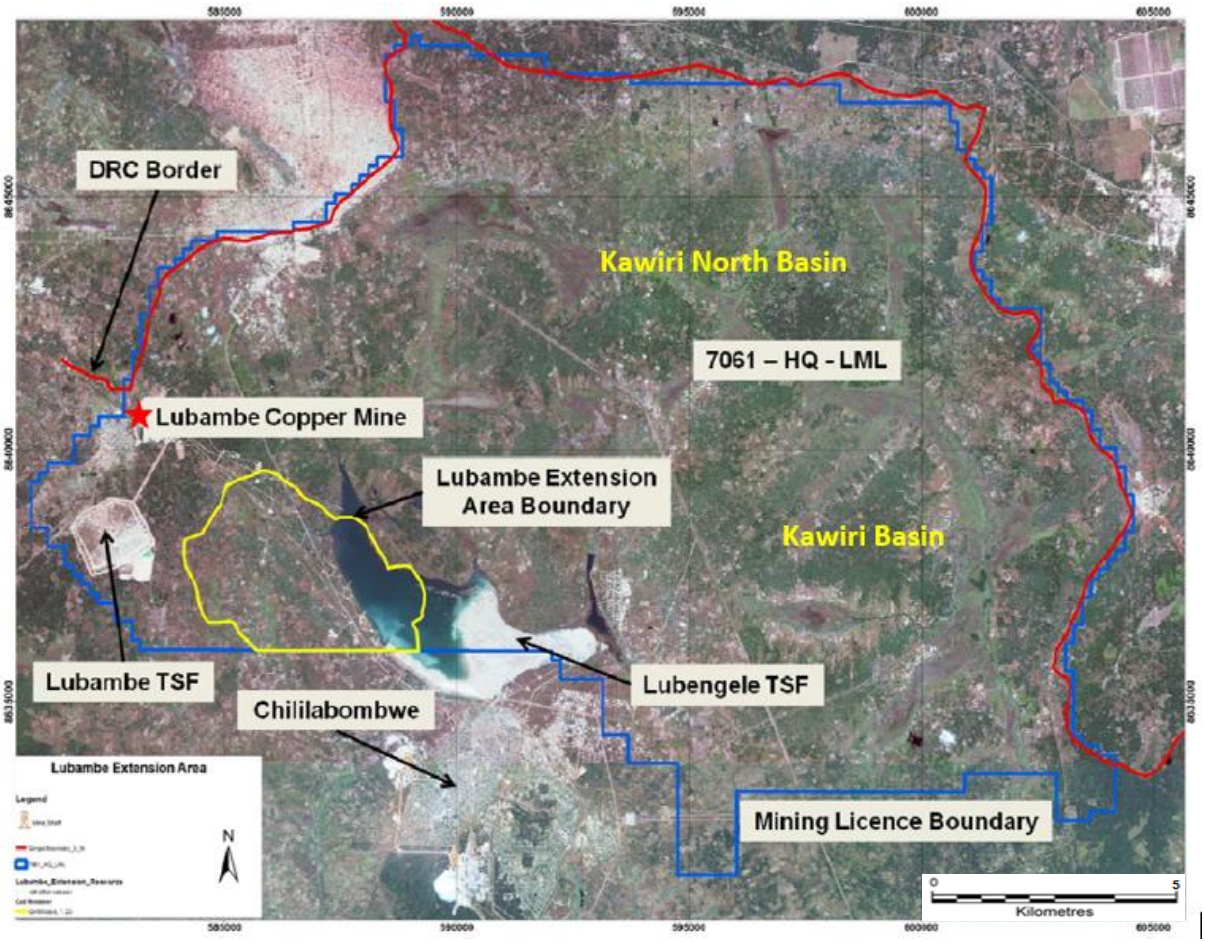

Figure 2-5: Google image showing the Lubambe License Area and the Kawiri basins targeted for geophysical exploration.

Detailed geophysical investigations were carried out in the Mining License 7061-HQ-LML from 1980 to 2012 with the aim of gaining more detailed information about the geological structures and to use the information to set drilling targets. Between the early 1980s to 1994, ground resistivity and frequency domain electromagnetic (EM) surveys were carried out by the University of Zambia on behalf of Zambia Consolidated Copper Mines Limited (ZCCM) during the latter part of state ownership. This geophysical work achieved limited depth penetration but was able to identify numerous NW-SE trending resistivity lows, interpreted as faults. NW-SE faulting was also interpreted from the EM data and this is also supported by the trend of various streams in the area (Carey and Cevallos, 2012).

Konnoco (Zambia) Ltd also carried out a detailed geophysical investigation in 1997. The geophysical methods used consisted of low-level aeromagnetics and semi-detailed gravimetric surveying. The acquisition was sub-contracted to a geophysical contracting company called Geodass (Pty) Ltd, which carried out the geophysical surveys on behalf of Konnoco (Zambia) Ltd. The aeromagnetic survey was carried out in September 1997 and the gravity survey in December 1997. Other geophysical datasets that included magnetics, radiometrics and electromagnetics to further understand the structures in the area were carried out by Avmin (Pvt) Ltd and Teal Zambia (Pvt) Ltd between the period 1995 to 2011. Vale Zambia (Pvt) Ltd also undertook gravity surveys in 2014 while Lubambe Copper Mine attempted to carry out seismic surveys in 2019, but were both unsuccessful due to improper procedures and adverse weather conditions (Mwelwa, 2020).

2.7.1 AIRBORNE ELECTROMAGNETICS

Variations in electromagnetic responses and magnetic texture/intensity across the Lubambe license area reflect compositional layering, lateral facies changes and unconformities between individual sedimentary sequences (Figure 2-6) (Nyoni, 1999). Major regional structures transect the project area and include predominantly east-west trending sinistral faults, thrust faults, anticlines, and major synclinal basins. Anticlinal features commonly form as fault propagation folds over thrust ramps or basement domes (Knupp, 2006). These anticlinal features can also be identified in the eastern domain and south-central region of the project area within the Mwashia Formation (Figure 2-6e). The preliminary analysis of selected discrete EM anomalies identified prospective target areas for copper mineralisation and subsequent follow-up exploration.

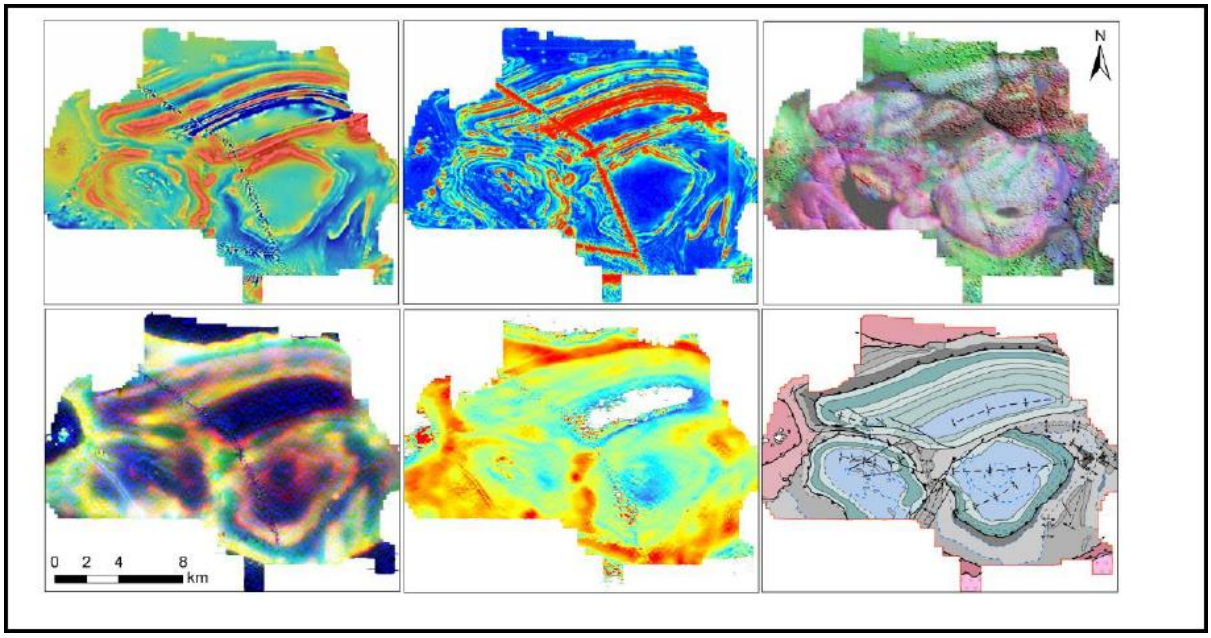

Figure 2-6: Magnetic and EM Images and Interpretations from the 2011 Fugro Airborne Survey (Carey and Cevallos, 2012).

(Clockwise from top left: (a) First Vertical Derivative overlain by the Total Magnetic Intensity Reduced to Pole (1VD TMI-RTP); (b) Horizontal Derivative; (c) Ternary of the Radiometric data overlain on the STRM; (d) fundamental Litho-structural interpretation; (e) Tau of the EM data (channels 14-21); and (f) Ternary of the EM data).

The techniques were essentially used to map sub-surface lithology and assist in the planning of collar locations. Late structures in the upper stratigraphy associated with palaeo-basin margin structures were identified when the aeromagnetic data was later combined with gravity data. A correlation between edges of gravity lows and deformation/juxtaposition of magnetic units was interpreted by Woodhead (2006) as proxies for sub-basin structures controlling mineralisation. Locations of

deformation features in stratigraphy overlying footwall clastics were noted to be spatially associated with palaeo-basin margin structures. Deformation and faulting of the Mwashia Formation was observed to be associated with underlying basement topography and structure (Carey and Cevallos, 2012).

2.7.2 AIRBORNE RADIOMETRIC

Airborne radiometrics were used in conjunction with airborne magnetics to map surface lithologies. The combined radiometric and litho-magnetic units from areas with distinctive signatures were correlated with geological data from surface mapping and drilling during interpretation. Radiometric potassic (K) anomalies indicate regions of alteration associated with epigenetic style mineralisation (Knupp, 2006). Coincident electromagnetic and radiometric anomalies associated with early basinal fault structures were considered highly prospective and highly ranked (Nyoni, 1999).

2.7.3 GRAVITY SURVEYING

Gravity data was collected between November 1996 and February 1997 by Geodass (Pty) Ltd of South Africa, on behalf of Konocco (Zambia) Ltd. The data acquisition was conducted on the exploration grid with lines spacing of 500 m apart. The gravity measurements were taken at 200 m intervals. The elevation data was collected using a Novatel Gizmo™ differential GPS system.

High resolution gravity data enabled detection of density variations associated with thickness variations in footwall stratigraphy. Thickness variations are controlled by sub-basin fault systems that provide a focus for mineralisation (Bhattacharrya, 1978). This provides an effective tool for targeting in the Konkola and Kawiri basins, in particular, the region to the east of Extension Area directly below the tailings dam. Gravity contrasts generated from juxtaposing formations were used in conjunction with aeromagnetic and radiometric data to positively identify controlling structures for deep-seated mineralisation. Gravity data also provided valuable information for features associated with the basin margins between Konkola and Kawiri Basin as well as the Kawiri/Kawiri North and Konkola/Kawiri North Basins.

2.8 MINING OPERATIONS AT LUBAMBE COPPER MINE

Lubambe Copper Mine copper mineralisation is virtually continuous over a very large area which extends from Musoshi mine in the Democratic Republic of Congo in the north, southwards into Zambia through Lubambe Mine and the Konkola Mine as far as Nchanga (Arthurs et al., 2009). The Lubambe Copper Mine plant covers 4.4 km² within the entire license area.

The mine started development in March 2011 with a 2.5 Mtpa copper operation and a life of mine of approximately 25 years at an average grade of 2.34% TCu. Mining of the East and South Limb orebodies started in the 1950s with approximately 200 000 t of copper ore extracted from No. 2 Vertical Shaft until the mine was closed due to low copper demand causing a drop in the copper price (AMEC, 2014). The mine was eventually flooded by water in the late 1950s due to prolonged dormancy.

Mining is currently taking place in the South Limb and the East Limb orebodies only. Access for extraction and exploitation of the underground resources is via two main points with each orebody having its own entry point. The South Limb is accessed via the No. 2 Shaft (Figure 2-7), which has been refurbished from the old operations, whilst the East Limb orebody can be accessed via a twin decline

to 100 m level which is the upper limit of stoping. At deeper levels, the mine is split into five separate sections, each with its own ramp (two in the South Limb and three in the East Limb).

The No.2 Shaft is also used as the primary material haulage channel for ore transportation from the South Limb. On the East Limb, ore is hauled through one of the drives which is equipped with conveyors for ore and waste haulaging.

The Extension Area is still under exploration with pre-feasibility studies almost complete.



Figure 2-7: Picture of No.2 Shaft (2011) at Lubambe Mine which provides access to the South Limb.

2.9 LUBAMBE EXTENSION AREA – BROWNFIELD EXPLORATION

The Lubambe Extension Area is situated to the south and southeast of the Lubambe Copper Mine and shares a common boundary with KCM to the southeast (Figure 2-8). The Extension Area has been the focus for exploration with the intention to outline a possible down-dip copper ore body currently being exploited by the mine on both the East Limb and the South Limb (Figure 2-8). Over 50,000 m of diamond and reverse circulation drilling combined with geochemical and geophysical surveys have been carried out in the past four decades under different license owners. A prefeasibility study carried out in 2010 indicated that there was a high probability of developing an extension to the existing Lubambe Copper Mine (AMEC, 2014). A further geological drilling programme was completed in 2014, 2018 and 2019, which significantly increased both the tonnage and grade of the Lubambe Extension Area (Reid, 2020). Of particular interest were the results completed towards the east, close to, and under KCM's Lubengele Tailings Storage Facility (LTSF). These conclusively demonstrated that the higher grades and thicker mineralisation intervals intersected in previous holes located close to the LTSF were continuous to the east (Stacey, 2020). The eastern limit of this easterly trend is still being explored. The Extension Area has generated great interest due to its high-grades and thicker orebodies. Economic grades in the OS5 Member have also been intersected in several holes, particularly on the Eastern side of the LTSF.

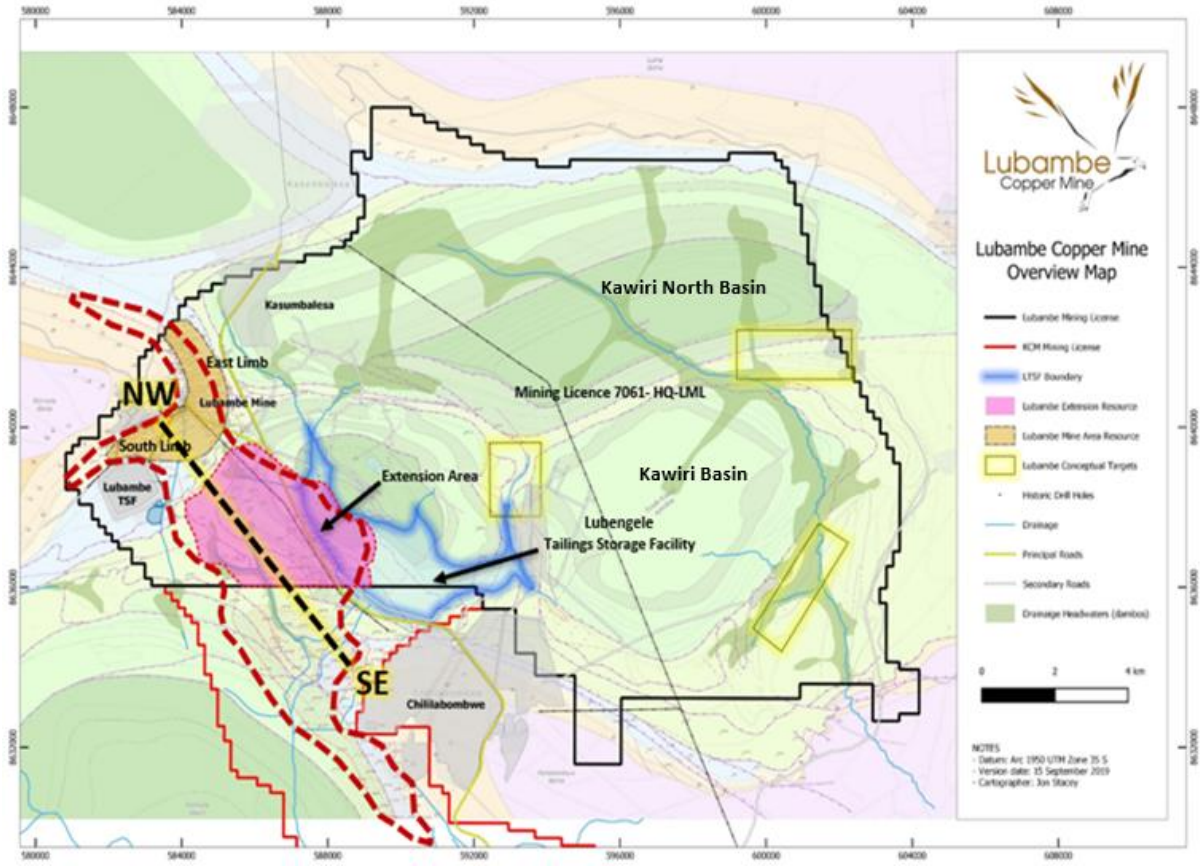

Figure 2-8: Location map showing the extent of the Extension Area (pink polygon) (modified from Stacey, 2020).

Konkola and Lubambe Extension Area orebodies are positioned on the hangingwall side of inverted growth faults (Figure 2-9). In the Extension Area, orebody intersections range in depth from 800 m to 1800 m.

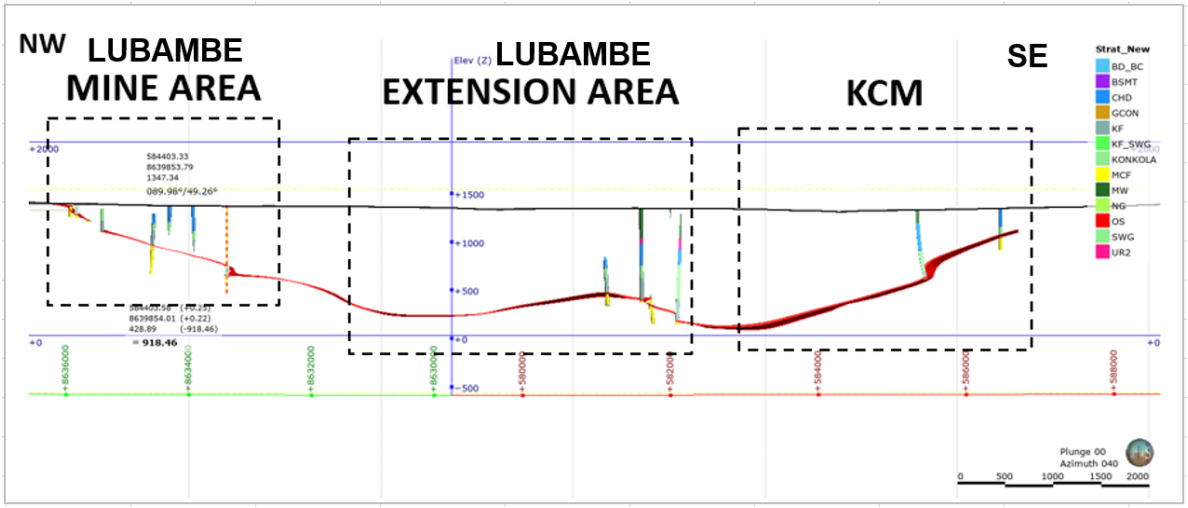

Figure 2-9: Cross section showing the orebody profile from the Lubambe Mine Area to KCM (Stacey, 2020).

The Lubambe Extension Area project is already one of the largest large-scale undeveloped copper resources in the world, with an estimated resource of 350Mt @ 3.72% TCu (Reid, 2020). Figure 2-10 shows the benchmark position of the Lubambe Extension Area in respect to other world-class undeveloped copper discoveries.

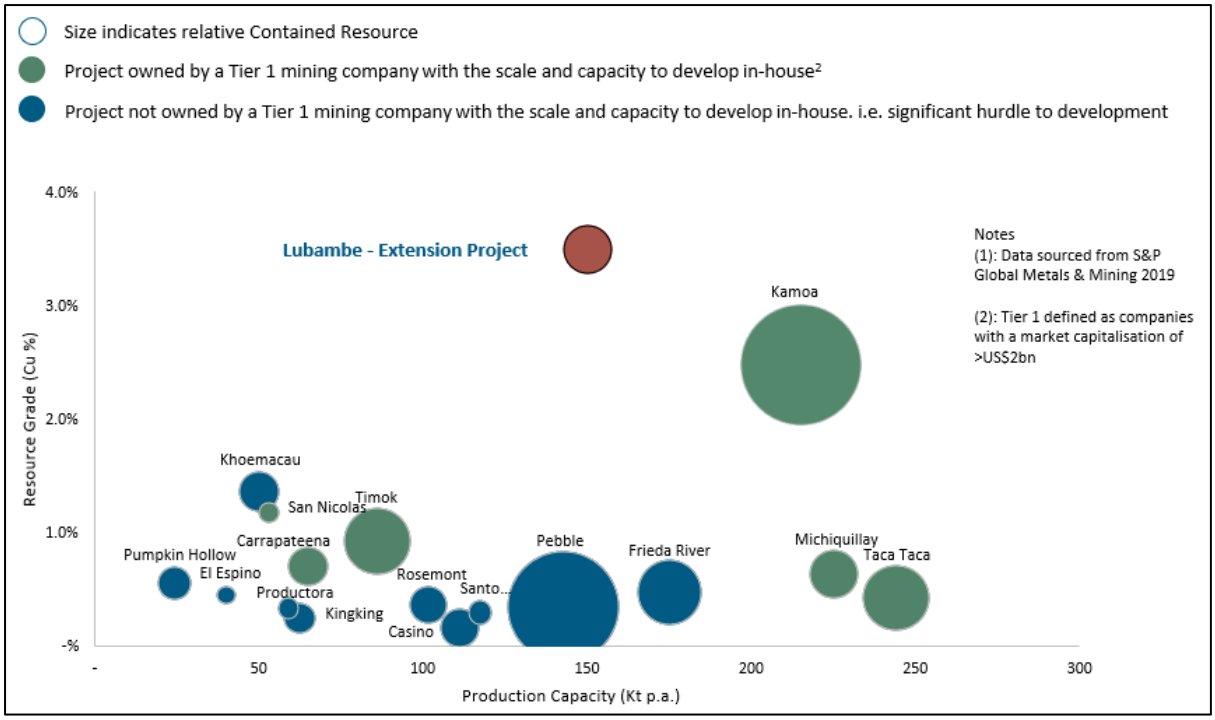

Figure 2-10: Graph showing production capacity plotted against resource grade for the Lubambe Extension Area project benchmarked in respect to other world-class undeveloped copper discoveries (Reid, 2020).

CHAPTER 3

METHODOLOGY

3.1 INTRODUCTION

Data acquisition and compilation was done during employment at Lubambe Copper Mine. As soon as the research topic was approved, a number of aspects of the methodology were incorporated into the routine work schedule at the mine. Below are some of the techniques used to achieve the set objectives of the study.

3.1.1 Surface Mapping of Outcrops

Areas of interest were selected from historical geological maps and geophysical images. Traverse lines were designed perpendicular to strikes of lithologies. Field mapping and ground truthing were carried out with the purpose of confirming lithological units and their contacts on the ground, measuring structural data and collecting samples for mineralogical and petrographic analysis. Outcrop exposures were only noted around the Konkola dome. Findings were plotted in ArcGIS and formed part of the geological illustrations and interpretation.

Other areas of geological importance outside the Lubambe license area such as the Kirilabombwe dome and Muliashi porphyry were also visited and samples collected. No field traversing and mapping was done in these areas since the property does not belong to Lubambe Copper Mine.

3.1.2 Core Logging

To ensure a good understanding of geological formations and their respective lithologies, structures, mineralisation and alteration patterns, a re-logging exercise was carried out on a number of historical boreholes as well as recent boreholes. The first step taken was to filter holes that intersected the OS1 unit from the database. The holes were then plotted using ArcGIS and Leapfrog to ascertain their spatial distribution. All re-logged holes were collared from the surface. A total of 72 drill holes were re-logged in detail, resulting in improved characterisation of stratigraphic contacts and a revision of the stratigraphic nomenclature. Re-logging was also undertaken to determine the reliability and consistency of existing data and aid correlation across the property.



Figure 3-1: Showing photos taken during the re-logging of core at Lubambe Copper Mine (a) marking lithological contacts (b) structural data collection using an IQ logger.

Core logging was carried out in manuscript on A3 size log sheets which have columns for the various codes required in the Acquire database. Four separate sheets were completed for each hole, one each

for geology, structure, mineralisation and alteration, and were filled in during separate logging runs on the same core. The sheets were later entered onto an excel sheet and then transcribed directly into the Acquire database. Re-logged and other existing drill hole data was used to compile 2D plans and sections and a 3D geological model using Leapfrog software. Outcomes were provided in free Leapfrog Viewer format and results compared with what was saved in the database.

3.1.3 Petrography

Petrography was carried out over a period of three days at the University of the Witwatersrand School of Geoscience Microscope and Imaging Laboratory. A total of eight samples were selected from different drill hole intersections in the project area. Samples for petrography were cut into half and quarter using a core cutting machine in the sample preparation laboratory at the School of Geoscience at the University of Witwatersrand. Positions to cut and polish the thin sections were drawn soon after sample cutting. Samples were then submitted to the technician to make thin polished sections. Sample lengths ranged from 5 to 15 cm.

Polished thin sections were examined using an Olympus DX41 Petrographic Microscope in transmitted light under both Plane Polarised Light (PPL) and Crossed Polarised Light (XPL) and mineralisation was examined in Reflected light mode.

3.1.4 GIS and Orebody Modelling

A GIS compilation and interpretation of all existing geological, geochemical and geophysical work within the property and surrounding properties was carried out.

Copper-bearing and related minerals like chalcocite, chalcopyrite, bornite, pyrite, copper oxides and limonite were plotted across the drilled areas to show the spatial distribution of the ore mineralogy. Structures were also superimposed to determine the structural influence against the orebody thicknesses and the grade intensities. Results were presented as ArcGIS illustrations.

All available geological and geophysical data covering the Lubambe East property and surrounding areas was used in compiling a new 2D geological interpretation map of the area. Historical data employed in this work included detailed exploration mapping (pre-1970s) and open-source data from the surrounding mine properties. Resource evaluation products for the Lubambe Mine and Lubambe Extension Area (AMEC, 2014, Subramani, 2018 and Reid, 2020) were also reviewed and compiled. This revised geology and structural interpretation was undertaken to reconcile differences between various historic maps and to extend the geological map into the adjoining mining properties. Outputs were plotted in an ArcGIS v.10.2 Map Package, Leapfrog Viewer as well as PDF and hardcopy formats.

The new map of the Lubambe property serves as a base on which to assess the subsurface mine and drill hole data, and to interpret the significance of airborne geophysical and surface geochemical anomalies.

3.1.5 Geochemical Assay Results Analysis from core

Selected and certified geochemical assay results were downloaded from the Lubambe Copper Mine database and used in the research project. Though multi-elements assay results are issued covering both major and minor elements, the focus of this research was mainly on copper-bearing minerals and associated alteration minerals. A 1% TCu assay cutoff was used to outline and define the ‘ore pick’ zone for each borehole. Assay results from drill core were composited and used to determine orebody true thickness based on hangingwall and footwall assay contacts, the copper distribution and spatial occurrence.

Since geochemical data was already available in the database, it is important to note the procedures and processes involved from core sampling to attainment of results from the laboratory. A specific sampling process was followed and routine quality control steps were undertaken as in compliance with the JORC code.

3.1.5.1 Summary of Core Handling, Preparation and Analysis Procedures

Core material obtained after drilling is transported to the Lubambe core shed for detailed logging, sample interval selection and sampling. Once the mineralised intersection is accepted according to the minimum specifications (recovery, orientation, fitted together, cleaned etc.), the core is photographed for geotechnical and reference purposes. The core is metre-marked and recoveries calculated for individual runs. Thereafter, the core is marked for splitting by diamond saw, making sure that the same side is sampled throughout the mineralised section. Broken core is pieced together and secured with masking tape. After splitting, both halves are placed in the core tray with split surfaces facing upwards and the core logged in detail. The geologist then marks the core for sampling using a china marker, taking cognisance of variations in lithology, mineralisation and alteration and utilising natural breaks as far as possible. Sample widths approximate to 0.5 m. The corresponding sample intervals and numbers are then marked on the remaining half core using enamel paint. Sampling details are captured on a standardised spreadsheet (sample no., from and to depths, dip, drilled thickness and true thickness. Sample numbers are prefixed with the borehole number and increase sequentially down the hole. Quality control samples are inserted and carefully recorded on a standardised spreadsheet. Other selected primary samples are further cut to quarter sample and split to create duplicate samples. Samples are assigned coded sample numbers, to conceal the identity of the borehole and of the control samples. The geologist then bags each sample, inserts two marked sample tickets, one of which is used during splitting at the laboratory.

Samples are then dispatched to ALS Laboratory in Ndola with a set of instructions for sample preparation and analysis. The ALS Ndola office carries out the initial sample preparation to reduce the sample size before sending the samples to ALS Chemex South Africa (Pty) Limited in Johannesburg.

Assay data once received from ALS Chemex South Africa is subjected to Quality Assurance / Quality Control (QA/QC) analysis to check for contamination, accuracy and precision during the assay analysis process. Once the batches pass the QA/QC analysis, results are formally accepted and saved into the database in both pdf and Microsoft Excel formats. Copper content results are normally indicated as percentages (%) of Total Copper (“TCu”) and Acid-soluble Copper (“ASCu”).

CHAPTER 4

RESULTS

4.1 INTRODUCTION

This chapter focuses on the results from the methodological techniques used to gather the required information or data in order to achieve this study's objectives. Techniques used include surface mapping, core logging, geological modelling, petrography, GIS plots of copper distribution maps, and geochemical assay results analysis.

4.2 SURFACE MAPPING OF OUTCROPS

The field mapping exercise carried out was not very successful in terms of generating adequate data of lithologies in the project area. Only a small portion of outcrops/hills lying on the northwestern side of the Lubambe Mine were mapped. The rest of the Lubambe license area is covered by deep regolith. Mapped units include the Kafufya Formation (sandstones, conglomerates, and arkoses) as well as the Konkola dome basement units (granites and gneisses). Mapping was extended slightly outside the license area in order to get a clearer picture of the lithologies and structural trends of units extending into the project area. Geological and geophysical signatures were verified and confirmed on the ground and interpretation was modified to suit ground confirmations. UTM Arc 1950 Zone 35 South was used as the datum and projection during field traversing and plotting of results.

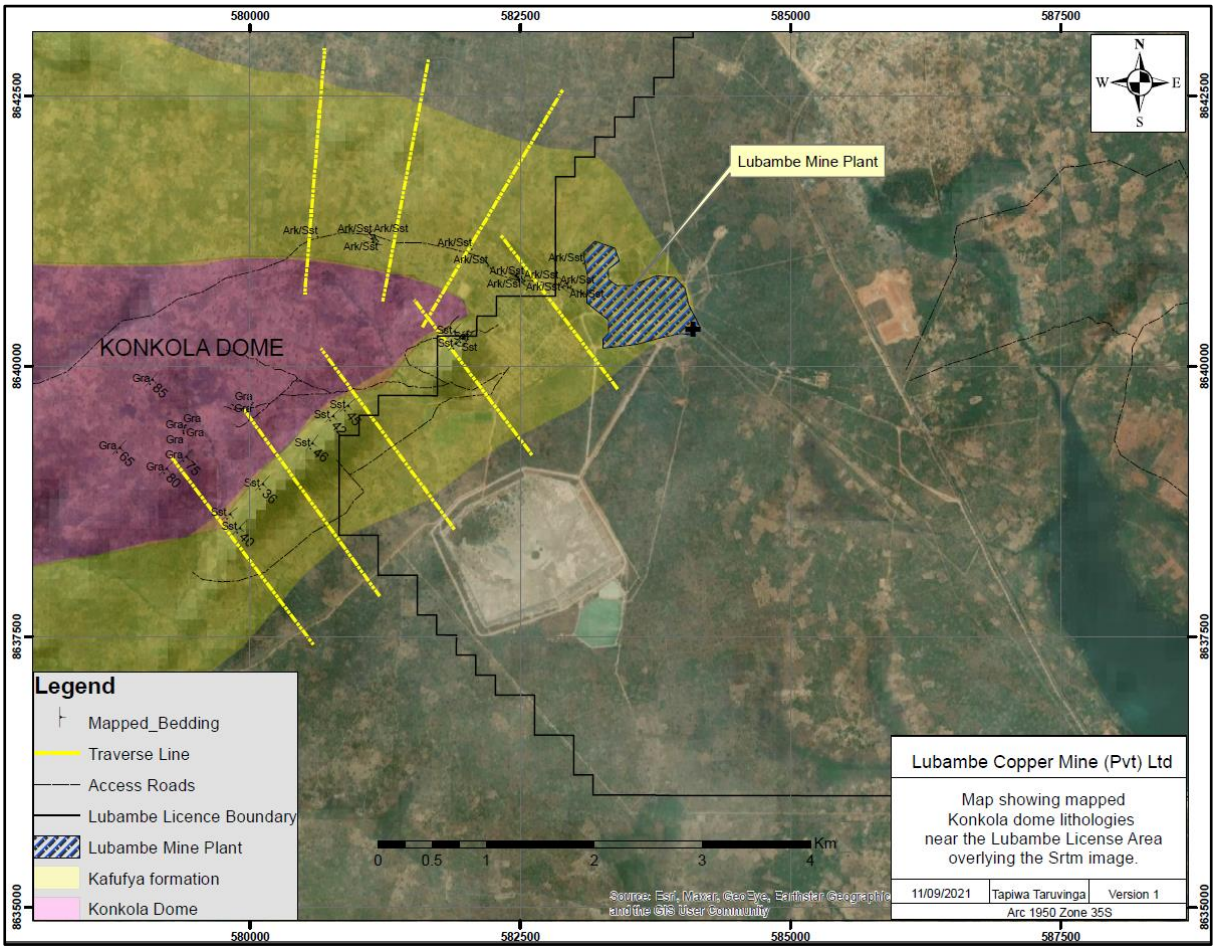

Figure 4-1: Plan showing the surface mapped portions within the Lubambe mining license area.

The ground-truthing and verification was important as it provided an overall understanding of the geology, stratigraphy and structures in the project area. Mapping results are summarised below.

4.2.1 KAFUFYA FORMATION OUTCROPS

4.2.1.1 Sandstones

The sandstones are generally bedded, greyish white with abundant visible medium grain-sized, rounded quartz and feldspar grains cemented by a white kaolinitic material (Figure 4-2). Palaeo-current cross-bedding structures are well preserved and prominent. Mineralogically, it is dominated by quartz, feldspars and some notable kaolinised bands parallel to bedding. Weathering was also observed as brown Fe-alteration rim, which could be seen a few centimetres into the specimens.

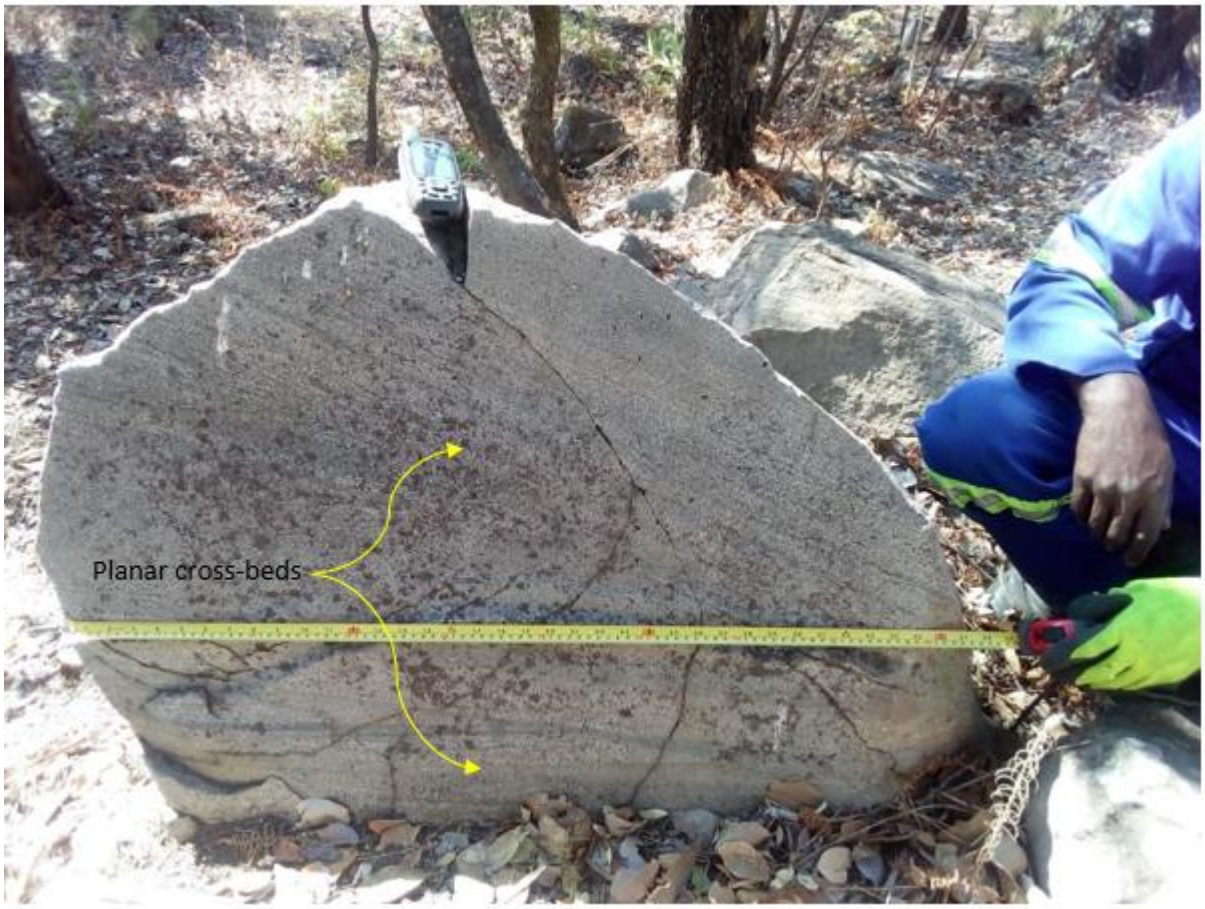

Figure 4-2: Photo showing a planar cross-bedded Kafufya Formation sandstone outcrop. Location: 581887E / 8640159N.

4.2.1.2 Arkose

Outcrops of arkoses are intensely weathered, medium grained, highly feldspathic and sericitised (Figure 4-3). Pink feldspathic clasts, vitreous quartz and pink to cream feldspathic and sericitic alteration residue is visible on outcrops and cut samples. The strike of arkose units varied depending on their position relative to the basement dome, whilst dips ranged between 05° - 55° (Figure 4-1). Dip-direction also varied depending on the location relative to the dome.

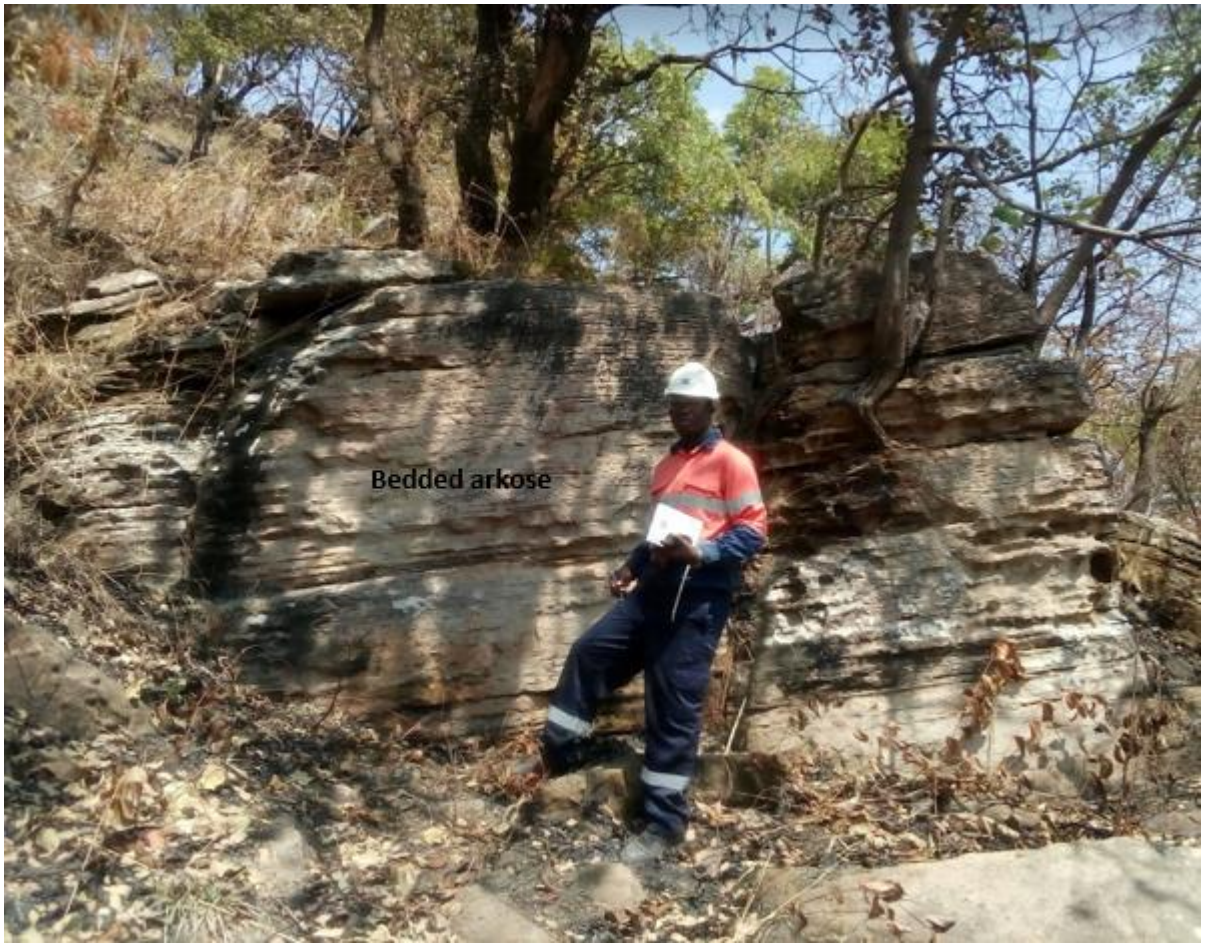

Figure 4-3: Photo showing bedded and weathered gently dipping Kafufya Formation arkose outcrop. Location: 581877E / 8640273N.

4.2.1.3 Conglomerate

The outcrops are mostly grey with some pinkish white stains on the outside with rounded quartz clasts embedded in an argillaceous matrix (Figure 4-4). Quartz is more resistant to weathering and hence a rough surface texture is developed on the outcrop (Figure 4-4). The outer parts of the rocks are hard and more resistant whilst the interior is soft, pinkish and shows intense K-feldspar and haematite alteration. The outcrops have varying strikes (202° - 298°) and dips ranging, 15° to 50° towards the northeast and southwest.



Figure 4-4: Photo showing a Kafufya Formation conglomerate outcrop undergoing selective weathering. Quartz resisting weathering formed a rough surface. Location: 579410E / 8639448N.

4.2.2 KONKOLA DOME OUTCROPS

4.2.2.1 Granites and Gneiss

The Konkola Dome granitic outcrops are pinkish, coarse grained with some reddish-brown haematite and feldspathic alteration stains on the exposed surfaces. The granite is dominated by feldspathic phenocrysts, quartz, micas, K-feldspar alteration products and sericite (Figure 4-5). The mineralogy can be summarised as feldspathic phenocrysts (50%), quartz (18%), biotite (15%), muscovite (7%), chlorite (2%) and other minerals 5%. The outcrops have NW – SE trending strikes.

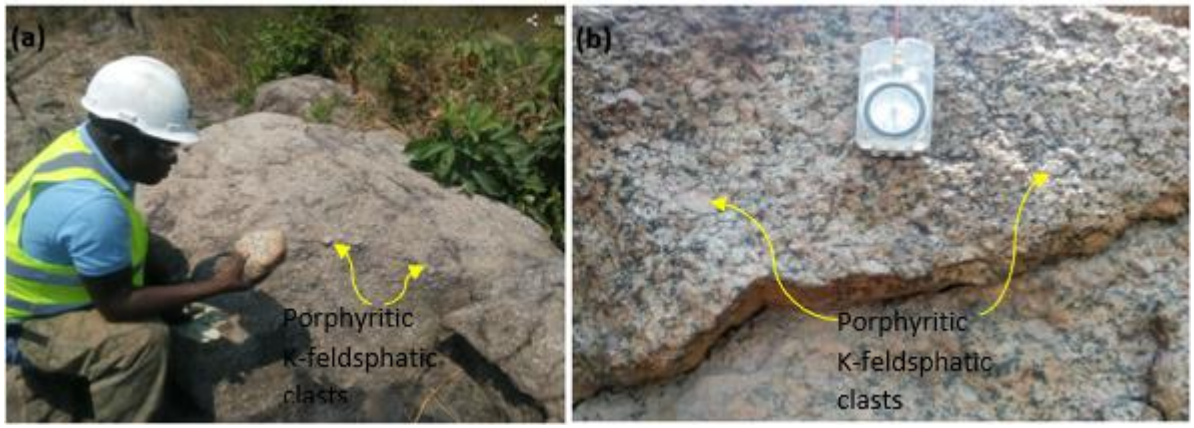

Figure 4-5: Photos showing Konkola Dome granite outcrop(a) porphyritic feldspathic clasts exposed after weathering (b) Pink subhedral coarse feldspathic phenocrysts outstanding in a granitic outcrop.

4.2.3 SUMMARY OF MAPPING RESULTS

Climatic conditions leading to poor exposure and deep weathering coupled with thick vegetation resulted in a poor expression of the geology in the project area. A few outcrops exist on the northwestern side of the Lubambe License Area (Figure 4-1), so geophysical surveys were carried out to generate sub-surface structural and lithological data and give a geological expression in areas which had no outcrops but with sufficient geophysical data for lithological extrapolation. Figure 4-6 is a geological map produced from the interpretation of geophysical data from aeromagnetic surveys by Woodhead (2006).

The portion mapped during field traversing, (Figure 4-1), correlate well with the detailed structures as observed in the aeromagnetics images. Similar major lineament trends such as the prominent NW-trending and the E-W-trending lineaments were observed (Figure 4-6).

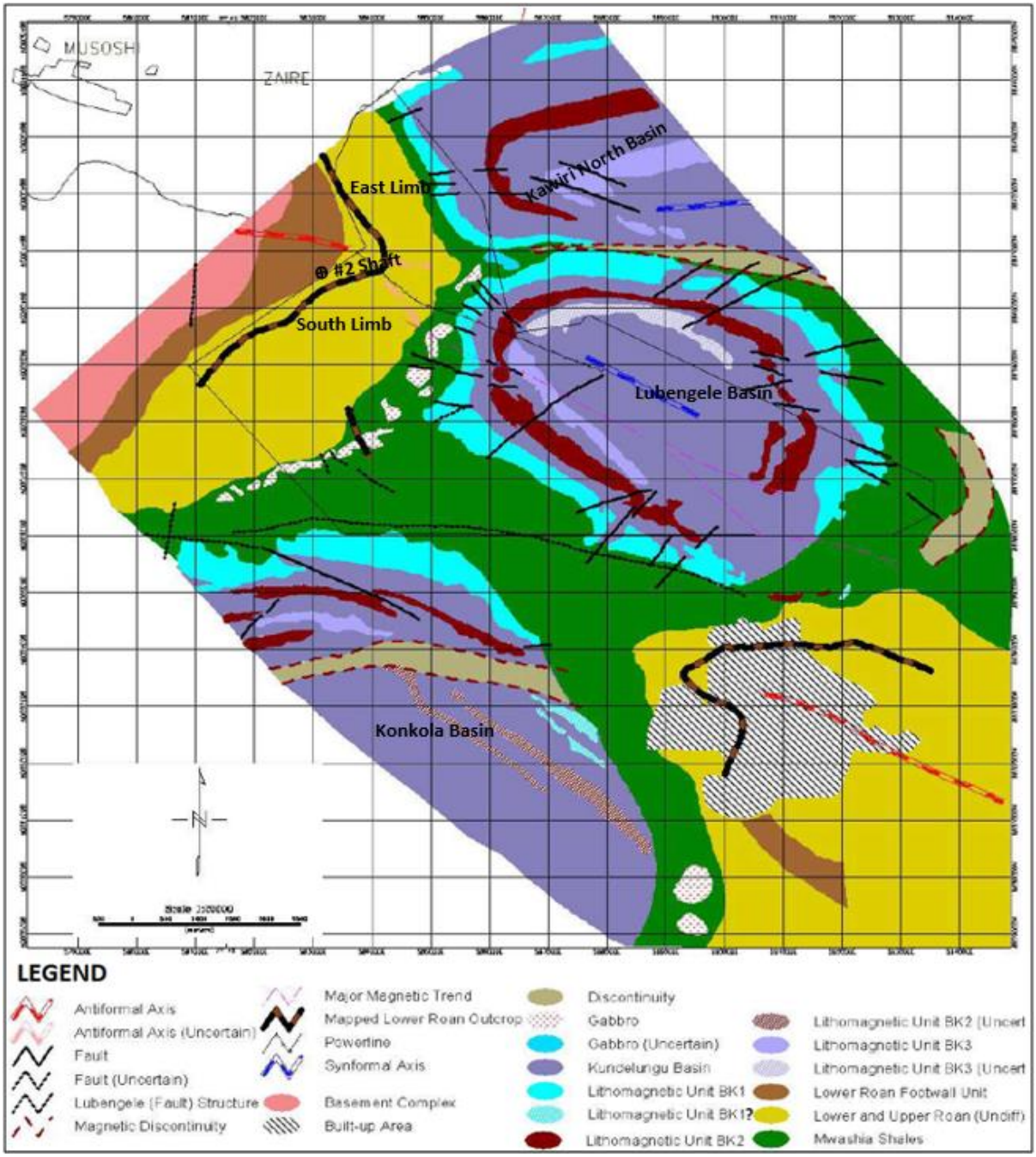

Figure 4-6: Revised geological map of the Lubambe mining license area showing the revised map based on compiled mapping and geophysical data interpretation (after Woodhead, 2006).

Data employed in the geological map (Figure 4-6), include detailed exploration mapping (pre-1970s) and open-source data from the surrounding properties. All available geological and geophysical data covering the Lubambe property and surrounding areas was used to compile an interpreted 2-D geological map of the Lubambe project area. The geological map produced provide a better understanding of sub-surface structures and lithologies so as to improve on targeting. to update historic maps and to extend the geological map into the adjacent mining properties.

4.3 CORE LOGGING

Core logging was undertaken as a way to gather primary stratigraphic information and ascertain how it correlates to mineralisation. The technique was used to determine and broaden an understanding of the Lubambe stratigraphy and also provide geological data for 3-D modelling purposes. At both local and regional scale, the analysis of the stratigraphic architecture from the geological modelling provides key focal points that can be essential in predicting grade distribution trends. A total of 72 boreholes were re-logged, spread across the entire project area. Re-logging was also used to assess and determine the reliability and consistency of stratigraphic information already in the database.

There are many stratigraphic classifications in the ZCB and mines generally formulate their own stratigraphic subdivisions based on convenient local mining terms and environment, which are not necessarily aligned to standard geological terms. Drilling carried out in the Lubambe license area intersected units from the Lower Kundelungu Group to the Lower Roan Group - Kafufya Formation (Figure 4-27). No drill hole has penetrated to the basement to date, although basement domes were confirmed during surface mapping.

The product of the core logging exercise is summarised in the subsections below and overall results presented in the form of a simplified stratigraphic log (Figure 4-27). Descriptive logging summary of units logged are sub-categorised into groups, formations and members and presented with reference to the stratigraphic log in full detail afterwards.

4.3.1 BASEMENT COMPLEX

No basement complex core was logged since no basement has been intersected from all the drilling carried out to date. All successful drill holes were terminated within the Kafufya Formation. Basement projections are currently based on literature from nearby mines and extrapolations from known basement outcrops.

4.3.2 LOWER ROAN GROUP

4.3.2.1 Kafufya Formation

In the Lubambe license area, the Kafufya Formation is the equivalent of the Mindola Clastic Formation and forms the basal unit of the Lower Roan Group. The Kafufya Formation rests unconformably over the underlying Basement Complex (Simposya and Hart, 2008). The total thickness is not yet known since its base has not yet been intersected whilst minimum thicknesses cannot be confirmed since holes were being terminated whilst in the Kafufya Formation. However, it is estimated that thicknesses extend beyond 1000 m in deepest portions (Condor Consulting 2014). Lithofacies range from pebbly conglomerate and gritty arkosic arenites to argillaceous sub-arkosic arenites which are typical alluvial fan sediments (Anglovaal Mining, 1999a). Core logging results on this formation showed that the formation consists of a fining-up cycle comprising, from base to top, the basal conglomerate and the basal arkosic and sandstone members, and a pebbly-sized conglomeratic unit just below the main OS1 orebody. Varieties of occasional beds of poorly sorted pebbly, vuggy and leached conglomerates, dominantly comprising arkoses and feldspathic sandstones were logged (Figure 4-7).

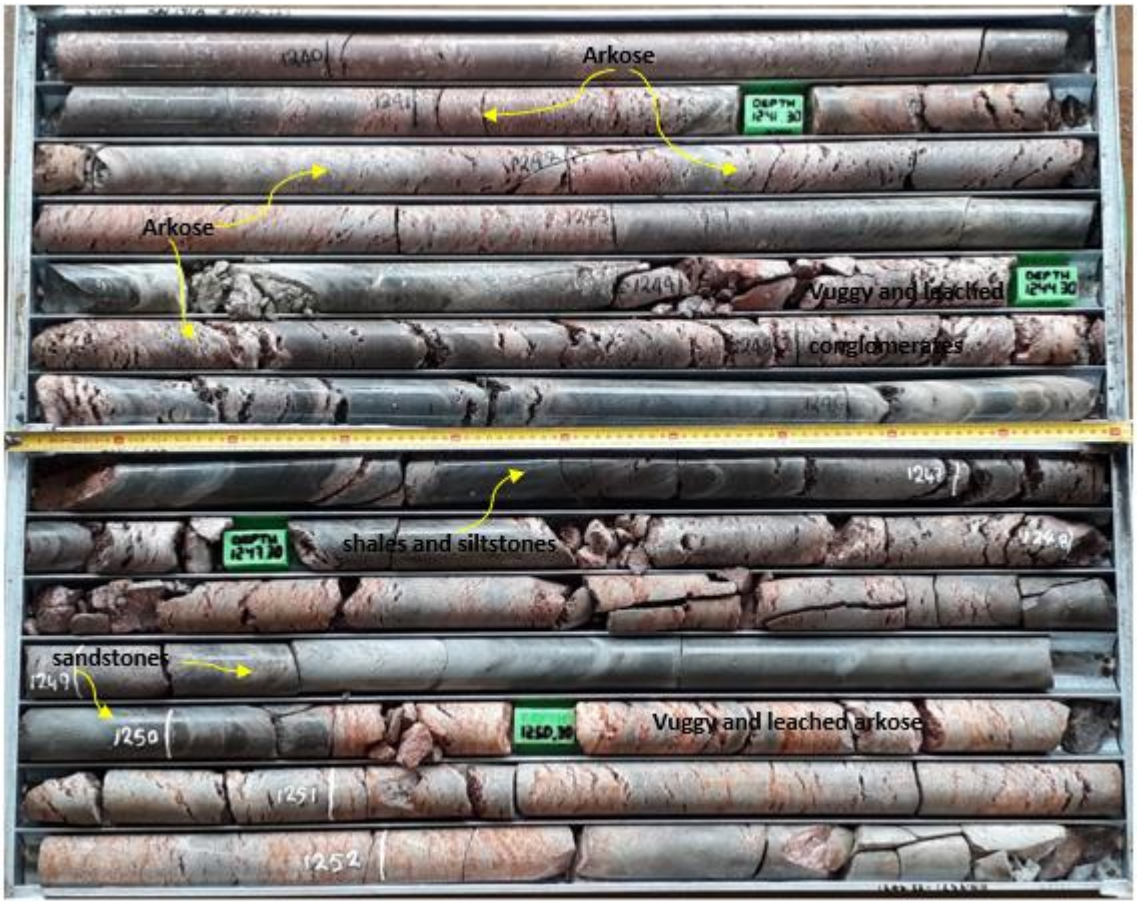

Figure 4-7: Photo showing the Kafufya Formation dominated by vuggy and leached sandstones, arkoses and conglomerates from borehole KN191A.

The topmost bed is a pink, coarse-grained, variably mineralised conglomerate with some cross-bedding layering with thicknesses ranging between 2 m to 6 m. The cross-bedding is characterised by heavy minerals laminae. Mineralised portions of the Kafufya Formation (Figure 4-8) are locally termed "Footwall Conglomerate" and make part of the Lubambe resource.

The Footwall Conglomerate shares a contact with the lowermost unit of the Nchanga Formation, called the OS1 Member, which is the main ore-bearing unit of the Lubambe deposit (Figure 4-8).

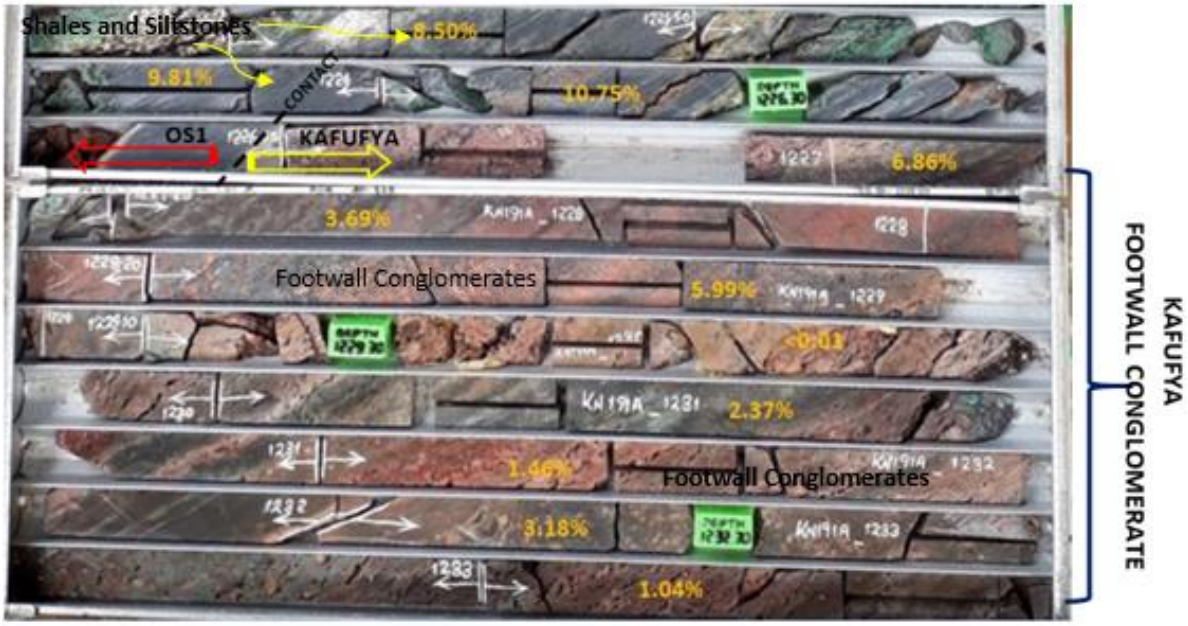

Figure 4-8: Photo showing the OS1 (shales and siltstones) / Kafufya Formation (Footwall Conglomerate) contact from borehole KN129. (Cu% grades labelled in orange).

The appearance of thin, silty intervals and an increase in argillaceous components (biotite-muscovite-chlorite) within the arkoses and conglomerates below the OS1 characterise the Footwall Conglomerate. These commonly appear as dark coloration accompanied by a bleached (pinkish-mottled) colour with copper oxides (malachite, azurite, chrysocolla). Towards the contact with OS1 there is also progressive accumulation of sulphide copper minerals. Sutton and Maynard (2005) attributed leaching of carbonate or anhydrite cements as the cause of pits and vugs in the Footwall Conglomerate that were then patched with haematite and limonite.

4.3.2.2 Nchanga Formation

The Nchanga Formation refers to the stratigraphic section comprising the Ore Shale members, that is from OS1 to OS6 (Figure 4-27). Thickness varies from 300 m to 650 m. The base of the Nchanga Formation consists of the OS1 Member which is the ore bearing member of the Lubambe deposits.

Ore Shale 1 Member (OS1)

The Ore Shale 1 (OS1) Member ranges 2 m to 18 m in thickness, and comprises a weakly metamorphosed, laminated, grey shale / siltstone unit with disseminated, blebby and vein-bound, hypogene and supergene copper minerals. The upper parts mostly consist of millimetre- to centimetre-sized, ellipsoidal nodules replaced by carbonates (mainly calcite and dolomite), quartz, K-feldspar and various ore minerals. Sutton and Maynard (2005) interpreted such nodules as being a result of alteration products of early diagenetic processes. The basal and upper contacts of the OS1 Member can be sharp or locally transitional over several metres and arkosic beds can occur throughout the unit making precise delineation difficult. Traditionally, the upper contact was defined

lithologically by the first appearance of arkose even without any copper mineralisation but for easy resource calculations and grade modelling, the presence of copper minerals has sometimes been used to define this contact. This has resulted in terminologies like “assay contact” and “lithological contact” being used to define and clarify the nature and position of the contact. In some instances, the assay and lithological contact coincide, as seen in Figure 4-9.



Figure 4-9: Photo showing mineralised OS1 unit from borehole KN191A with upper assay and lithological contact coinciding. (Cu% grades labelled in orange).

Very fine-grained Cu-sulphides are disseminated in the siltstone and occur as slightly coarser grains in thin lenticles along bedding planes and fractures. They are usually associated with red-brown and yellowish limonite staining or brownish haematite stains. There is a tendency for the limonite staining occurring at the bottom of the mineralised section. Bleaching of the siltstone is common in the Extension Area. Figure 4-10a, b and c, shows some mineralised core pieces from the OS1 Member.



Figure 4-10: Photos showing mineralised core samples in OS1 Member (a) Massive chalcocite mineralisation from borehole KN192; (b) malachite filling vugs in borehole KN44; (c) blebby and bedding-parallel chalcocite from borehole KN101B.

Ore Shale 2 to Ore Shale 6 Members (OS2 – OS6)

The OS2 – OS6 Members are characterised by a cyclical, upward-coarsening succession of units which includes shales/siltstones, sandstones and arkoses. Condor Consulting (2014) interprets it as a reflection of a prograding, fluvio-deltaic environment on the basis of the patterns displayed during sediment accumulation. The patterns are pronounced to mirror underlying basin configurations as a result of continued slow subsidence (Condor Consulting, 2014).

From the core logging carried out, the OS2 Member lies above the OS1 Member with thicknesses ranging between 10 m to 150 m (drilled thickness). It consists of a relatively thickly-bedded, greyish to pale pink, mottled, arkosic arenite with prominent, layer-parallel dissolution vugs due to anhydrite dissolution. The OS2 Member is locally termed the 'Porous Sandstone'. The upper part is mostly coarser-grained and dominantly arkosic in composition and mostly associated with cyclic sequences of interbedded sandstones and arkose units.

The OS2 is generally overlain by a pale-pink K-feldspar and silica-rich, recrystallised, arkosic unit locally termed the 'Lower Pink Arkose Marker' (Figure 4-11), which marks the base of the OS3 Member. The pink arkose marker generally contains random quartz veins along with dark alteration spots composed of iron-carbonate minerals. Generally, the OS3 Member is a variable (mixed), cyclical unit of thinly-bedded, dark-grey, argillaceous siltstones and gritty to granular, cream to pink, K-feldspar dominant arenites. This unit varies considerably in thickness from 5 m to 230 m (drilled thickness).



Figure 4-11: Photo showing OS2 Member (greyish interbedded arkose and sandstones) and OS3 Member (Lower Pink Arkose Marker) from borehole KN190.

In between the Pink Arkose Markers lies a unit locally known as the "Arkose with Shale Member" which is usually variable in terms of mineralogy, grain-size and thickness (Figure 4-11). The Arkose with Shale Member is dominated by K-feldspars, quartz and mica minerals and characterised by variable cyclic sequences of arkosic grits and feldspathic sandstones interbedded on the centimetre to decimetre scale with rare shaly beds. Two to three distinctive units of strongly-feldspathic and siliceous, pink arkosic units are commonly present with each potentially representing the top of an upward-coarsening cycle. All are identical in character to the Lower Pink Arkose. The uppermost unit is generally the well developed and is locally termed the 'Upper Pink Arkose Marker', and marks the beginning of the OS4 Member.

Overlying the OS3 Member is the OS4 Member with drilled thickness ranges from 80 m to 310 m. This unit is characterised by an abrupt change from an arkosic-dominant unit to a well-banded interbedded, argillaceous siltstone (commonly dolomitic) with gritty arkosic beds. Despite having similar lithofacies with the underlying OS3 unit, the OS4 is distinguished by a marked increase in dark, laminated shales/siltstones, conspicuous layering, and the prevalence of soft-sediment deformation structures (e.g., slump folds, contorted beds, and clastic dikes). This unit is commonly thick and generally uniform over several metres and is locally referred to as the "Shale with Arkose", and mostly characterised by the dominance of fine-grained shales / siltstone (Figure 4-12).



Figure 4-12: Photo showing interbedded sequences of the OS4 Member (Shale with Arkose) from borehole KN120.

Overlying the OS4 Member is an interbedded and thinly-laminated, dolomitic, shaly-siltstone unit called the OS5 Member commonly characterised by a fining-upward trend at a gross scale. The unit has drilled thickness ranging from 2 m to 50 m and has been noted as the second major redox boundary in the Lubambe Area (Reid, 2020). Due to extensive weathering, dark brown to pale brown, bleached, soft, friable and fragmented siltstones and shales are the essential characteristics of the OS5 bottom unit. Soft sediment deformation can be seen in better preserved cores. Dolomites up to a few metres thick are common at the base and the top of the OS5 Member. The dolomites are fine-grained, crystalline, pale grey and distinctively striped with thin wavy laminae of shale reflecting evidence of folding and partial brecciation (Figure 4-13). Above these is commonly a thin, fine-grained, gritty and muddy shaly-siltstone, which is dark brown or dark grey with a strong haematite presence, malachite, chrysocolla and manganese stains. In some drill holes, traces of pyrite and chalcopyrite are observed locally developed at the base along with scapolite and carbonate ± quartz pseudomorphs after prismatic evaporite minerals.

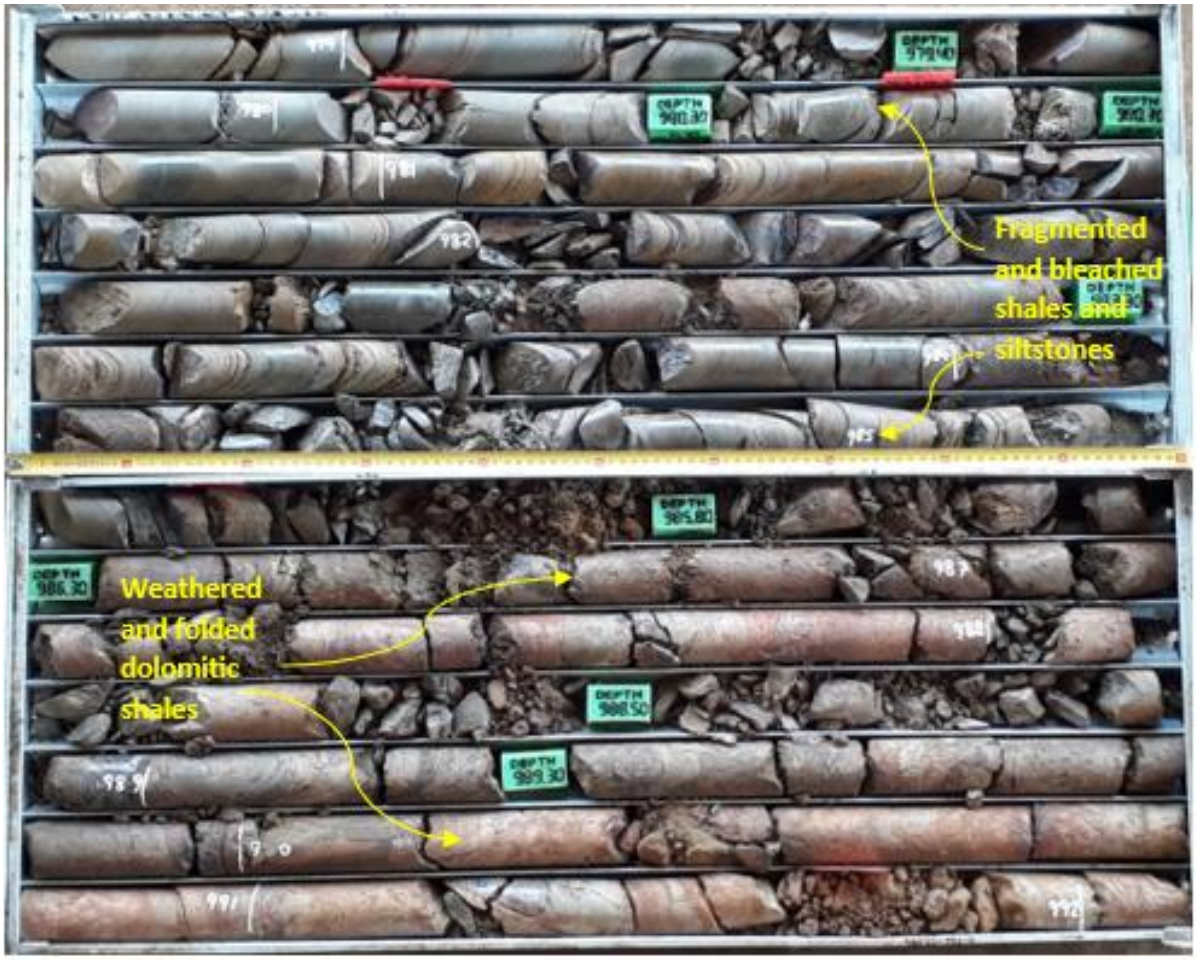

Figure 4-13: Photo showing Dolomitic Shale unit (at the bottom) with folded and slump structures grading to shales within the OS5 Member of borehole KN191A.

Previously, the OS5 Member was regarded as uneconomic but the 2019 – 2020 drilling on the eastern side of the Lubambe license area has revealed some economic grades above the current mining cutoff grade of 1% TCu with true thicknesses ranging from 1 m to 8 m within the OS5 Member. It is commonly mineralised with fine-grained chalcopyrite and traces of pyrite mostly occurring at the base of the unit along with scapolite and carbonate ± quartz pseudomorphs after prismatic evaporitic minerals. Core samples from holes drilled on the eastern side of the project area show strong bornite mineralisation along bedding planes and replacement of bornite blebs by chalcopyrite within OS5 shales and dolomites (Figure 4-14).

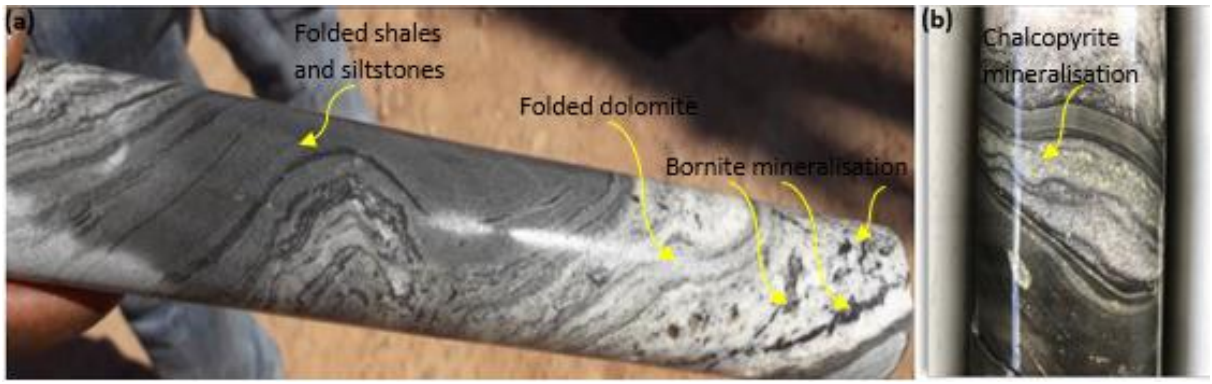

Figure 4-14: Photos showing mineralised core samples from the OS5 Member of borehole KN194D1 (a) strong blebby bornite mineralisation along folded bedding in shales and blebby chalcopyrite disseminations in dolomite; (b) chalcopyrite mineralisation parallel to bedding and lamination planes in shales.

Overlying the OS5 Member is the OS6 Member, which marks the top of the Nchanga Formation. The OS5-OS6 Members contact is generally fragmented, friable and decomposed (yellow-brown, limonitic where oxidized and leached), with indications of a progressive return to arkosic dominant compositions (OS6 Member). The member has varying drilled thicknesses from 3 m to 25 m.

4.3.2.3 Shale with Grit Formation

The Shale with Grit Formation marks the upper limit of both the Kitwe formation and the Lower Roan Group according to the revised Lubambe core logging sequence nomenclature (Figure 4-27). It comprises two members, that is, the Konkola Member and the Shale with Grit Member.

Konkola Member

The Konkola Member conglomerate is a pink pebbly arkosic conglomerate with drilled thicknesses ranging 5 to 25 m. The unit is quite distinct and very widespread, representing a significant basin-ward shift in facies according to Arthurs et al. (2009). The Konkola Member conglomerate has a sharp erosional contact base with the underlying OS6 unit of the Nchanga Formation. The unit was descriptively and consistently logged as pink, coarse-grained, thickly-bedded clast-supported and poorly sorted conglomerate with sub-rounded and sub-angular quartzo-felspathic clasts and white feldspathic alteration rims in most of the drill holes that intersected it. Dark heavy mineral laminae parallel to bedding are very prominent throughout the unit. K-feldspar clasts have average sizes ranging from 1 mm to a maximum of 40 mm, set in a gritty matrix (Figure 4-15).

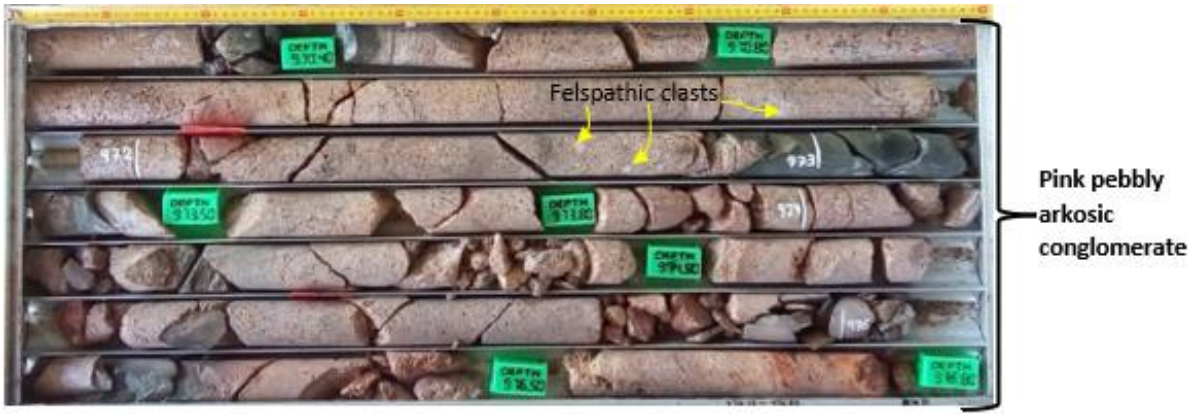

Figure 4-15: Photo showing the bedded pebbly arkosic conglomerate of the Konkola Member in borehole KN120.

The conglomerate grades upwards into a thick sequence of thinly interbedded arkose, shales, siltstone and grit cycles, commonly known as the Shale with Grit Member ("SWG").

Shale with Grit Member (SWG)

The overlying SWG generally consists of a uniform succession of approximately 80 to 300 m of grey-green, interbedded mudstone, gritty siltstone and subordinate medium- to coarse-grained arkose. It is characterised by distinct alternation of fining-upward cycles of dark grey shales and siltstones with gritty bands, ripple cross-laminated arkoses at the bottom (Figure 4-16). The cyclic sequences have thicknesses ranging from 10 cm towards the base of the member to about 1 m at the top.

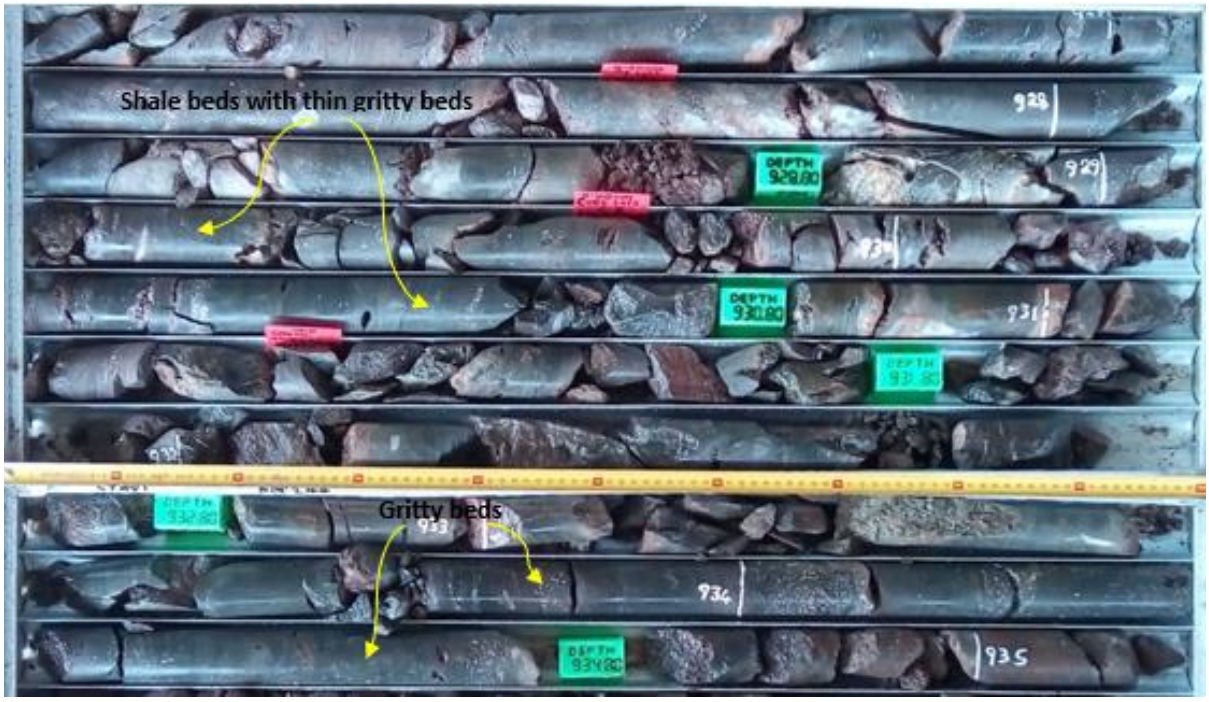

Figure 4-16: Photo showing the Shale with Grit (SWG) Member in borehole KN190. Gritty beds thicknesses increasing with depth.

Figure 4-16 shows matrix-supported gritty bands comprising granules of quartz and feldspar in mudstones. Common characteristics include micro-folds and micro-faults, disrupted lamellae, sand-filled mud cracks and pinch-and-swell beds with disseminated specular haematite. Condor Consulting (2014) interpreted such features as indicating an intermittently emergent, supratidal to intertidal, evaporitic, mudflat environment. Wavy bedding and ripple laminations are very common within the unit.

4.3.3 UPPER ROAN GROUP

4.3.3.1 Chingola Dolomite (CHD) Formation

The Chingola Dolomite Formation is an interbedded sequence comprising greenish argillaceous shales/siltstones capped by brick-red silicified dolomites and massive dolomitic siltstones with a graded contact with the underlying SWG Member. Mwelwa (2020) articulates that the transitional contact between the SWG and the CHD represents a gradual flooding of a gentle, shoaling-up cycle of mudflat to evaporitic-carbonate platform ultimately producing a layer-cake stratigraphy with lateral persistency. Fibrous dolomite-quartz bands and vuggy to brecciated textures indicate the former presence of massive anhydrite and other evaporite minerals (Anglovaal Mining, 1999a).

Core logging results noted thick sequences of pale greenish-grey argillaceous shales and dolomitic siltstones with gritty spots (Figure 4-17) interbedded with fine grained, red, massive, vuggy and highly silicified dolomites (Figure 4-18). Drilled thicknesses vary from 100 m to 350 m. The silicified dolomites are commonly haematite-stained to an intense brick-red with abundant cavities filled with haematite (Figure 4-18). Cavities have various sizes ranging from centimetre to decimetre scale. Carbonate dissolution and haematisation commonly results in prominent iron staining and cavitation (Binda and Porada, 1995). Up-section, dolomitic beds become thicker and more dominant.

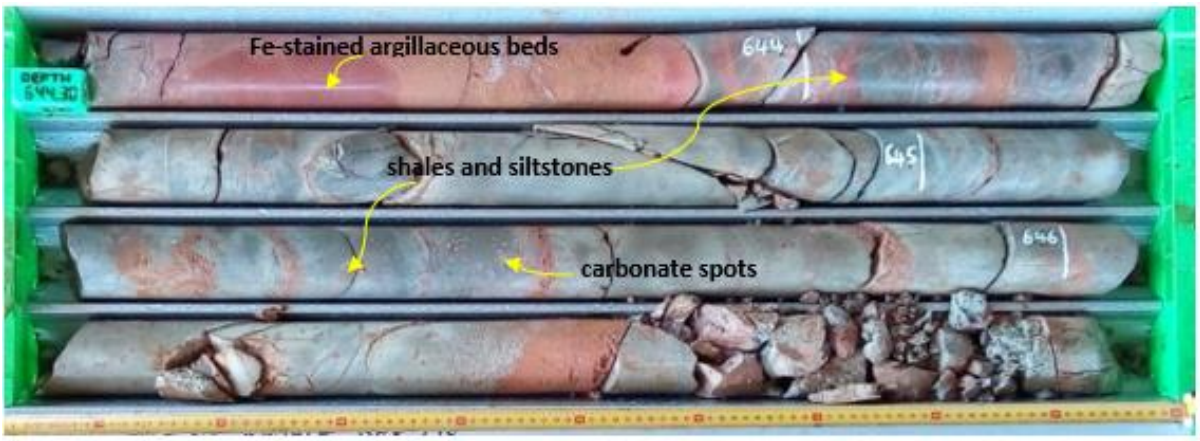

Figure 4-17: Photo showing greenish argillaceous shales and siltstones with white gritty spots of the Chingola Dolomite Formation in borehole KN191A.



Figure 4-18: Photo showing the highly oxidised and silicified dolomites of the Chingola Dolomite Formation in borehole KN191A.

4.3.3.2 The Breccia Formation

Overlying the CHD Formation is The Breccia Formation which marks the beginning of the Mwashia Formation but still categorised under the Upper Roan Group. Thickness varies from 50 m to 250 m. During core logging, two types of breccias were noted, the "stockwork/crackled breccia and "conglomeratic breccia."

The crackled breccia is clast supported, with broken and veined angular and sub-angular dolomitic clasts of sizes ranging from 1 to 50 mm cemented by carbonates, chlorite, ankerite, talc and phlogopite (Figure 4-19). The colour is dominantly creamish white with grey to black vein fillings.

The conglomeratic breccia formation consists of unsorted, matrix-supported, heterogeneous assemblage of laterally variable polylithic, sub-rounded to rounded, conglomeratic clasts of siltstone and dolomite set in a matrix with varying amounts of dolomite, magnesite, anhydrite, quartz, albite, chlorite and talc (± K-feldspar, sericite and phlogopite) (Figure 4-19). The conglomeratic breccia is locally termed as a "collapsed breccia" and typically lacks shear or foliation fabric. The colour ranges from grey through grey-green, brown to red.

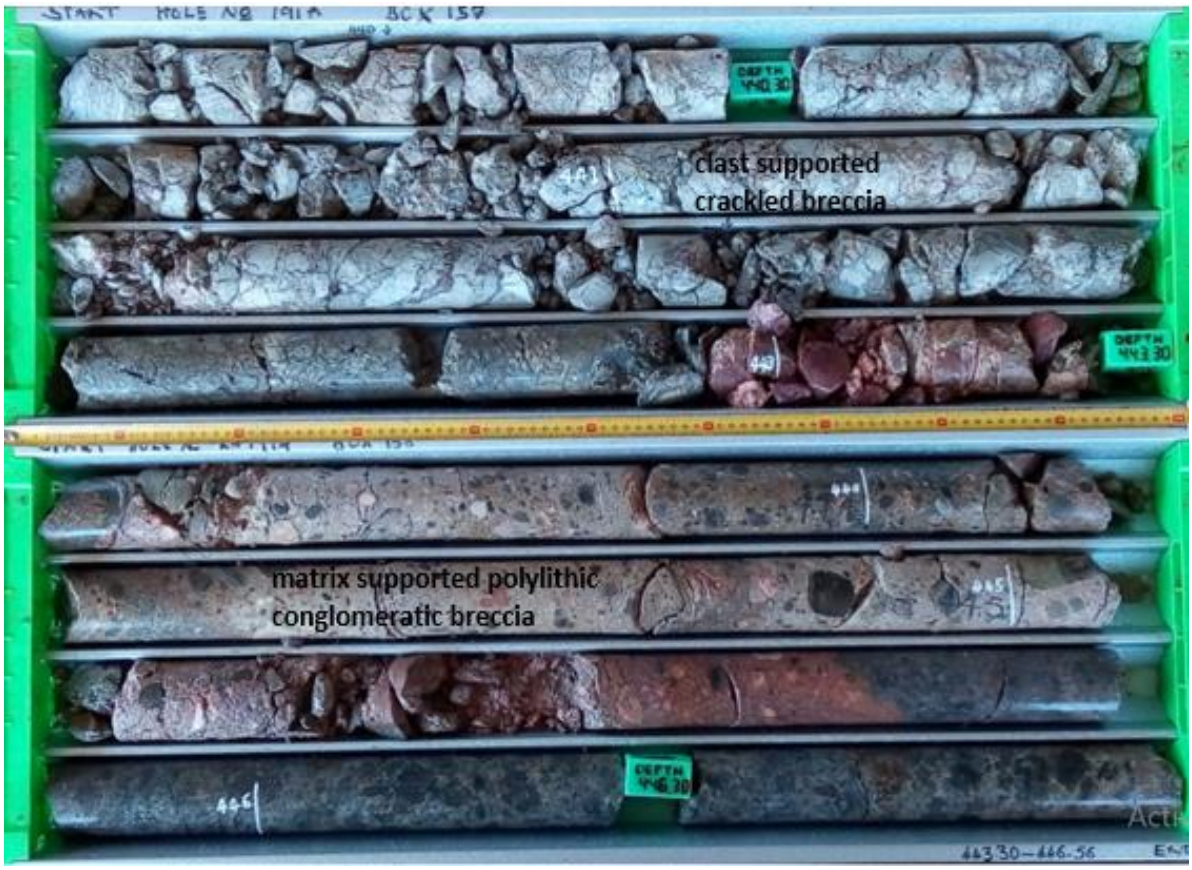

Figure 4-19: Photo showing a clast supported crackled breccia and matrix supported polylithic conglomeratic breccia in borehole KN191A.

The Breccia Formation comprises anhydrite-bearing dolomite and highly-altered medium to coarse grained meta-gabbros, locally termed 'amphibolite sills'. The unit was consistently intersected in all holes over the entire Lubambe License Area, hence, concordant and recognized as a sill. Drilled thicknesses vary from 5 m 45 m. Mineralogically, it is dominated by pyroxenes, hornblendes, chlorite, plagioclase, biotite and epidote. The topmost contacts of amphibolite dykes are generally magnetite-rich, commonly banded, brecciated and veined whilst having secondary chlorite, silica and/or albite alteration (mostly accompanied by scapolite) (Figure 4-20). It is considered that the sills intruded and

were emplaced during thrusting and assimilated with country rock (dolomitic siltstone), in the presence of fluidised dolomitic breccias thus no chilled margins or skarnification is observed (Rainaud et al, 2005).



Figure 4-20: Photo showing brecciated meta-gabbros (amphibolite dyke) in borehole KN116.

4.3.4 MWASHIA GROUP

4.3.4.1 Mwashia Formation

Overlying the Roan Group are a series of interbedded dolomites, dolomitic siltstones and shales of the Mwashia Formation which are predominantly shallow marine in origin (Broughton, 2014). Bull et al. (2011) note that the base of the Mwashia Formation reflects a decollement surface that was likely reactivated during basin inversion and subsequent sinistral translation. The Mwashia Formation also represents a basin flooding event which is taken to indicate hydrological re-connection of the Roan basin after a prolonged period of intermittent isolation and evaporite accumulation that formed the Upper Roan sequences (Broughton, 2014; Bull et al., 2011). Mwashia Formation shales can be sub-categorised into smaller units comprising laminated and carbonaceous siltstone-shale, dolomitic siltstones, laminated dolomite, a unit of anhydrite-rich, scapolite rich shales/mudstones as well as crackled shales/mudstones with carbonate secretion veins. However, this brings about subjectivity and lack of consistency so only major and prominent units were sub-categorised during logging.

Core logging results showed thickness variations ranging from 400m to 780 m. The Mwashia Formation is largely composed of grey, laminated shales and thin white dolomitic siltstones (Figure 4-21). Biotite porphyroblasts are common within certain beds, reaching 3 mm in size and overgrowing the lamination and contain cores of magnetite. Disseminated pyrite (± pyrrhotite) of approximately 1 – 3 mm size are very common in most parts of the formation. Mineral compositions range from weakly carbonaceous shales to dolomitic siltstones with various forms of alteration depending on stratigraphic position.

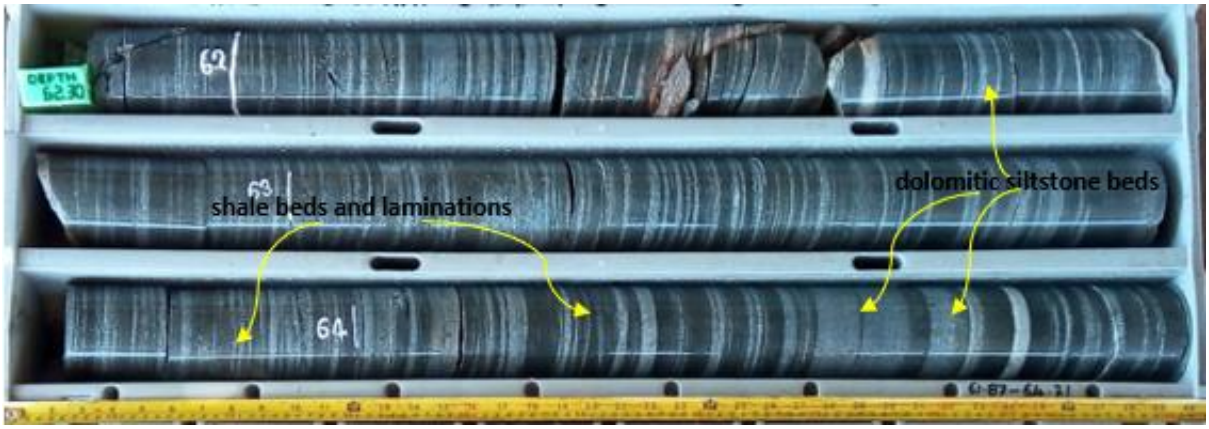

Figure 4-21: Photo showing laminated / banded shales with carbonate veins parallel to bedding and biotite porphyroblasts within the Mwashia Formation in borehole KN110.

The base of the succession is generally more dolomitic in composition, and it mostly comprises dolomitic siltstones with phlogopite disseminations (Figure 4-22). This unit commonly shows some degree of veining or brecciation accompanied by a salmon pink, albite-carbonate alteration.

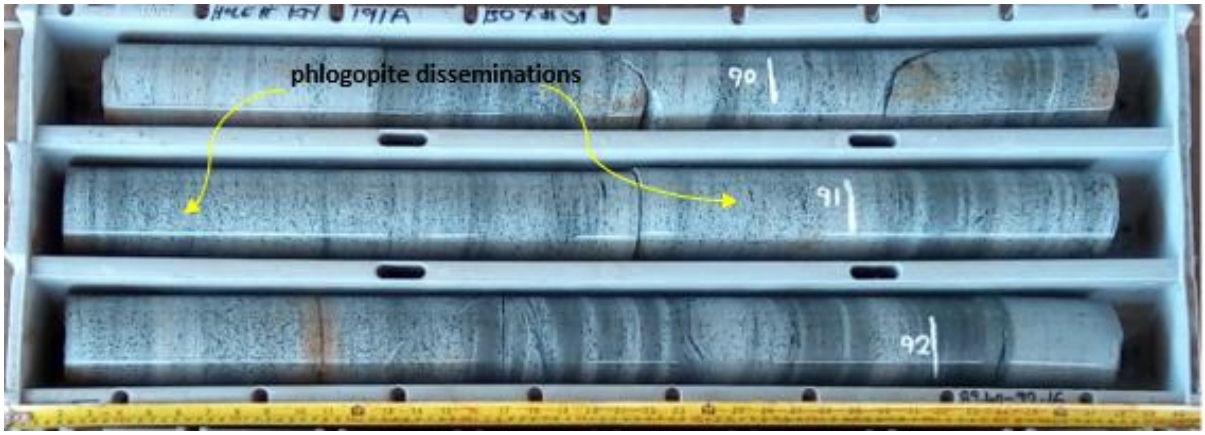

Figure 4-22: Photo showing dolomitic siltstones unit with phlogopite spots within the Mwashia Formation in borehole KN191A.

Scapolite-bearing shales and siltstones also make part of the Mwashia formations (Figure 4-23) and normally occur in association with albite. Arthurs et al. (2009), notes that the presence of scapolite suggests locally high concentrations of Cl, Na, CO_2 and SO_3 during metamorphism with a possible source for these components being the dissolution of evaporites that formed during sedimentation.

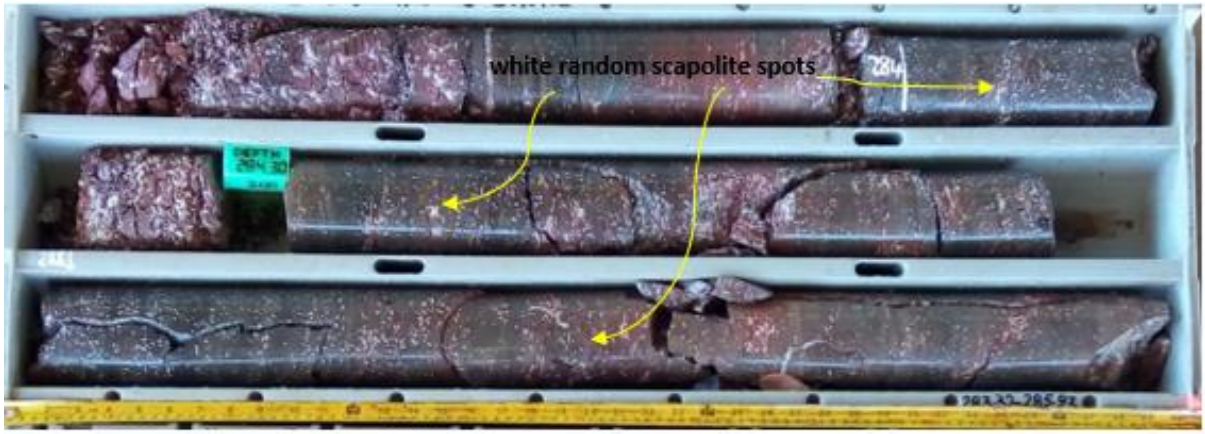

Figure 4-23: Photo showing crackled mudstones and shales with scapolite spots, borehole KN190.

White scapolite spots transition to irregular quartz-carbonate secretion veins (Figure 4-24). A deepening-upward trend is evidenced by an increase in thinly bedded, well-laminated, dark-grey (carbonaceous) siltstone and shale.

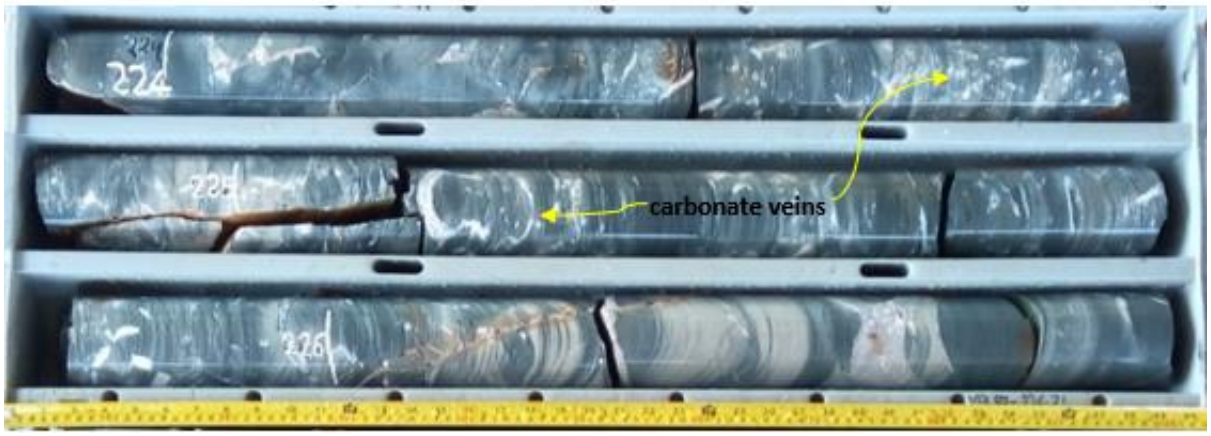

Figure 4-24: Photo showing shales with irregular carbonate veins, borehole KN121B.

Magnetic susceptibility measurements carried out indicate that magnetite is largely restricted to some of the Mwashia units.

4.3.5 LOWER KUNDELUNGU GROUP

The Kundelungu Group can be separated into two units, the Lower (contains the basal Grand Conglomerate and Kakontwe Formations) and the Upper (basal Petite Conglomerate). Both units unconformably overlie the Mwashia Formation within the cores of the major synclines within the CACB (Bull et at, 2011; Sillitoe et al., 2017). The project area has to date noted three units of the Lower Kundelungu Group, which are, are the Grand Conglomerate Formation, the Kakontwe Formation and some of the Lower Kundelungu Member shales and dolomites (Figure 4-27).

4.3.5.1 Grand Conglomerate Formation

The Grand Conglomerate Formation of the Lower Kundelungu Group marks the base of the Nguba Formation (Chilekwa, 2015; Wendorff and Key, 2009) (Figure 4-27). The formation was intersected in three boreholes in the project area. Thickness varies from 15 m to 65 m. The Grand Conglomerate Formation mainly comprises of diamictites, whilst shales and mudstones dominate the matrix. Diamictites were mostly comprising rounded and sub-rounded stretched granules to pebble-sized polylithic clasts of varying sizes, ranging from 1 to 10 cm in a shaly/muddy matrix which mainly comprises dolomitic and calcitic carbonates, phlogopite, feldspars, muscovite and silica clasts, (Figure 4-25). Also noted is a yellow and red alteration colour on some of the core surfaces due to iron alteration.

The foliation is typically continuous and pervasive throughout the rock unit defined by stretched clasts and oriented biotite grains. Quartz and feldspar commonly occur along foliation whilst the dolomitic matrix is light grey and occurring more as layers parallel to biotite foliation.

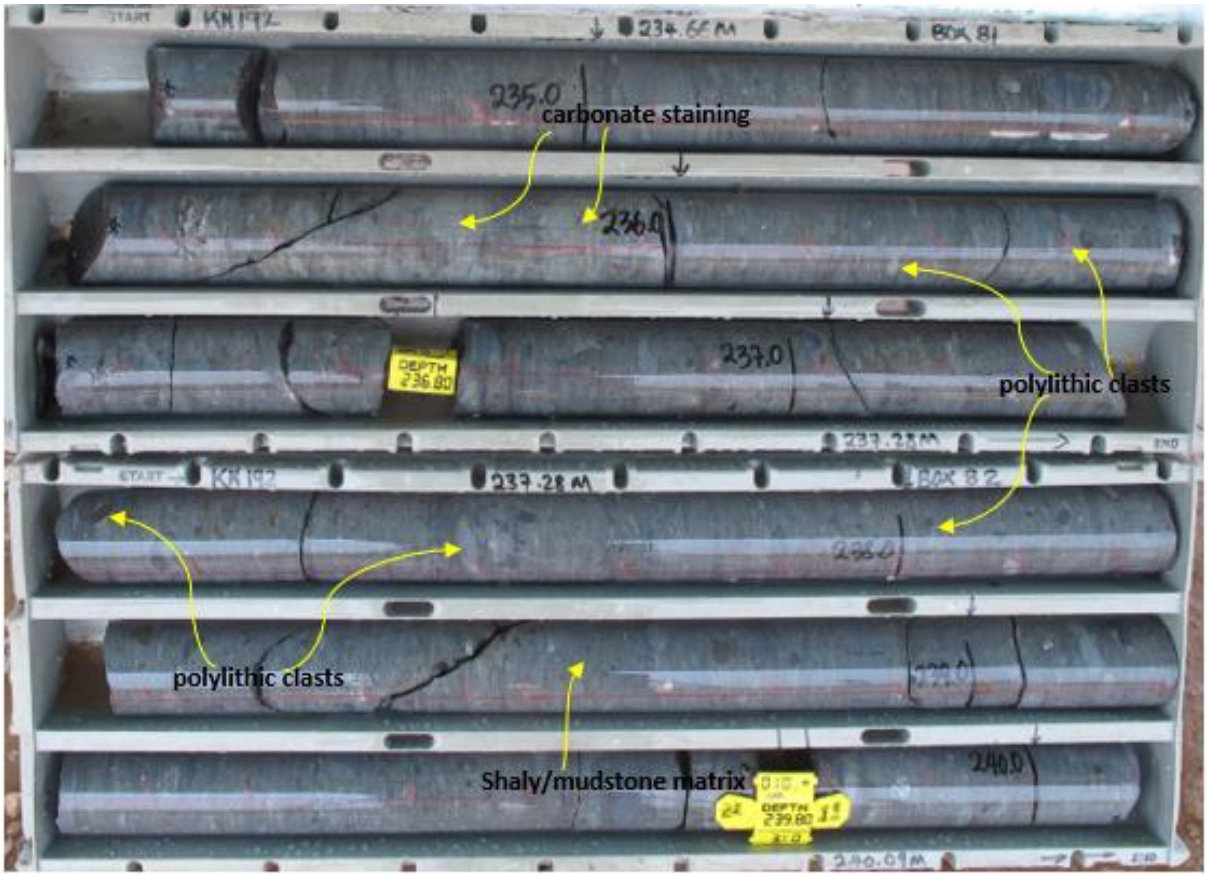

Figure 4-25: Photo showing the Grand Conglomerate Formation with some polylithic clasts in a shaly matrix, borehole KN192.

4.3.5.2 Kakontwe Formation

The Kakontwe Limestone Formation overlies the glacio-marine Grand Conglomerate (Wendorff and Key, 2009) and has drilled thicknesses varying from 20 m to 80 m. It is perceived to have formed from a low-topography graded shelf during and immediately post-glacial period (Master and Wendorff, 2011). The Limestone Member is commonly a fine-grained creamish to greyish limestone (Figure 4-26). It formed as a marginal marine stratum.

Core logging results showed the Limestone Member as a greyish to creamish white, fine grained, thickly bedded to massive, highly silicified and cherty limestones rich in calcite and carbonates and fizzing strongly in hydrochloric acid. The Kakontwe Formation is characterised by huge cavities which resulted in zero core recoveries and open fractures in some logged sections.

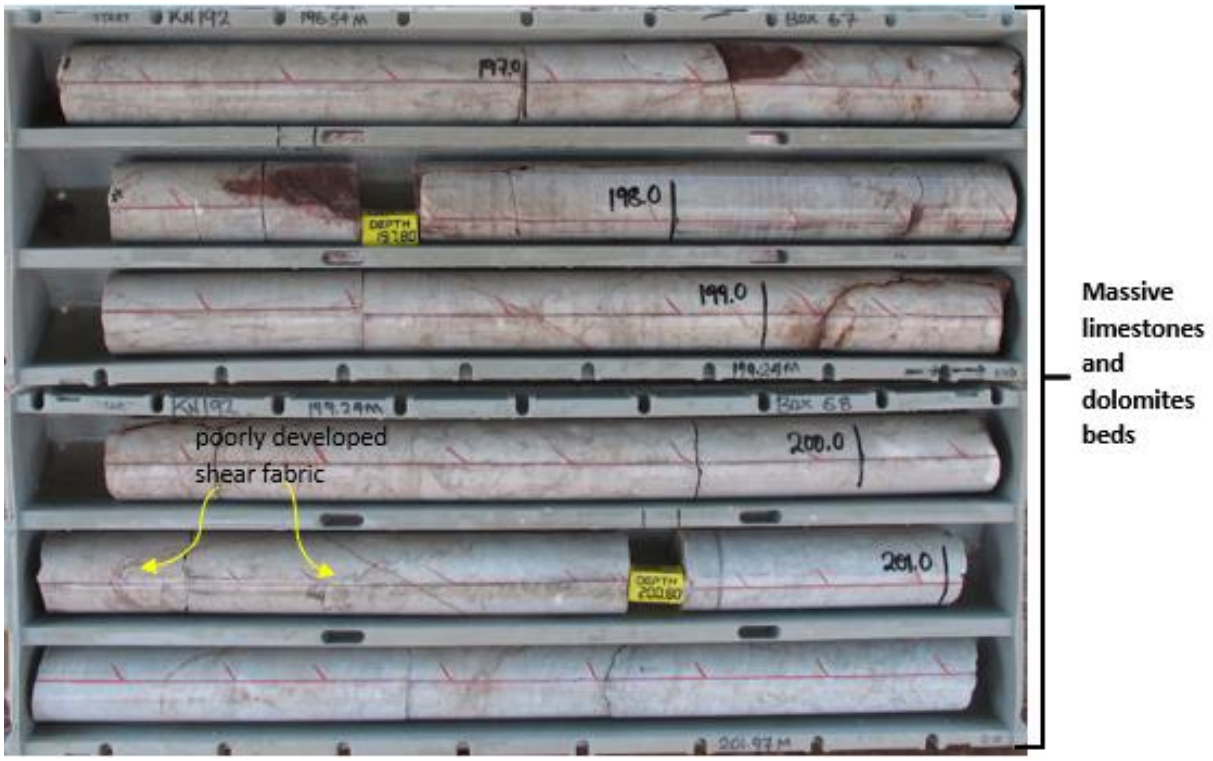

Figure 4-26: Photo showing the Kakontwe Formation from borehole KN192 comprising calcite rich limestones and dolomites.

4.3.5.3 Shales and Dolomites of the Lower Kundelungu Group

The shales and dolomites of the Lower Kundelungu Group are currently the topmost members intersected in the project area and occur at the top of the revised Lubambe stratigraphic log (Figure 4-27). The units were intersected in two recently drilled boreholes (drilled between 2019 and 2020) on the eastern side of the project area across the LTSF. Drilled thicknesses extend beyond 200 m as logged in borehole KN192. The units comprise cyclic sequences of interbedded shales and dolomites, with shales generally greenish grey, laminated and thinly bedded and talcose with planar joint surfaces whilst the dolomites are cream-white, silicified, micro-veined, moderately brecciated and vuggy with undulating joint surfaces. The vugs and joints in the dolomitic units were normally filled with a reddish-white mixture of iron and carbonate stains. The unit grades to become shale dominant at the top.

4.3.6 CORE LOGGING RESULTS

Core logging carried out was used to generate, modify and update information about the stratigraphic successions within the Lubambe License Area (Figure 4-27). Additional units such as the Kakontwe limestones, shales and dolomites above the Grand Conglomerate Member were added to what was previously available in the database and stratigraphic plots were updated. Additional units (Kakontwe limestones, shales and dolomites of the Lower Kundelungu) and structures were logged from recent boreholes (2019 – 2020), and it was the first time those units were intersected in Lubambe diamond drilling. Formational and Member boundaries from historical logging were changed to suit observations and interpretations made during the study. Changes included recognition of the SWG unit as a member on its own and as a formation when combined with the Konkola Member. The Breccia Formation and Chingola Dolomite Formation were added onto the updated stratigraphic log. Mwashia remained categorised as a Group and a Formation as per the Lubambe Mine nomenclature. The Kakontwe Formation (Limestone Member) and the Lower Kundelungu Group (Shales and Dolomites Members) were also added to the stratigraphic log based on new data from the 2019 - 2020 drilling carried out.

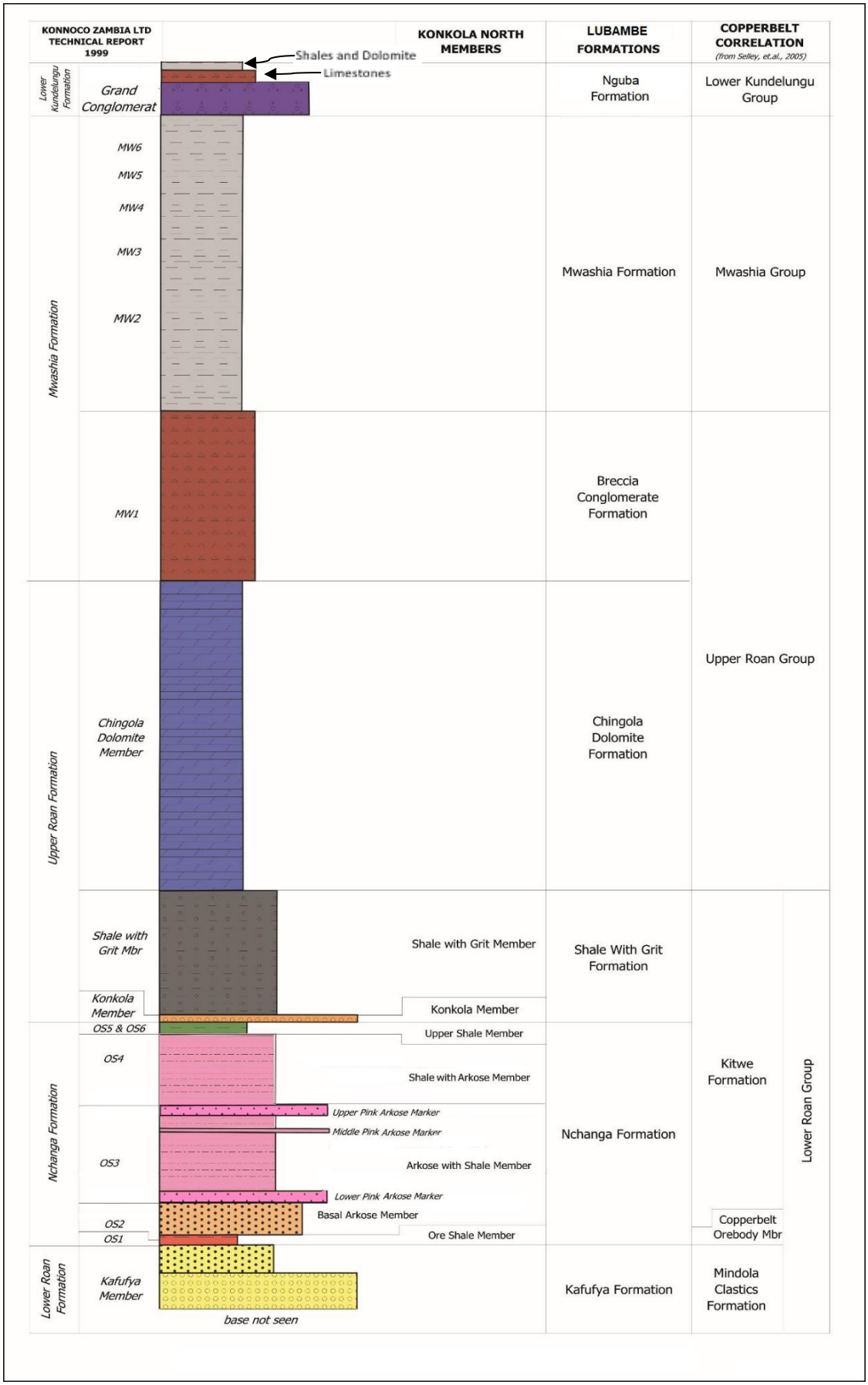

Figure 4-27: Simplified stratigraphic log of the Lubambe Area based on the core logging carried out (modified from Arthurs et al., 2009).

4.4 GEOLOGICAL MODELLING

The Lubambe stratigraphic and mineralisation models were created using Leapfrog software. The stratigraphic model includes all units from the surface down to the Kafufya Formation. The mineralisation model is basically derived from the delineation of the OS1 unit through core logging and geochemical assay results to define the orebody. The combination of the two models gives an understanding of the relationship between stratigraphy and mineralisation.

4.4.1 STRATIGRAPHIC MODELLING

Lubambe utilises the Acquire database to capture and manage its exploration data and information. The Lubambe Acquire database contains 654 drill holes including those from underground drilling which were excluded from the resource estimate. Out of the 654 drill holes, 11 were drilled for the metallurgical test work and 351 contained geochemical analyses. The resource estimate is based on the 351 drill holes that contain assay information. Drill spacing varies from 25 m for underground drilling to over a 1000 m for exploration drilling in the area between Lubambe Mine and the Extension Area (AMEC, 2014). The general spacing for drill holes in the Extension Area ranges between 300 and 500 m (Reid, 2020).

Because significant geological inconsistencies occur due to logging errors and database problems, further revision was carried out as part of the validation process. A total of 72 drill holes were re-logged, resulting in improved characterisation of stratigraphic contacts and a revision of the stratigraphic nomenclature. Re-logging of selected historic drill core was also undertaken to determine the reliability and consistency of existing data and aid correlation across the property. Results were compared with the data recorded in the database.

The database contains collar, survey, geology and assay data. Figure 4-28 is a plan view showing some of the drill holes in the Lubambe database for the drilling carried out up to 2018. Drilling carried out between 2019 to 2021 is not displayed. Re-logged drill hole collars are shown as green circles. The model limits are shown in green. The orientation of the drill holes is almost vertical with most of the drill holes dipping at 90. Some deviation is observed for the deeper drill holes. Many of the deeper holes have multiple deflections to generate more reef interceptions.

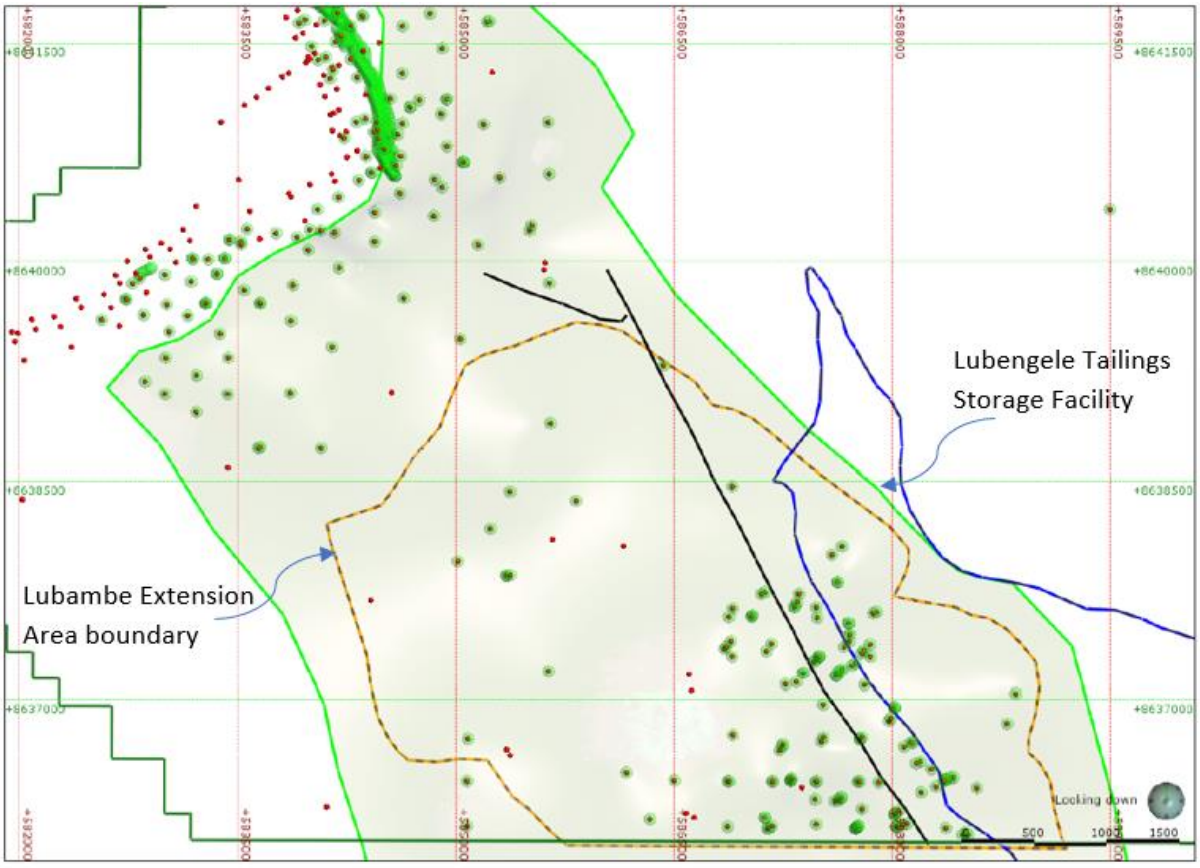

Figure 4-28: Plan showing collar positions of the drilling carried out in the Lubambe license area up to 2018. (Green circles show re-logged drill holes validated for modelling in this study).

The geological model, Figure 4-29, allows for the examination of stratigraphic architecture and thickness trends. Such features commonly reflect structural controls on sediment accumulation patterns and can potentially assist exploration targeting. Ongoing revision of the drill hole data and the resulting model is necessary to better constrain key geological components that could be used to show stratigraphic architecture for the purpose of defining depositional trends and their relationships to copper distribution.

During lithological modelling of the Lubambe deposit, most correlation with historically logged holes was found to be consistent on major contacts, formation classification, mineralisation types and alterations. At a regional scale (refer to Figure 1-3), Konkola, Lubambe and Musoshi (DRC) deposits all lie within the same basin and show near-identical stratigraphic sections with only local variations in lithofacies and thickness.

Re-logged and other existing drill hole data was used to compile a 3D geological model of the Lubambe-Konkola area. Outcomes were provided in free Leapfrog Viewer format (Figure 4-29), for ongoing use in drill hole planning and stratigraphic analysis.

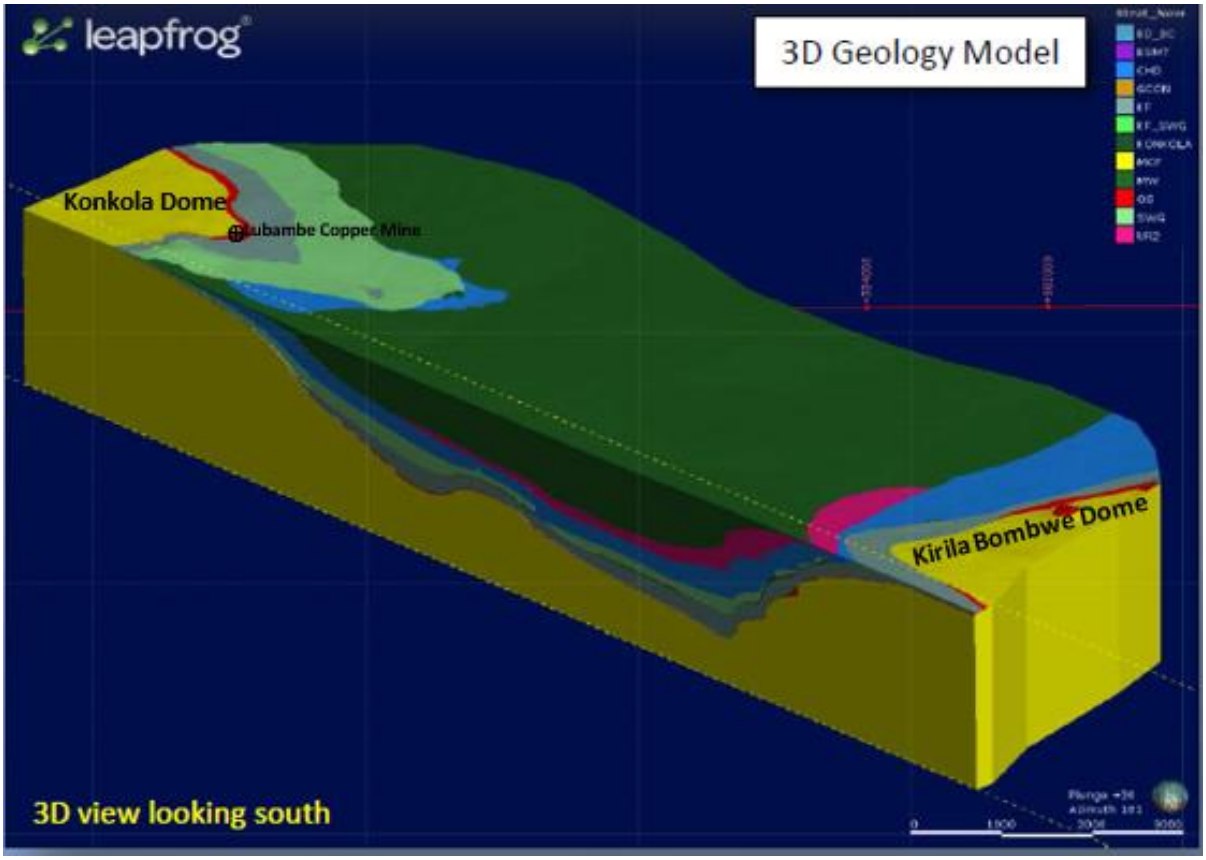

Figure 4-29: Image showing Geological / Stratigraphic Model of the Lubambe area.

The modelled lithological units in Figure 4-29 include: Kafufya Formation (MCF); Ore Shale 1 Member (OS); Nchanga Formation comprising Interbedded sequences of arkose, siltstone (KF); Konkola Member (KONKOLA) and Shale with Grit Formation (KF_SWG and SWG); Chingola Dolomite (CHD); Interbedded dolomite, dolomitic siltstone, limestone (UR2); Mwashia Formation Shales and dolomitic siltstones (MW); and Grand Conglomerate (GCON) units within each sedimentary package. Several unassigned units from the Lower Kundelungu Group within the Lubengele Syncline which lacked lateral continuity/extrapolation were also logged as BS_MT and BD_BC.

4.4.2 OREBODY ELEVATION VARIATION IN THE KONKOLA - LUBAMBE AREA

Orebody correlations (Figure 4-30), show that the Ore Shale extends northwards but becomes less distinctive and sub-economic towards the north. The thickness of the basal Kafufya Formation below Ore Shale 1 Member has so far not been determined unless deep penetrating geophysical techniques or drill holes are used, but what is clear is that the orebody thins towards the north from 16 m to 2 m. Maximum thickness of units above the Ore Shale 1 Member locally exceeds 1400 m towards the southeast.

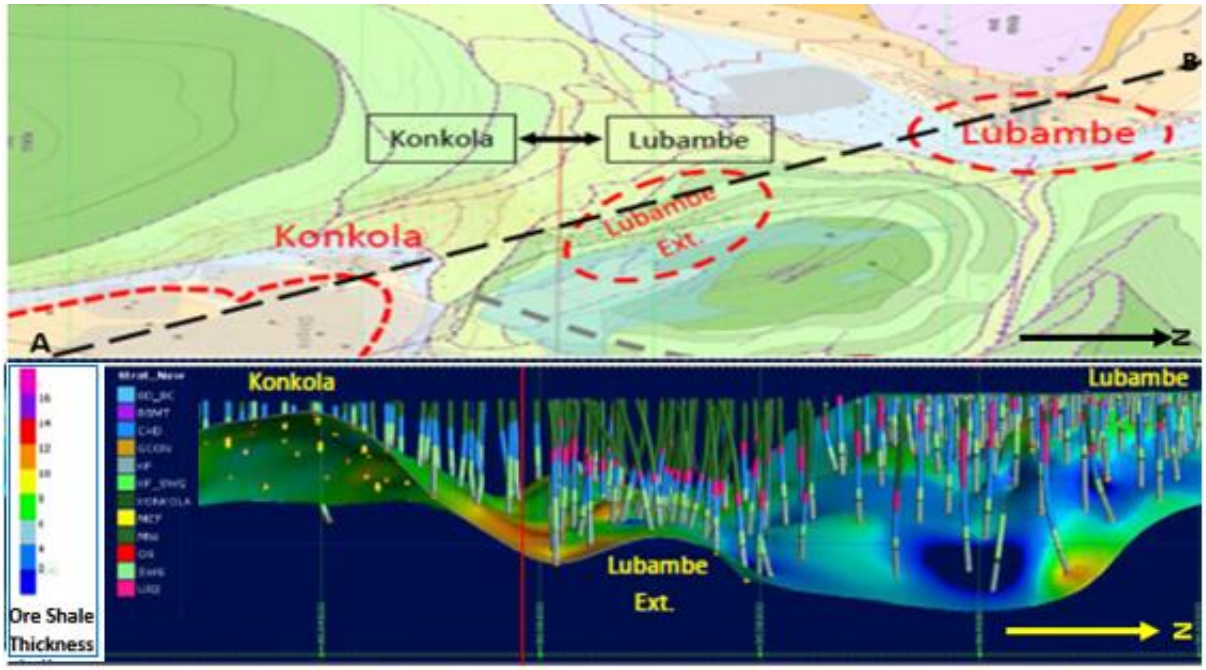

Figure 4-30: Sectional image showing the orebody elevation profile from Konkola to Lubambe based on drilling (image along the line A-B). Orebody is shown by the continuous surface in the image.

4.4.3 MINERALISATION MODELLING

The Lubambe mineralisation is closely associated with the litho-stratigraphic OS1 unit. However, mineralisation is not limited to this unit and is therefore stratiform as opposed to stratabound in nature (Figure 4-31), as it is sometimes above and/or below the OS1 unit.

Figure 4-31 mineralisation section was created in Geosoft just to show the stratiform nature of the Lubambe project area lithologies. The Interval selection tool allows interactive selection of samples to include in the mineralised zone. A cutoff grade of 1.00% TCu was used as a guide to indicate which samples should be included into the mineralised zone. In order to create a continuous mineralisation zone internal samples below 1.00% TCu are included, resulting in some samples that are below the cutoff being included inside the mineralised zone.

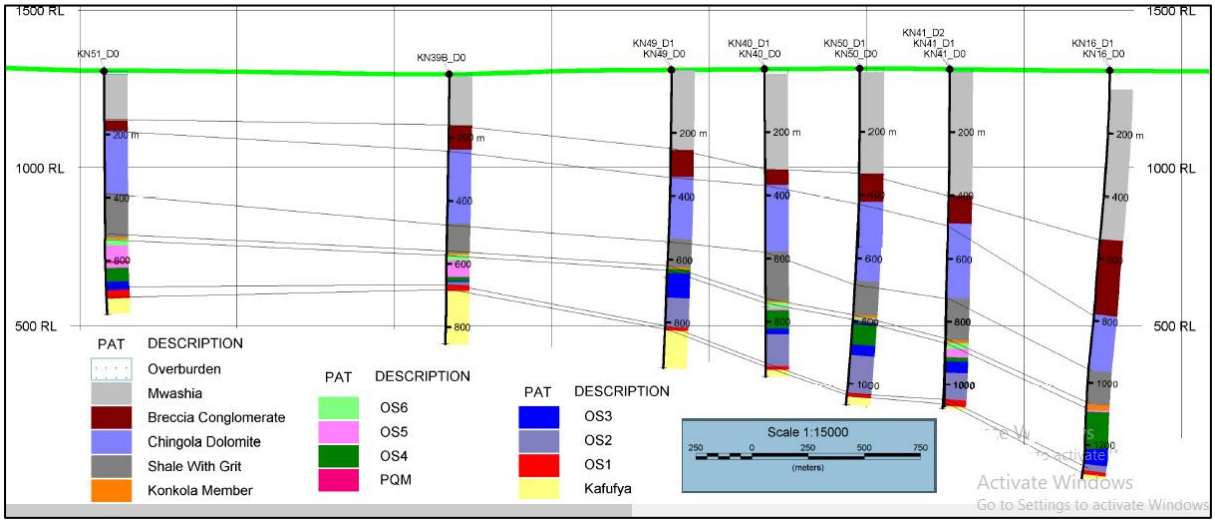

Figure 4-31: Section showing the stratiform nature of mineralisation within the Lubambe license area. (Litho-stratigraphic unit OS1 mineralised zone (red) at the bottom) (modified after Mwelwa, 2020).

Results from a mineralisation section cut from KN51 and KN16 (Figure 4-31) show the stratiform nature of the OS1 Member consistently lying above the Kafufya Member. The OS1 member varies in thickness sizes and elevation across the section and also shows the general dip of the units. This enables the generation of a continuous OS1 Member 3-D planar surface map using Leapfrog software (Figure 4-32).

Selected intervals were modelled into an envelope (Figure 4-32), using the Veining Tool in Leapfrog. Pinching out of the vein in areas of absent mineralisation was applied, meaning in a drill hole where there is no grade intersection above indicator cutoff, the wireframe would pinch out. The extents of the wireframe away from drilling was manually controlled by limiting the boundary of the geological model using a polyline. This is to ensure good confidence in the position and thickness.

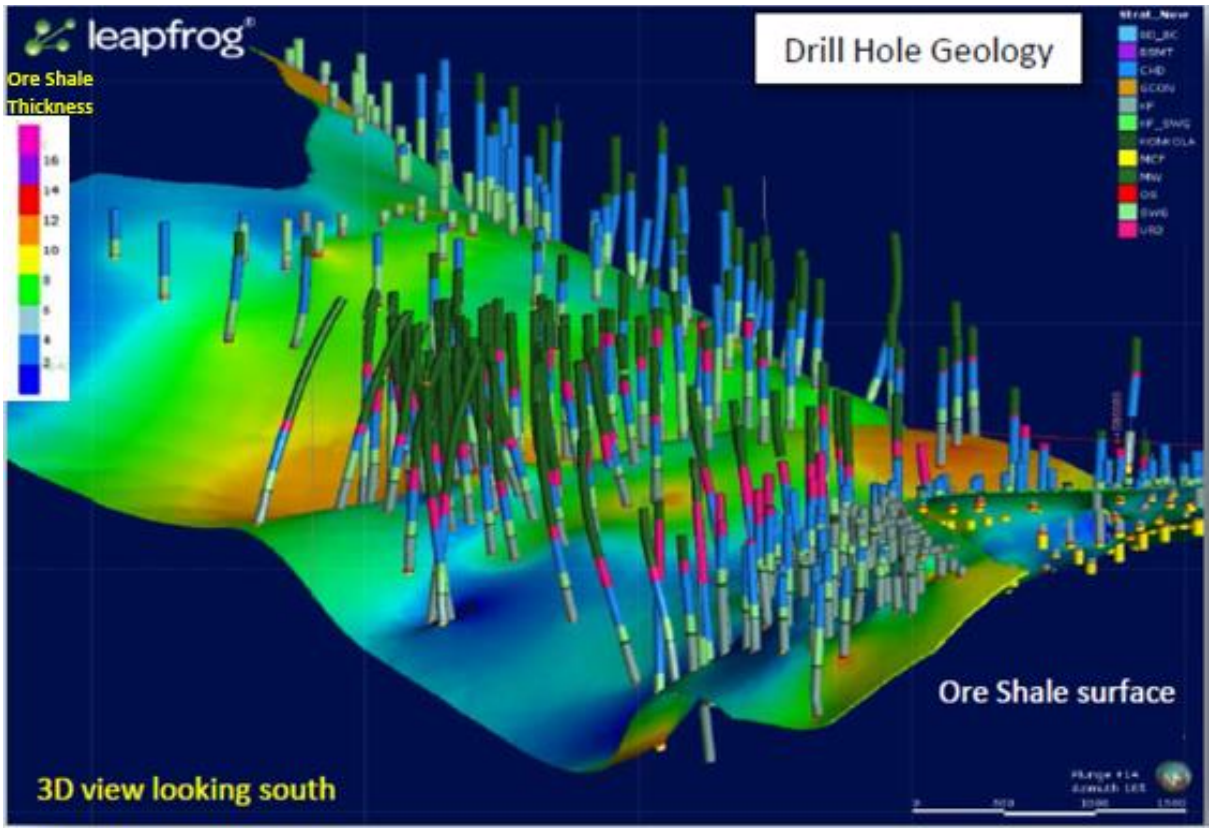

Figure 4-32: Image showing modelled mineralised envelope based on drill hole intersections in the Lubambe License Area.

4.5 PETROGRAPHY

Mining activities are currently taking place in the East and South Limbs whilst the Extension Area and the Eastern side of the license area (Figure 4-33), have been noted to have their own forms of mineralisation (Subramani, 2018). The Lubambe Mining Area eastern side is where recent drilling (2019 – 2020) has been carried out. Two samples were selected from four (4) major areas with sample locations indicated in Table 1 and Figure 4-33. This section focuses on petrographic descriptions of thin sections as observed under the microscope. Focus has been put on studying the mineralogical variations, type, intensity, association, texture, and distribution.

Table 1: Summary information of selected samples for petrography within the Lubambe license area.

Sample ID	Hole ID	From (m)	To (m)	Rock Name	Formation	Supergroup	Location
TT017	KN34	573.40	573.55	Shales/Siltstones	OS1	Katanga	East Limb
TT018	KN55	375.70	375.82	Shales/Siltstones	OS1	Katanga	East Limb
TT019	KN146	697.30	697.45	Shales/Siltstones	OS1	Katanga	South Limb
TT020	KN89	428.55	528.70	Shales/Siltstones	OS1	Katanga	South Limb
TT021	KN126	1114.00	1114.15	Shales/Siltstones	OS1	Katanga	Ext. Area
TT022	KN191A	1216.65	1216.80	Shales/Siltstones	OS1	Katanga	Ext. Area
TT023	KN192	1566.40	1566.55	Shales/Siltstones	OS1	Katanga	East of LTSF
TT024	KN194D1	1506.35	1506.50	Shales/Siltstones	OS1	Katanga	East of LTSF

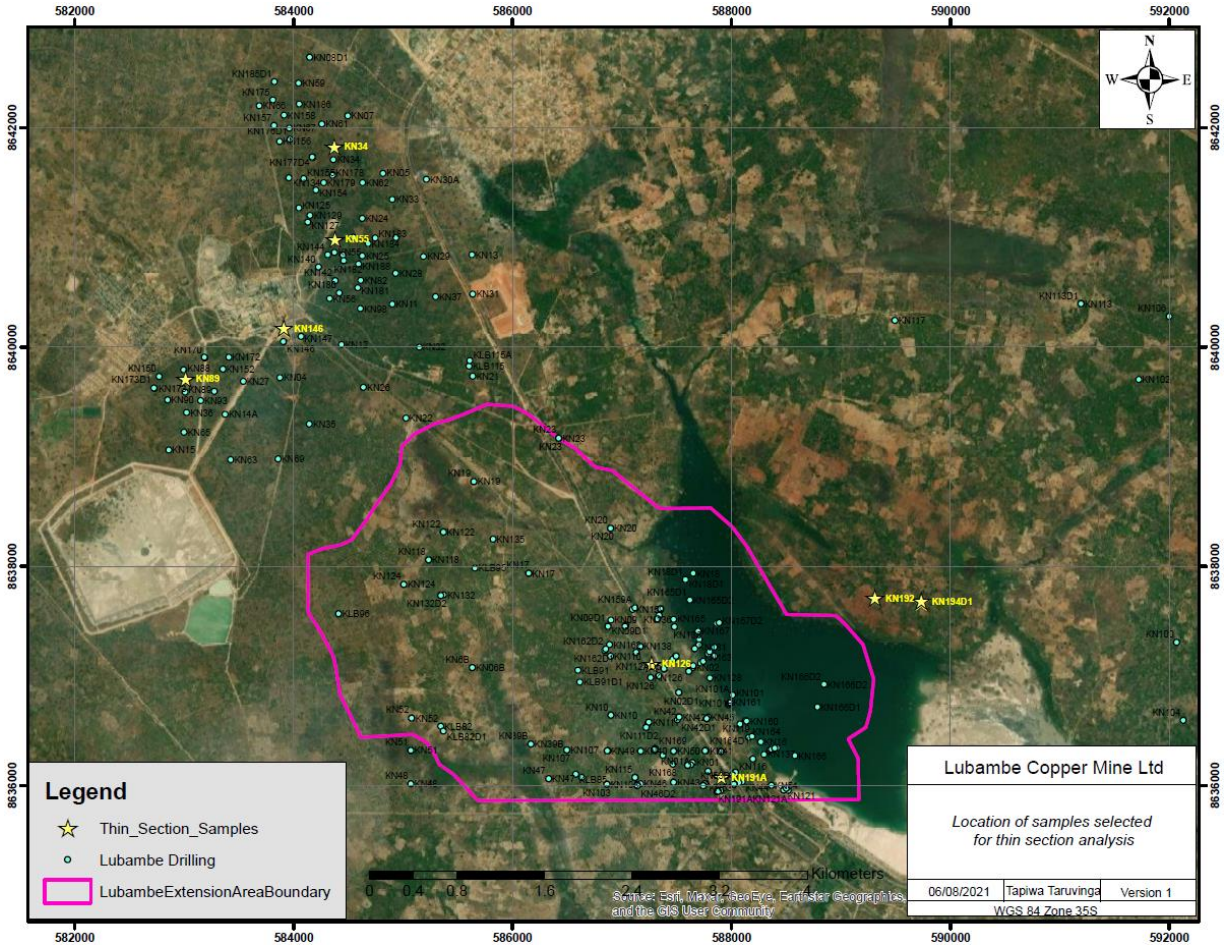

Figure 4-33: Map showing collar locations of drill holes from which samples for micro-petrographic analysis were taken.

4.5.1 MICRO-PETROGRAPHIC ANALYSIS

4.5.1.1 TT017 Petrography

TT017 was sampled from borehole KN34 in the East Limb at a depth of 573.40 m. The rock is a grey fine grained, banded, weakly foliated and laminated siltstone with shale intercalations. The hand specimen, Figure 4-34, shows thin shaly and silty laminations and minor carbonate filling silty laminae which reacted weakly to cold dilute hydrochloric acid. Chalcocite mineralisation filling pits.

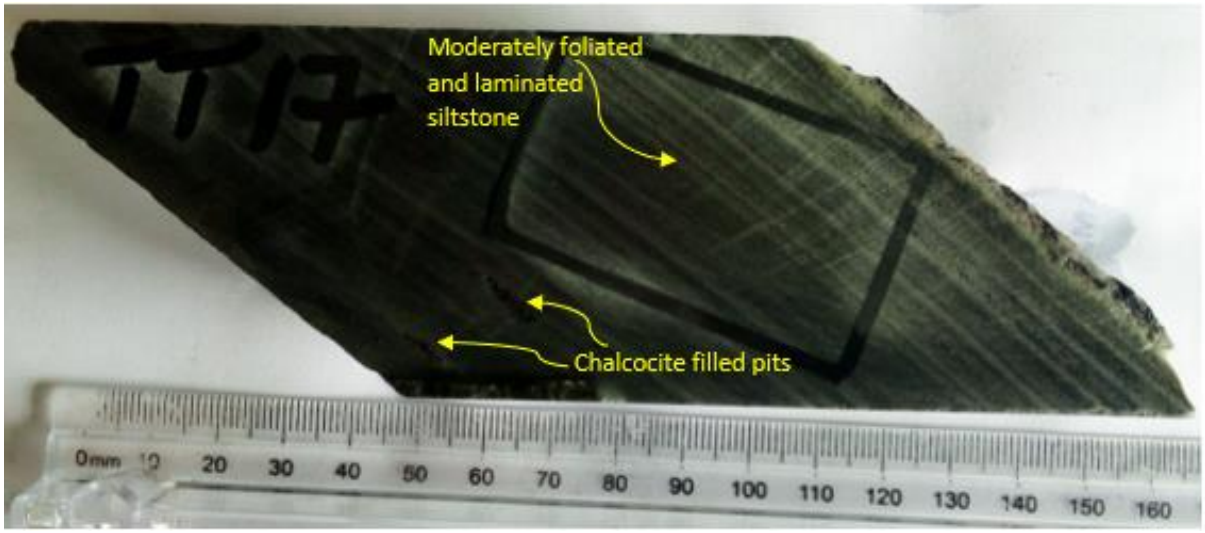

Figure 4-34: Photo showing TT017 hand specimen.

Under crossed polarised light (XPL) (Figure 4-35), quartz is fairly evenly distributed throughout the section, commonly showing undulose extinction although it commonly occurs in fairly small aggregates. Micas in the form of muscovite (elongate multi-coloured plates) and biotite (brownish to dark elongate minerals) also dominate together with sericite (greenish-grey matrix). Opaque minerals are fairly evenly disseminated throughout as fine to coarse grains, or aggregate bodies aligned to the foliation direction and parallel to bedding. Blebby opaque mineral grains are more significant on the left side of the image. Biotite is more irregularly distributed than either the quartz or the opaque minerals, tending to be preferentially concentrated in bedding or laminated layers.

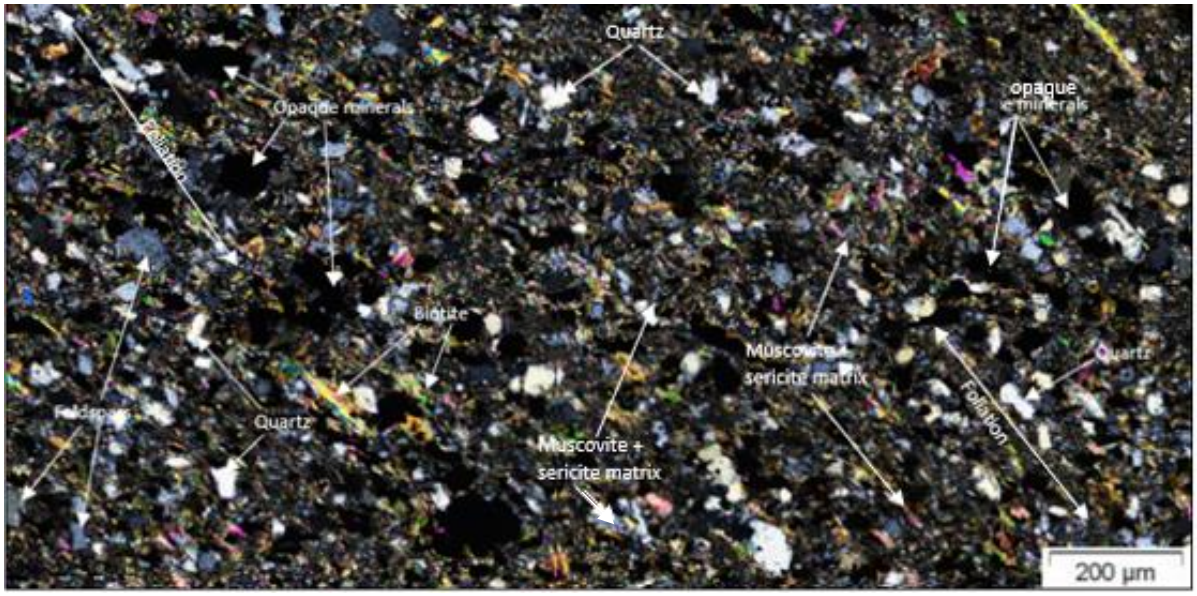

Figure 4-35: Photomicrograph showing TT017 image under XPL.

Under reflected light (Figure 4-36), the sample is strongly mineralised with chalcocite occurring as disseminations parallel to bedding/laminations. Chalcocite is the dominant opaque phase but is accompanied by considerable amounts of chalcopyrite and isolated pyrite grains. The chalcopyrite occurs in four main modes; i) disseminated in the slightly silty matrix. ii) as small grains marginally embedded in or attached to the edges of large chalcocite grains; iii) as relict grains in chalcocite, iv) chalcopyrite also occurs surrounded and being replaced by iron oxides on some of the observed mineral grains. The copper-bearing ore minerals occur together with haematite and limonite.

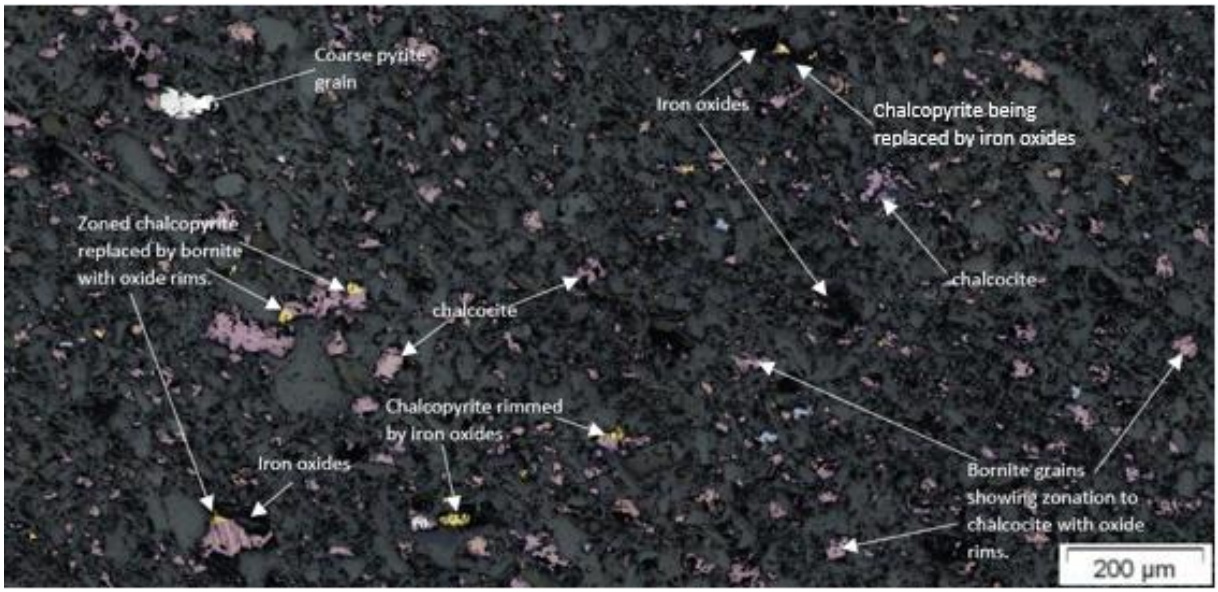

Figure 4-36: Photomicrograph showing TT017 image under reflected light.

4.5.1.2 TT018 Petrography

TT018 is from the East Limb and was sampled from borehole KN55 at a depth of 375.70 m. The hand specimen (Figure 4-37) is a greenish-grey, fine-grained, moderately foliated and laminated siltstone. Mineralisation observed in hand specimen consists of very fine chalcopyrite disseminations.

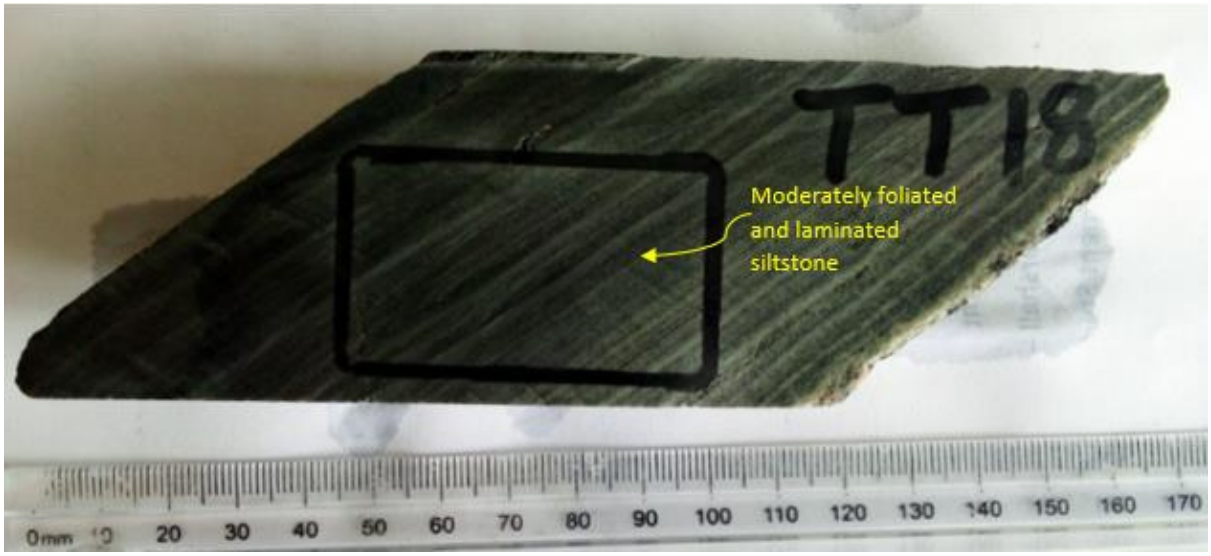

Figure 4-37: Photo showing TT018 hand specimen.

Under XPL (Figure 4-38), TT018 shows angular grains of quartz and feldspars and white and muscovite clasts (multi-coloured, thin plates) defining the foliation. Quartz and feldspar are embedded in a muscovite, haematite and goethite matrix which appears multi-coloured and finely speckled (Figure 4-38). Also notable are disseminations of opaque minerals (black), which are elongate and parallel to foliation. Opaque mineral grains are fairly evenly disseminated throughout the sample.

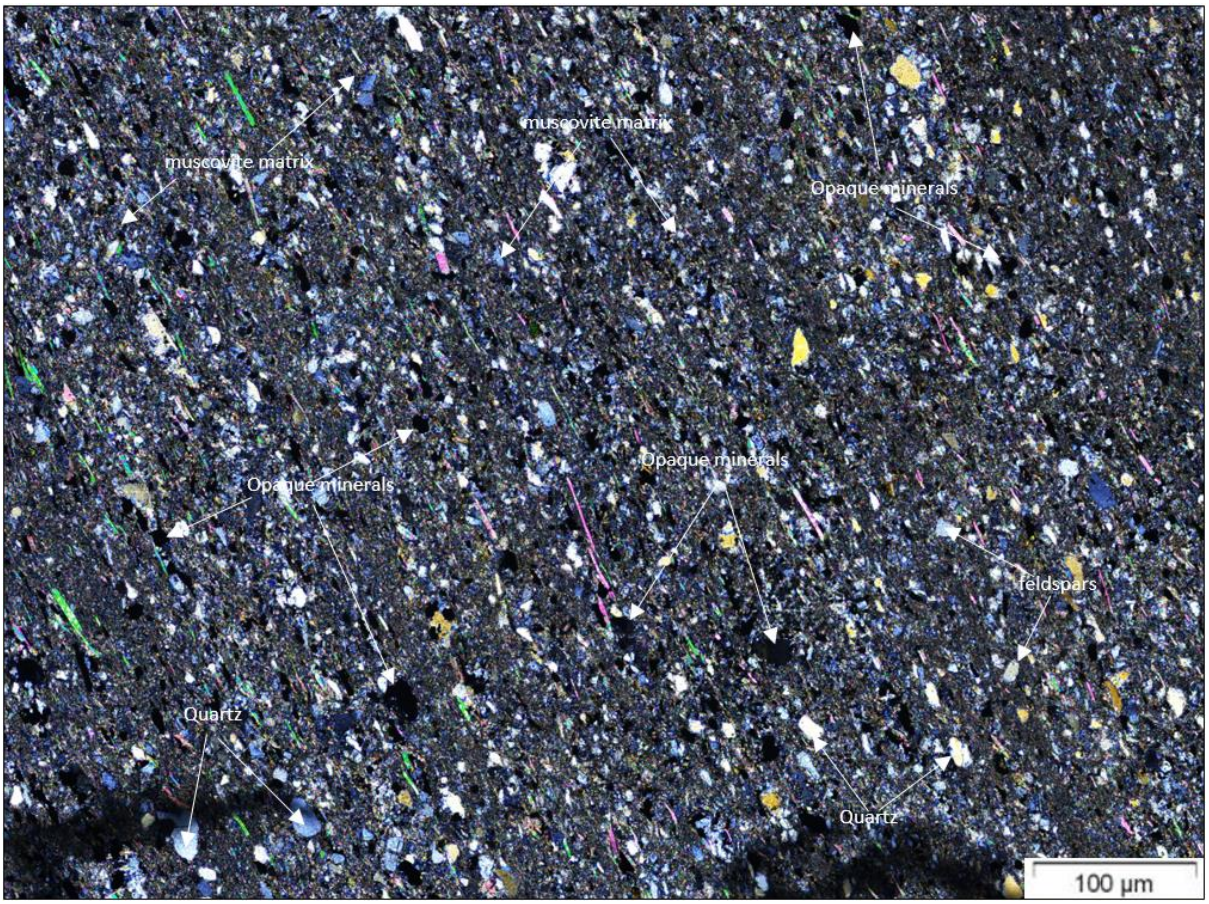

Figure 4-38: Photomicrograph showing TT018 image under XPL.

Under reflected light (Figure 4-39), chalcopyrite grains appear as roughly elongate grains, yellow with sub-rounded edges. Chalcopyrite grains are evenly distributed and also interlocked with the surrounding gangue mineral grains. Isolated flakes of fine grained covellite are also observed. Chalcopyrite and bornite grains are elongate and parallel to foliation.

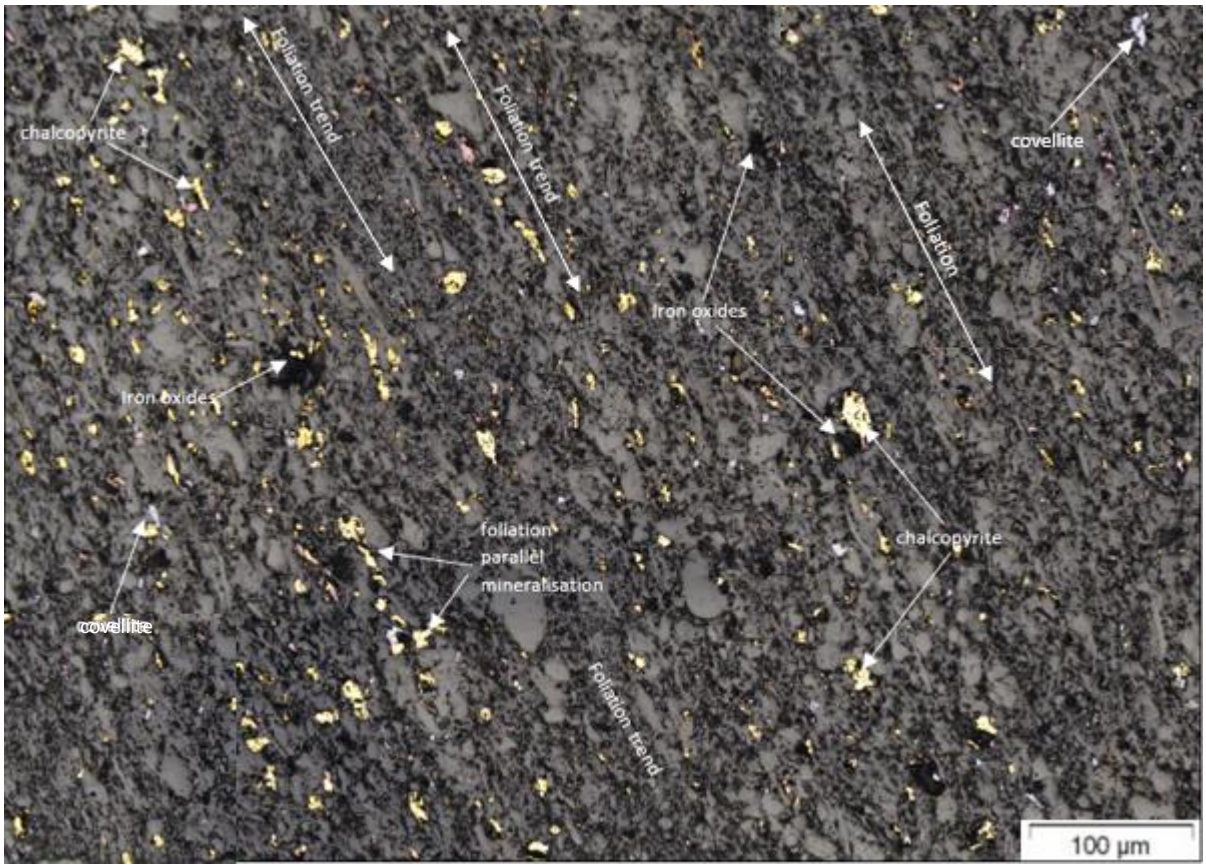

Figure 4-39: Photomicrograph showing TT018 image under reflected light.

4.5.1.3 TT019 Petrography

TT019 was cut from borehole KN146 at a depth of 697.30m. The sample was collected from the OS1 Member on the South Limb. The hand specimen is carbonaceous with notable banding, bedding and laminations (Figure 4-40). Primary mineralisation dominantly comprises very fine chalcocite disseminations and minor bornite. Veins with chalcopyrite and malachite/chrysocolla can be seen in the hand specimen. Chalcopyrite is the main secondary mineral along veins and occurs in close association with malachite and chrysocolla as secondary mineralisation.

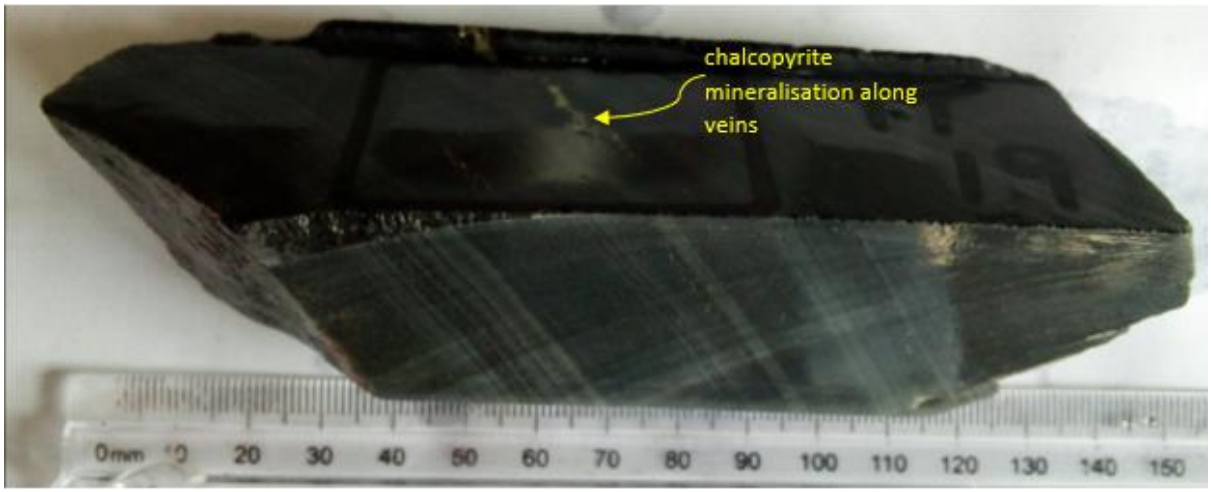

Figure 4-40: Photo showing TT019 hand specimen.

In crossed polarised transmitted light (Figure 4-41), there is dominance of quartz and feldspars giving a whitish and greyish colour and notably quartz displaying an undulose extinction characteristic whilst feldspar clasts are occasionally twinned. The matrix is dominated by sericite (greenish grey, multi-coloured, finely speckled), muscovite grains (multi-coloured, thin plates) and very fine biotite flakes mostly displaying a dark brownish to dark planar elongated minerals in the image. Opaque minerals filling the main vein as secondary sulphides, copper oxides and gangue minerals and displaying a black colour.

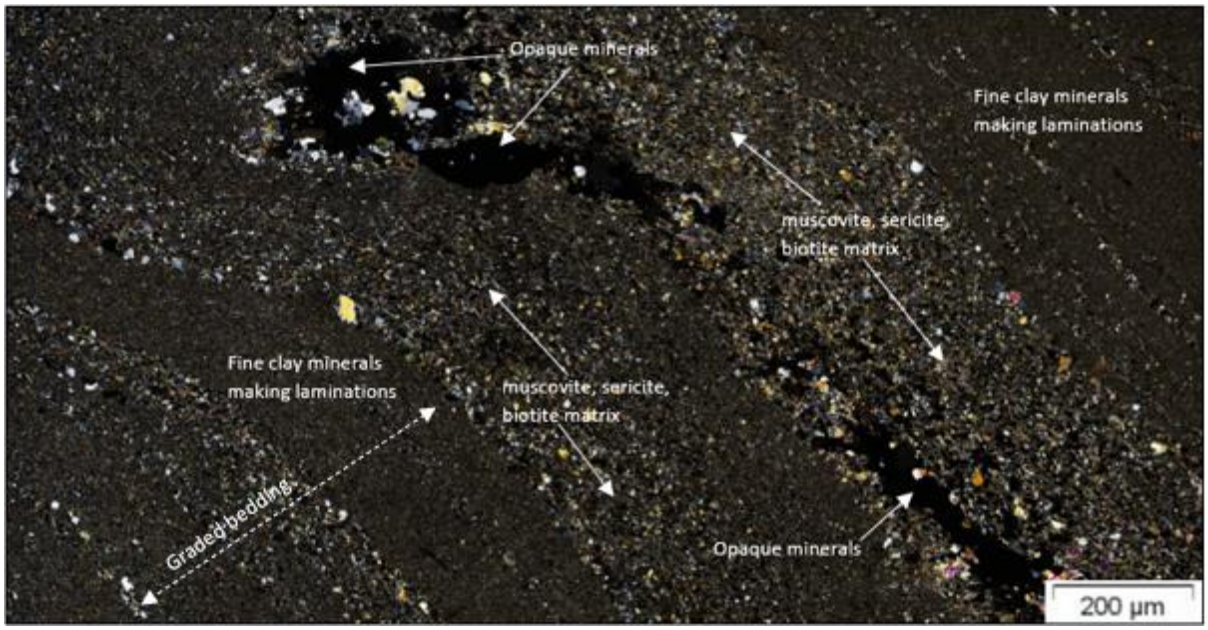

Figure 4-41: Photomicrograph showing TT019 image under XPL.

Under reflected light (Figure 4-42), primary mineralisation is observed as fine chalcocite (shiny grey-blue) following lamination bands and bedding. It is more pronounced in silt-sized grains than fine shaly laminated portions. Chalcopyrite (yellow, elongated grains) is the main secondary mineral filling the vein or micro-fractures. The chalcopyrite is associated with iron hydroxides mostly haematite/goethite (fine platy, white) in a darker band. Copper oxides, visibly noted in hand specimen as malachite and chrysocolla, concentrated on flexural zones where there are openings due to bending and curving and also occur along edges of the main vein. This is quite significant as the flexural-fold zones induced by tension gashes increase porosity which enables secondary copper oxide minerals dissolved in water to accumulate and concentrate thereby increasing the copper mineral content in the unit. However, within the vein, there is dominance of chalcopyrite and less of copper oxides as there is insufficient space for accumulation and concentration of secondary minerals.

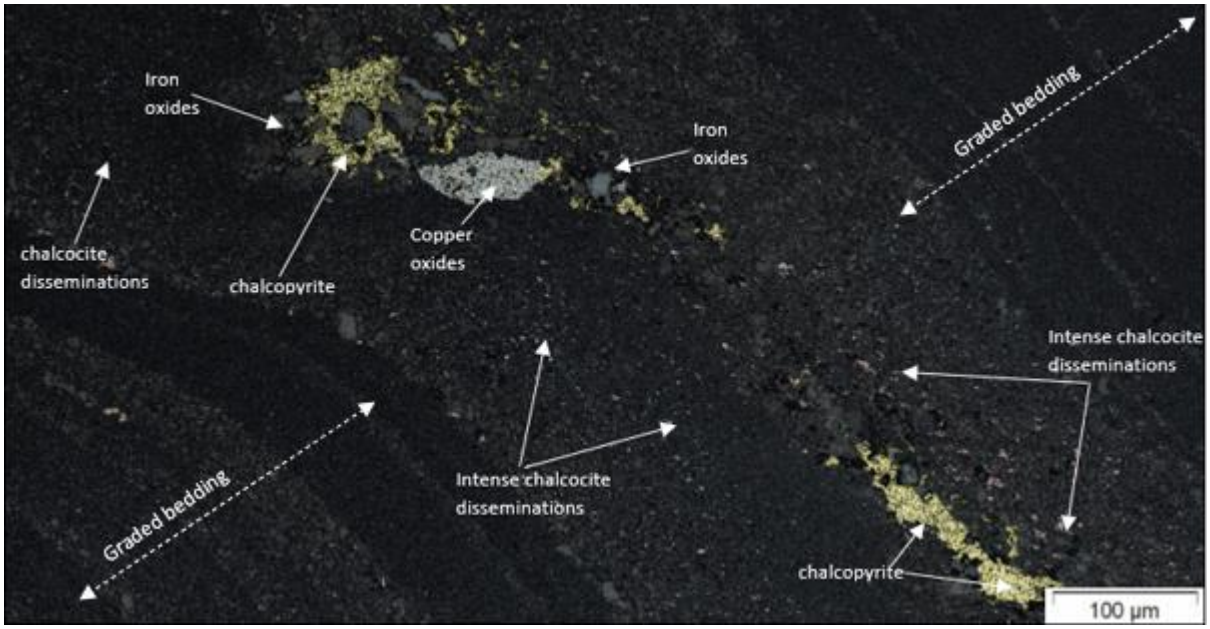

Figure 4-42: Photomicrograph showing TT019 image under reflected light.

4.5.1.4 TT020 Petrography

TT020 was cut from borehole KN89 at a depth of 428.55 m in the South Limb. The sample was cut from the OS1 Member. The hand specimen is greyish, banded, laminated and thinly bedded shale/siltstone (Figure 4-43). Predominantly moderately metamorphosed with clastic sedimentary textures and lamination bands. Primary mineralisation is dominated by chalcocite which occurs embedded within the matrix. Veins parallel to beddings and laminations are very outstanding and filled with chalcopyrite and secondary copper oxide minerals.

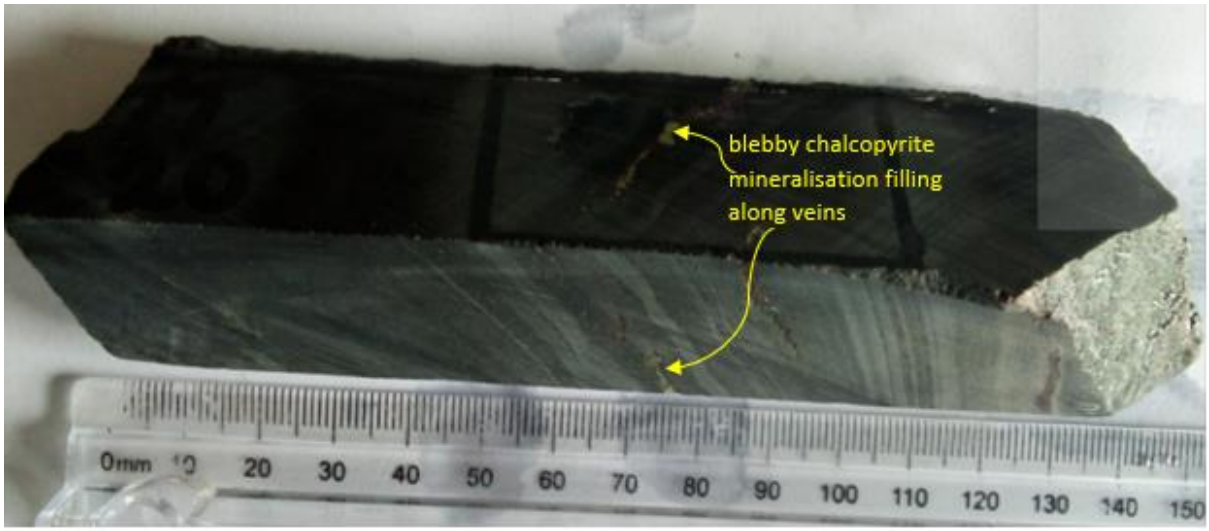

Figure 4-43: Photo showing TT020 hand specimen.

In XPL, concordant veins with blebby opaque minerals (black) running parallel are the most notable feature (Figure 4-44). The matrix is dominated by quartz, sericite, biotite, muscovite and opaque mineral disseminations. Clay minerals define the lamination, whilst quartz and feldspathic minerals represents the coarse grains. Muscovite clasts appear as pinkish, multi-coloured thin plates, biotite mostly consists of small brownish finely speckled plates whilst sericite comprises greenish fine grained matrix material. Disseminated opaque minerals are black. A strong, parallel lamination banding/bedding is noted with a preferred orientation defined by muscovite and biotite plates. Opaque minerals consist of copper minerals, iron oxides and gangue minerals appearing black on the vein and within the matrix.

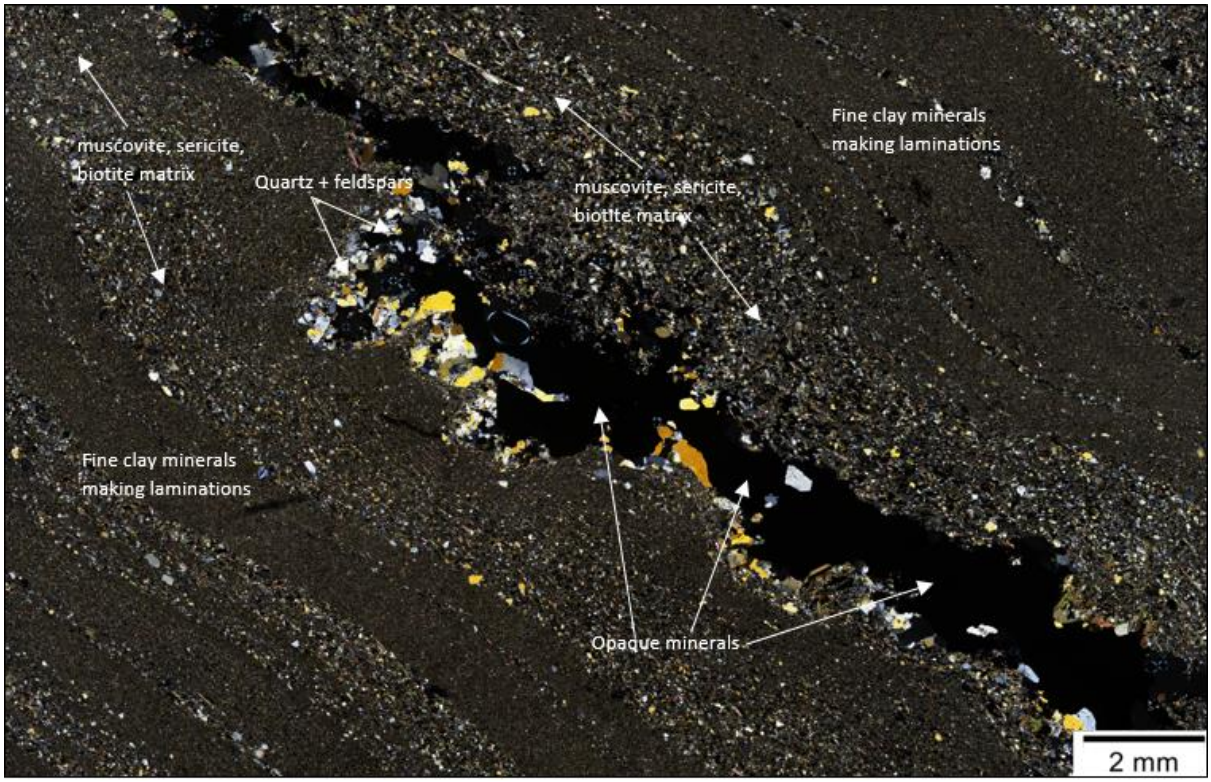

Figure 4-44: Photomicrograph showing TT020 image under XPL.

Under reflected light (Figure 4-45), a mineralised vein can be seen cutting across the image diagonally from the top left to the bottom right corner. The main vein consists of concentrations of larger, irregular anhedral, skeletal masses of chalcopyrite with some greyish and dark alteration margins which represents replacement by secondary copper oxides possibly brought about through oxidation reactions. The replacement has taken place in a highly irregular manner, mainly around the margins of the chalcopyrite grains but also partly penetrating into it and occasionally found as small dark inclusions. Flanking the vein is fine chalcocite +/- bornite grains appearing blue-grey forming part of the matrix.

Pale and dark grey coarse mineral grains can also be observed as chalcopyrite grains. These are iron hydroxide minerals mainly haematite and goethite. Some goethite, with dark red internal reflections is developed mainly around the margins of the replacing haematite aggregate masses.

The bottom right corner of Figure 4-45 shows replacement of chalcopyrite by copper oxides with a waxy pale blue colour.

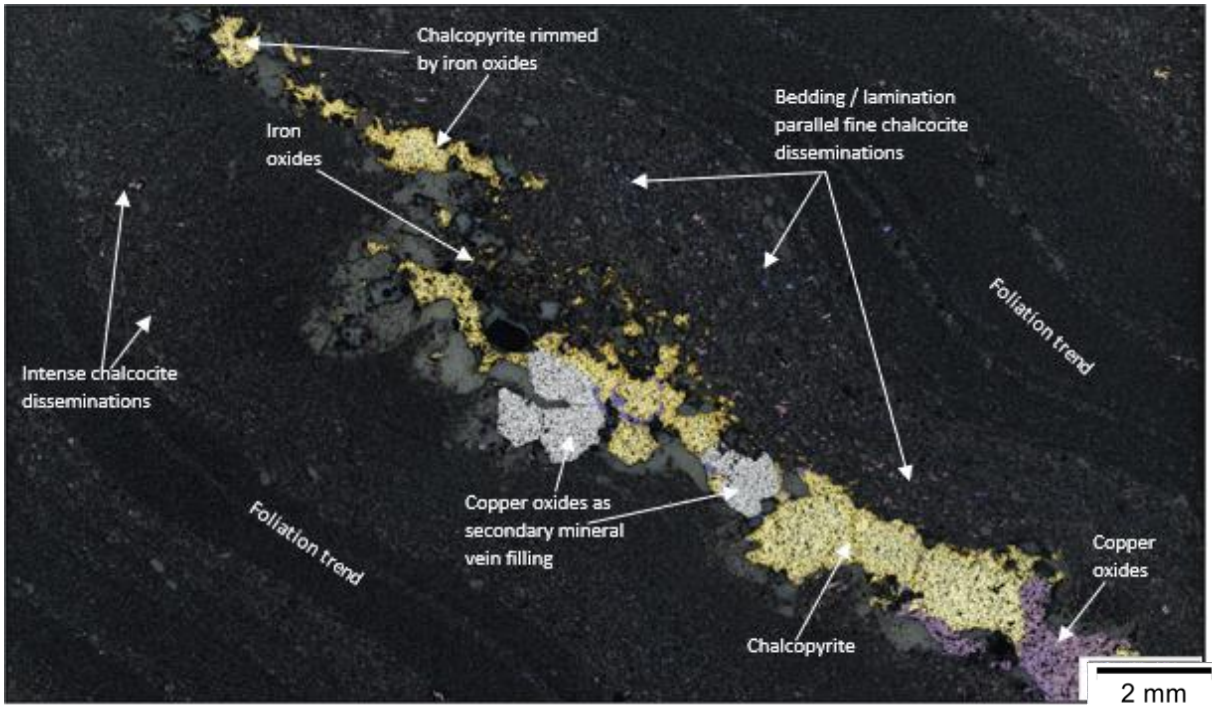

Figure 4-45: Photomicrograph showing TT020 image under reflected light.

4.5.1.5 TT021 Petrography

TT021 was obtained from borehole KN126 at a depth of 1114.00 in the OS1 Member of the Extension Area. The host rock is a moderately metamorphosed siltstone with shale intercalations, greyish, fine grained with well-developed foliation (Figure 4-46). Visible mineralisation is dominantly chalcopyrite and some specks of chalcocite both of which are elongated and parallel to foliation.

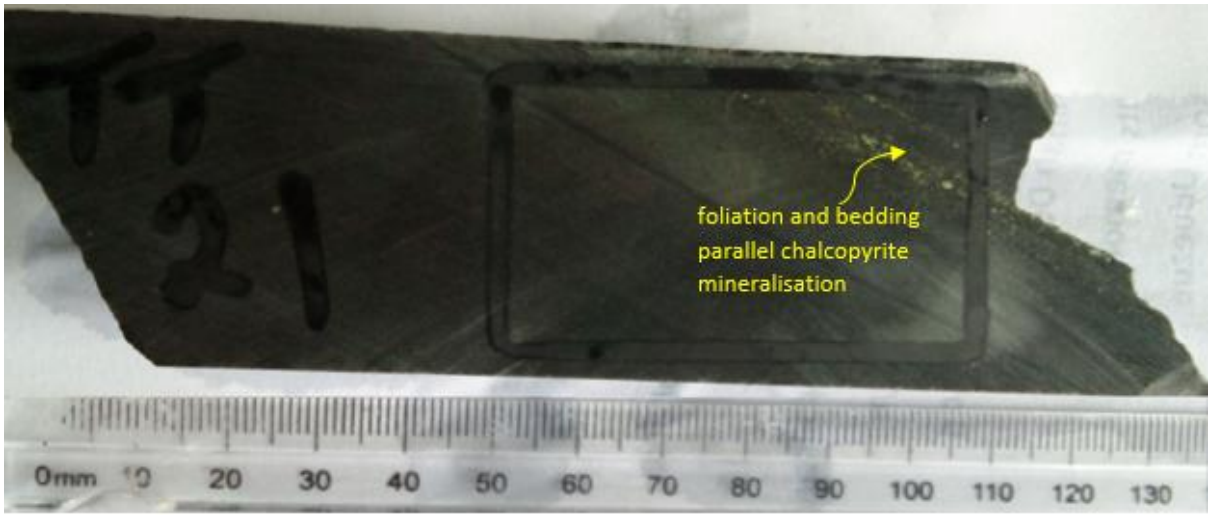

Figure 4-46: Photo showing TT021 hand specimen.

Under XPL transmitted light (Figure 4-47), a moderate to strong foliation is defined by the preferred orientation of muscovite (multi-coloured), biotite (brown to grey) plates, paralleled by a weak metamorphic foliation defined mainly by the preferred orientation of phyllosilicate mineral plates. Mineral banding corresponding to primary bedding is related to mineral variations in the matrix, clasts and grain size contents.

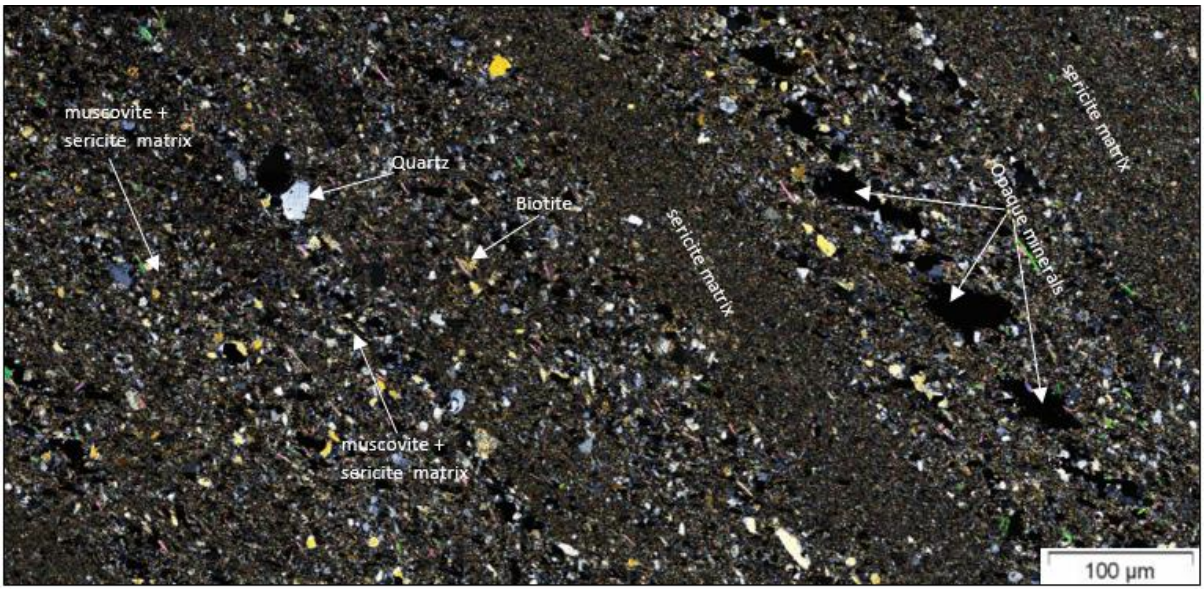

Figure 4-47: Photomicrograph showing TT021 image under XPL.

A linear array of coarse opaque minerals (black) can be seen on the right side surrounded by a medium-grain sized matrix. Disseminated fine- to medium-sized opaque minerals is observed aligned to bedding and foliation. Somewhat larger opaque mineral grains tend to be preferentially concentrated along the more silt size to arkosic microbands and laminae with smaller grains being abundantly and fairly evenly finely disseminated in between, especially in the more shaly microbands and laminae.

Under reflected light (Figure 4-48), coarse opaque minerals on the right side are mainly dominated by coarse chalcopyrite (yellowish) grains. A large isolated pyrite grain (pale yellowish white) is noted growing and replacing a chalcopyrite grain (Figure 4-48). Bornite (pinkish grey) is also notable within the top part of the aligned coarse matrix. Possible zonation on the top left side from pyrite to chalcopyrite to bornite. Fine grained chalcocite, bluish-grey grains, are embedded in the matrix covering most parts of the image. The mineralisation observed occurs in association with haematite (medium grey) and goethite (darker grey) (Figure 4-48).

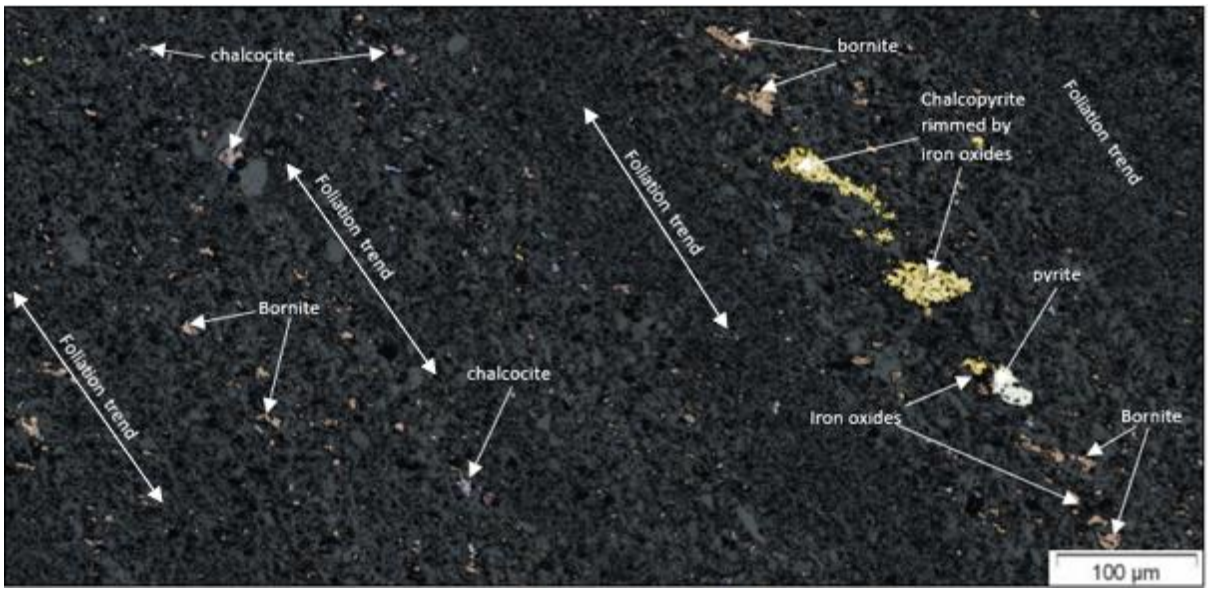

Figure 4-48: Photomicrograph showing TT021 image under reflected light.

4.5.1.6 TT022 Petrography

TT022 was obtained from borehole KN191A at a depth of 1216.65 m. The sample lies within the top section of the OS1 Member of the Extension Area dominantly comprising chalcopyrite, oxidized secondary mineral copper stains and minor flakes of chalcocite (Figure 4-49). The hand specimen shows a weakly metamorphosed, well laminated and banded shale with lenses filled with chalcopyrite. Chalcopyrite mineralisation is parallel to thin laminations. Also notable are thin white dolomitic micro-veins.

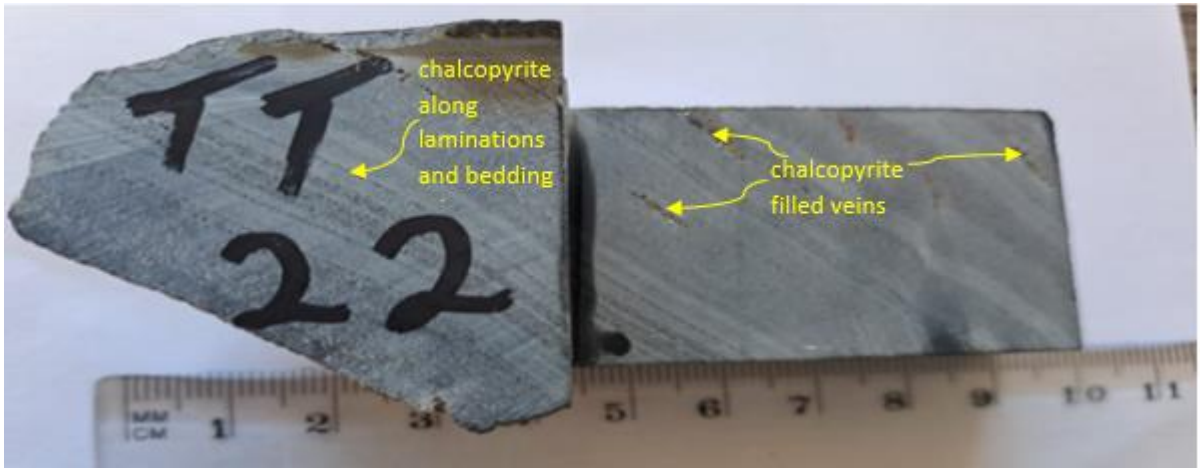

Figure 4-49: Photo showing TT022 hand specimen.

Under XPL (Figure 4-50), the image shows banding and lamination due to subtle variations in matrix and clast contents as well as some bedding-parallel concentration of fine- to coarse-grained opaque minerals. Quartz and feldspar clasts (white and grey) make up part of the fine matrix. Muscovite (multi-coloured, thin plates) and biotite flakes are parallel and aligned to define the bedding foliation. The sericite matrix is greenish-grey and finely speckled whilst biotite has brownish elongated mineral flakes.

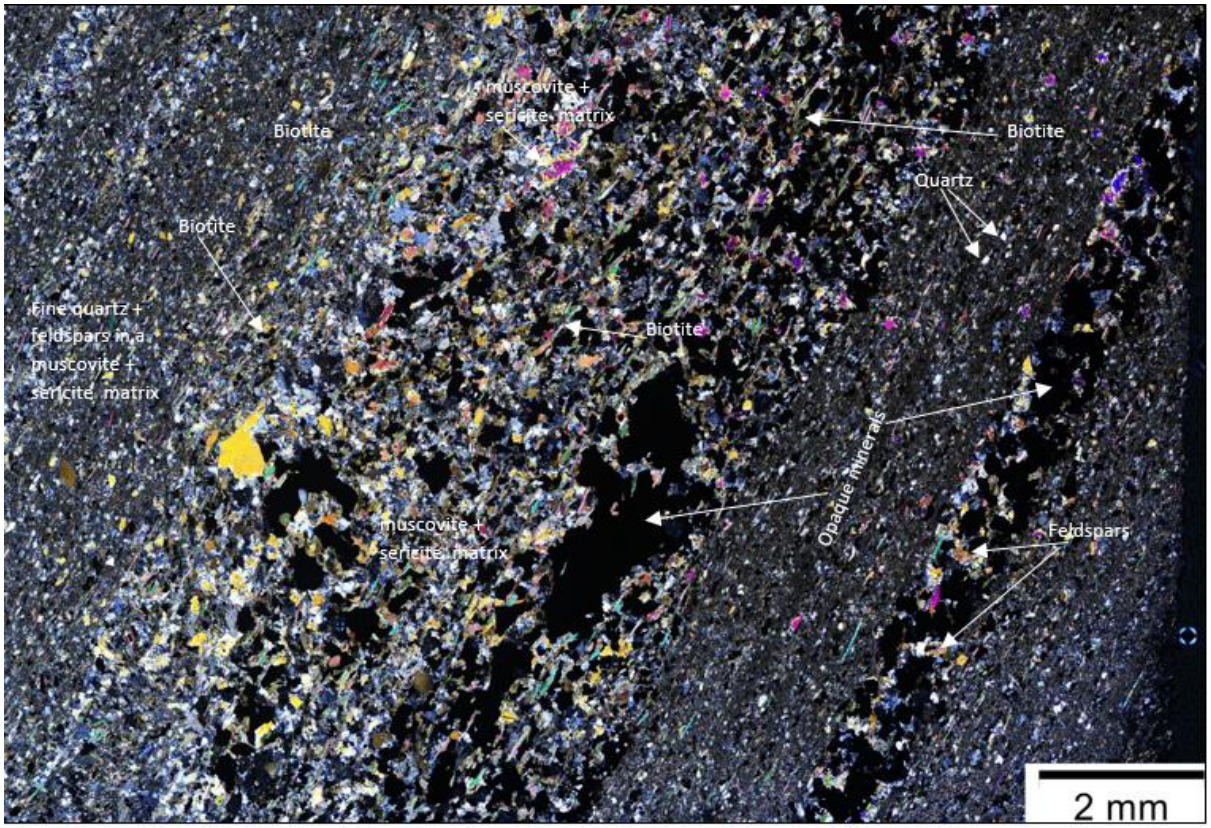

Figure 4-50: Photomicrograph showing TT022 image under XPL.

Under reflected light (Figure 4-51), there is a well-developed mineral banding and lamination which is probably primary bedding-related. Chalcopyrite mineralisation is observed between a finer-grained, bedded and laminated siltstone with some shale intercalations (Figure 4-51). Isolated bornite grains (pink) marginally attached or embedded within the chalcopyrite grains. Chalcopyrite occurs in association with iron oxide minerals. These are mostly in the form of haematite, limonite and goethite.

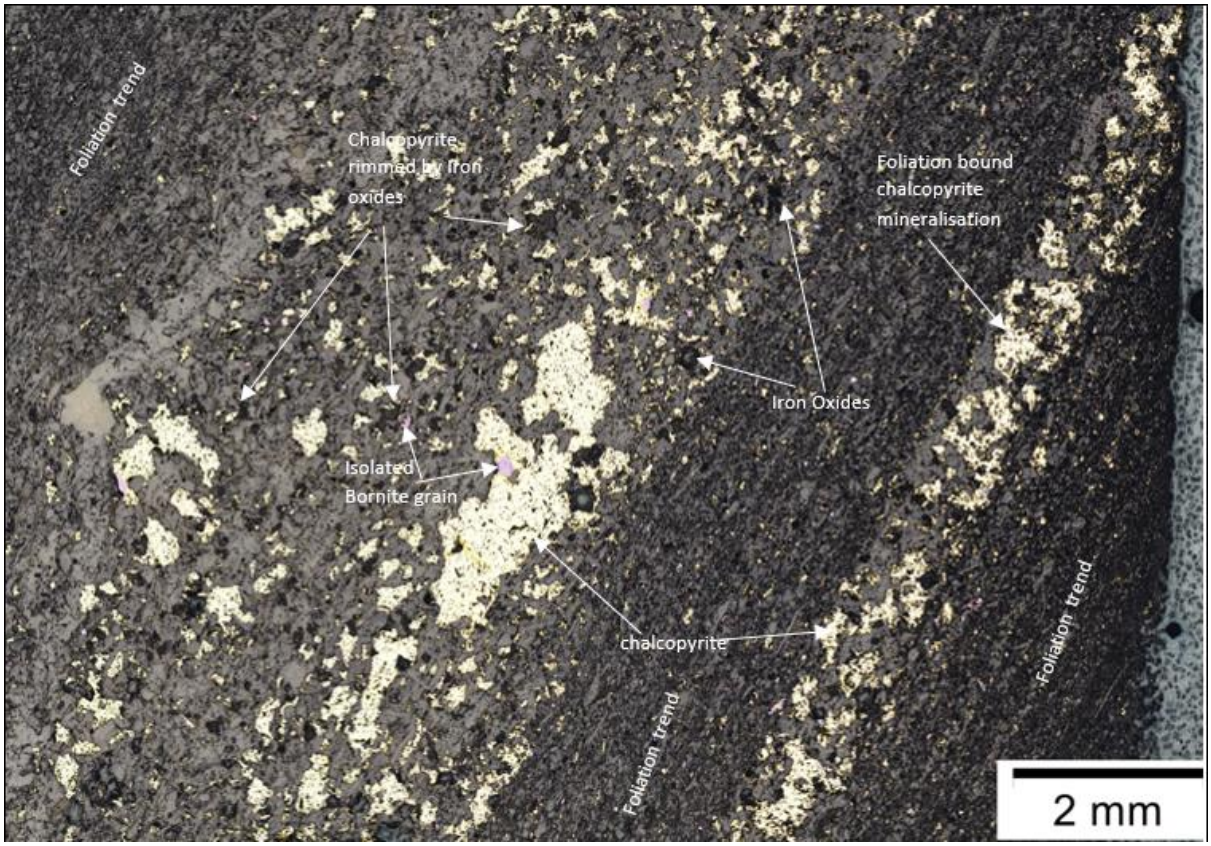

Figure 4-51: Photomicrograph showing TT022 image under reflected light.

4.5.1.7 TT023 Petrography

TT023 was obtained from borehole KN192 at a depth of 1566.40 m. The hand specimen is a silty and shaly, fine-grained siltstone from the OS1 Member (Figure 4-52). The specimen has very fine chalcocite and bornite disseminations whilst chalcopyrite and oxidised copper occupy the corner of the thin section (Figure 4-52).

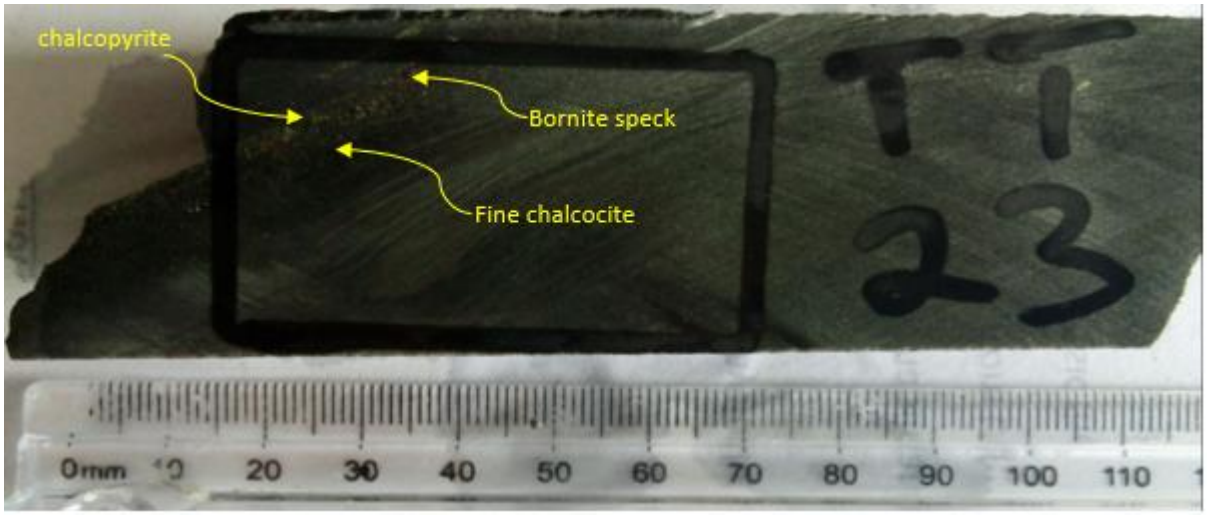

Figure 4-52: Photo showing TT023 hand specimen.

Under XPL transmitted light (Figure 4-53), quartz clasts appear white and grey exhibiting an undulose extinction characteristic. The matrix comprises muscovite, biotite and some fine quartz and feldspar minerals. Muscovite clasts (multi-coloured, thin plates) show a preferred orientation to define a weak foliation. Biotite is brown with elongated grains also defining the foliation direction. The image has significant darker microbands due to high concentration of opaque minerals. There is a higher concentration of opaque minerals (black) on the bottom left corner whilst the rest are disseminated throughout the image.

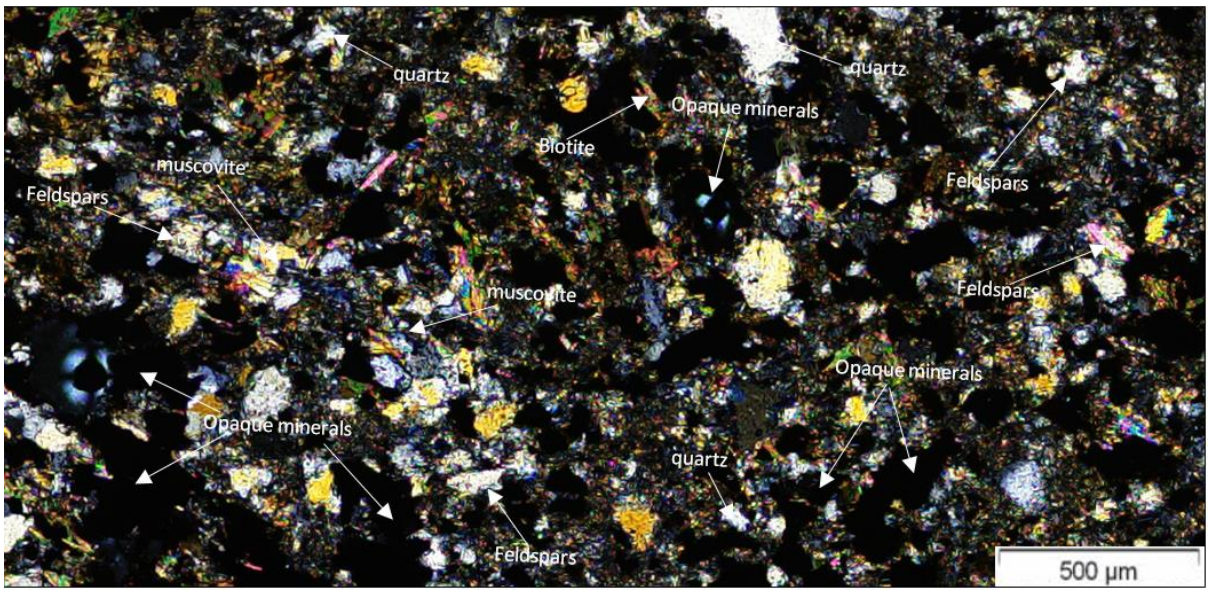

Figure 4-53: Photomicrograph showing TT023 image under XPL.

Under reflected light (Figure 4-54), a significant amount of sulphide copper-bearing minerals which include chalcocite (bluish-grey), bornite (pinkish-brown) and chalcopyrite (yellow skeletal grains) can be observed. Chalcocite and bornite are the most abundant, whilst chalcopyrite is confined to the bottom left corner (Figure 4-54). Copper-bearing sulphides have grains partially to completely surrounded and/or replaced by haematite and variable amounts of goethite.

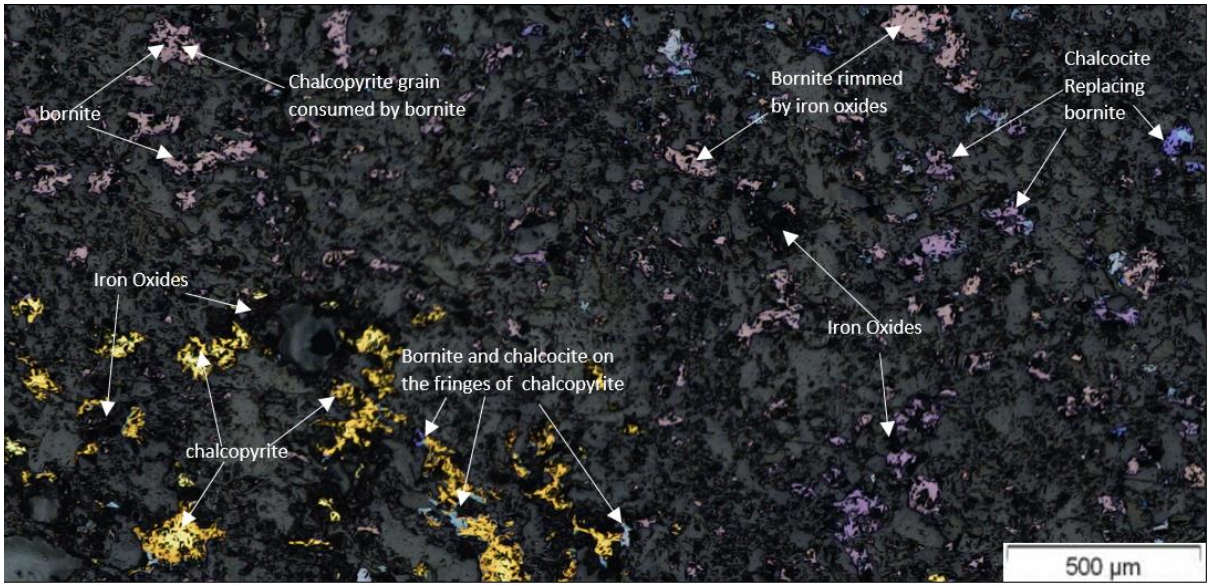

Figure 4-54: Photomicrograph showing TT023 image under reflected light.

4.5.1.8 TT024 Petrography

TT024 (Figure 4-55), was sampled from the OS1 Member of borehole KN194D1 at a depth of 1506.35 m. The hand specimen is a grey, fine grained, laminated, weakly foliated low-grade metamorphosed siltstone. Visible mineralisation is dominantly chalcocite and chalcopyrite. Bornite and chalcopyrite are dominant as vein fillings. In most portions bornite can be seen interlocked on the edges of chalcopyrite. Away from veins there are also some visible fine grained chalcocite disseminations. Mineralisation is parallel to bedding and foliation.

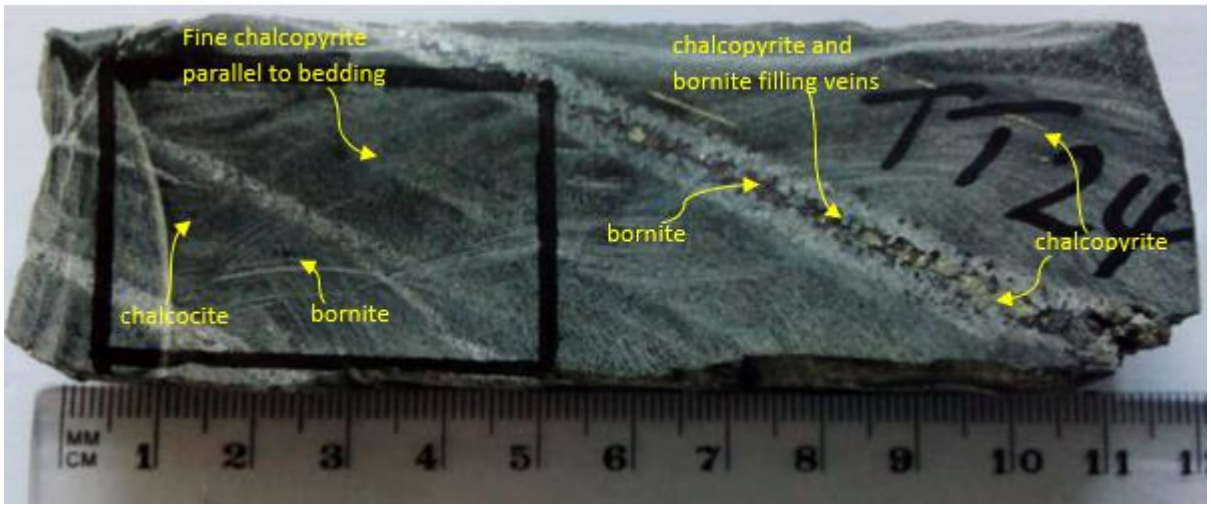

Figure 4-55: Photo showing TT024 hand specimen.

Under XPL, Figure 4-56, most of the image comprises muscovite (white and pink thin multi-coloured plates) occurring in a silty matrix. Also present is sericite (greenish-grey, finely speckled), mostly associated with silty laminations. Feldspathic (white and bluish-grey, angular grains) and biotite (brownish elongated and foliation parallel) are very significant. Opaque minerals are observed as black minerals.

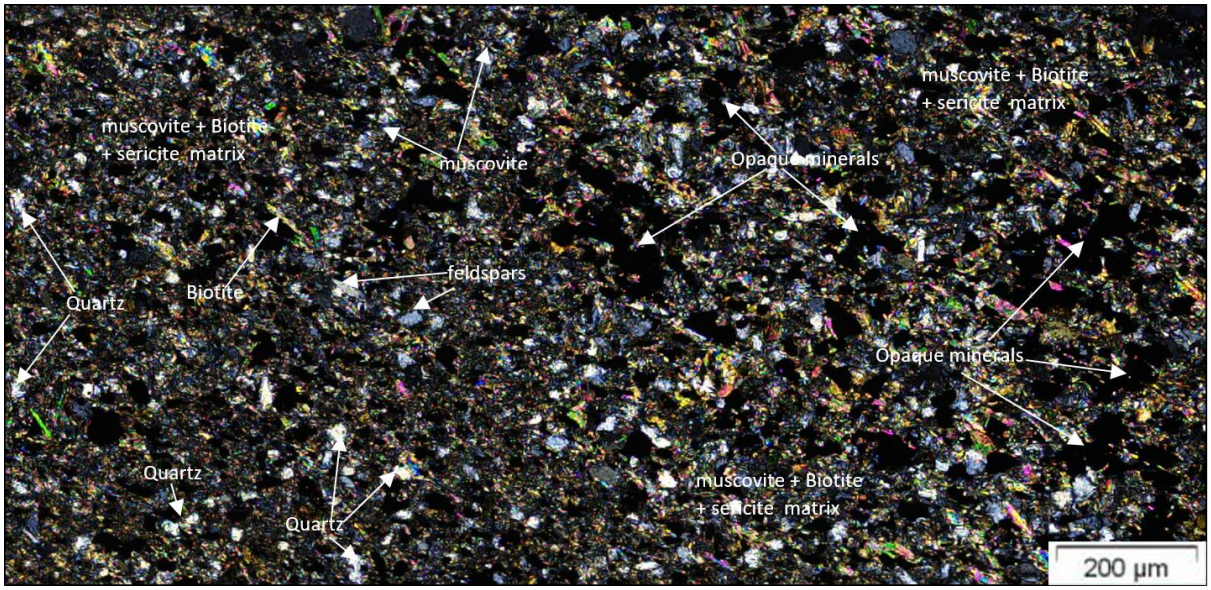

Figure 4-56: Photomicrograph showing TT024 image under XPL.

Under reflected light (Figure 4-57), there is a typical banding defining mineralisation zones. Fine chalcocite (greyish-pink grains) is mostly observed on bottom left to central part of the image. Chalcopyrite grains (yellow skeletal) cover the northeastern part of Figure 4-57, with some isolated pyrite (bright white) disseminations. Bornite (pinkish-brown) is observed interlocked with chalcopyrite and also replacing chalcopyrite. Iron hydroxide minerals comprising haematite and goethite surround and replace sulphide copper-bearing minerals.

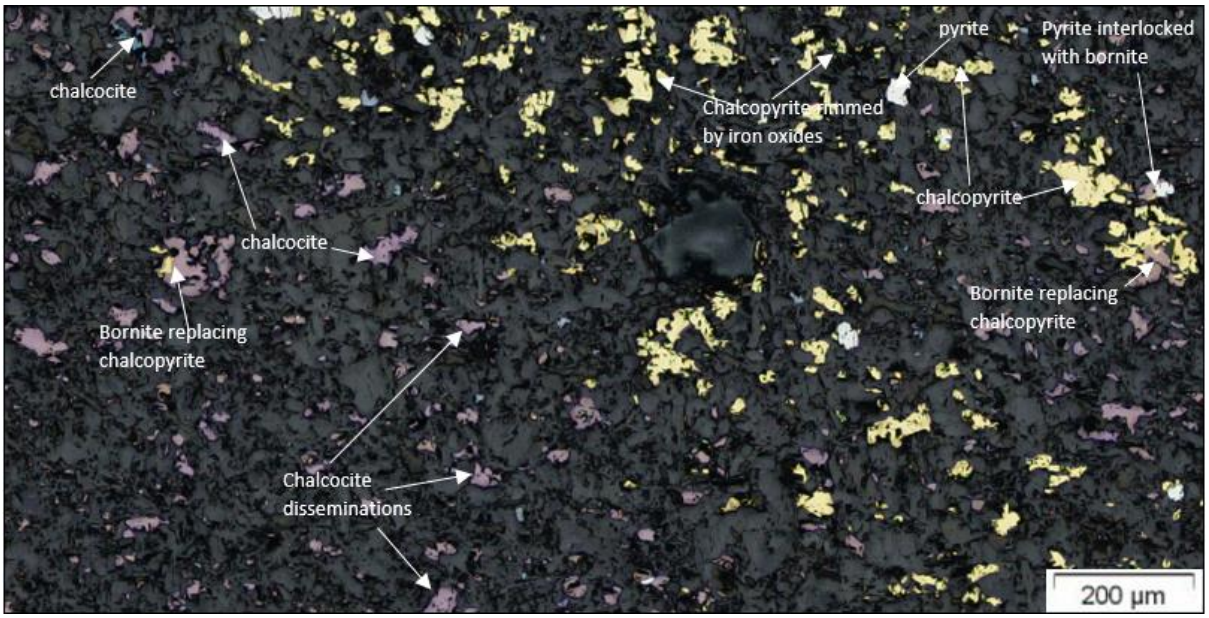

Figure 4-57: Photomicrograph showing TT024 image under reflected light.

4.6 SPATIAL DISTRIBUTION OF COPPER-BEARING MINERALS IN THE LUBAMBE MINING AREA

4.6.1 DATA COLLECTION PROCEDURE

The Lubambe ACQUIRE database has OREMIN1, 2, and 3 as the three fields of observation for the ore minerals. A style code is allocated for each individual mineral species entry and estimated percentages of the proportion present each mineral represent over specified intervals. In the case of Lubambe, each field (OREMIN1, 2 and 3) can be filled by any copper mineral depending on its dominance on that interval which makes it difficult to tie in or search for a specific dominant mineral for the entire member. The method adopted in this study was to text sort (using the excel spreadsheet functions) separate fields for different copper-bearing minerals such as chalcocite, chalcopyrite, bornite, malachite, chrysocolla, pyrite and limonite with the minerals whose quantities were visually estimated in the logs. The visual estimates are presented as texts in a variety of statements. These statements were then converted to numerical quantities with percentage estimates for each mineral over each sample interval (Table 2).

Table 2: Numerical values derived from text in the ACQUIRE database

Text Statement	Numerical Conversion %
<1%	0.5
1-2%	1.5
2-3%	2.5
2-4%	3
2-5%	3.5
4-6%	5
5-10%	7
trace	0.2
moderate	2
minor	1

A weighted average for each mineral in each sample over of the total mineralised interval in each hole was then calculated. The table was then imported into ArcGIS project and a series of plots showing distribution of ore minerals over the whole project area plotted (Figure 4-53 - 59).

4.6.1.1 Chalcopyrite

The drill holes on the edges of the East Limb and South Limb were meant to intersect the orebody at shallow levels. Figure 4-58 shows little chalcopyrite mineralisation on the edges of the East Limb as well as the South Limb. This is due to orebody intersections being attained whilst in the oxide zone. However, chalcopyrite is noted in the drill holes further away from the edges of the orebodies and there is a distinctly higher percentage of chalcopyrite on the South Limb than the East Limb (Figure 4-58). On the East Limb, general average percentages of chalcopyrite are below 3% whilst in the South Limb, chalcopyrite percentages get as high as >3%. Also notable is a significant number of holes with chalcopyrite on the southeastern part of the Extension Area. The central part of the Extension Area has some isolated areas with slightly elevated chalcopyrite which may be attributed to the reduced drilling density.

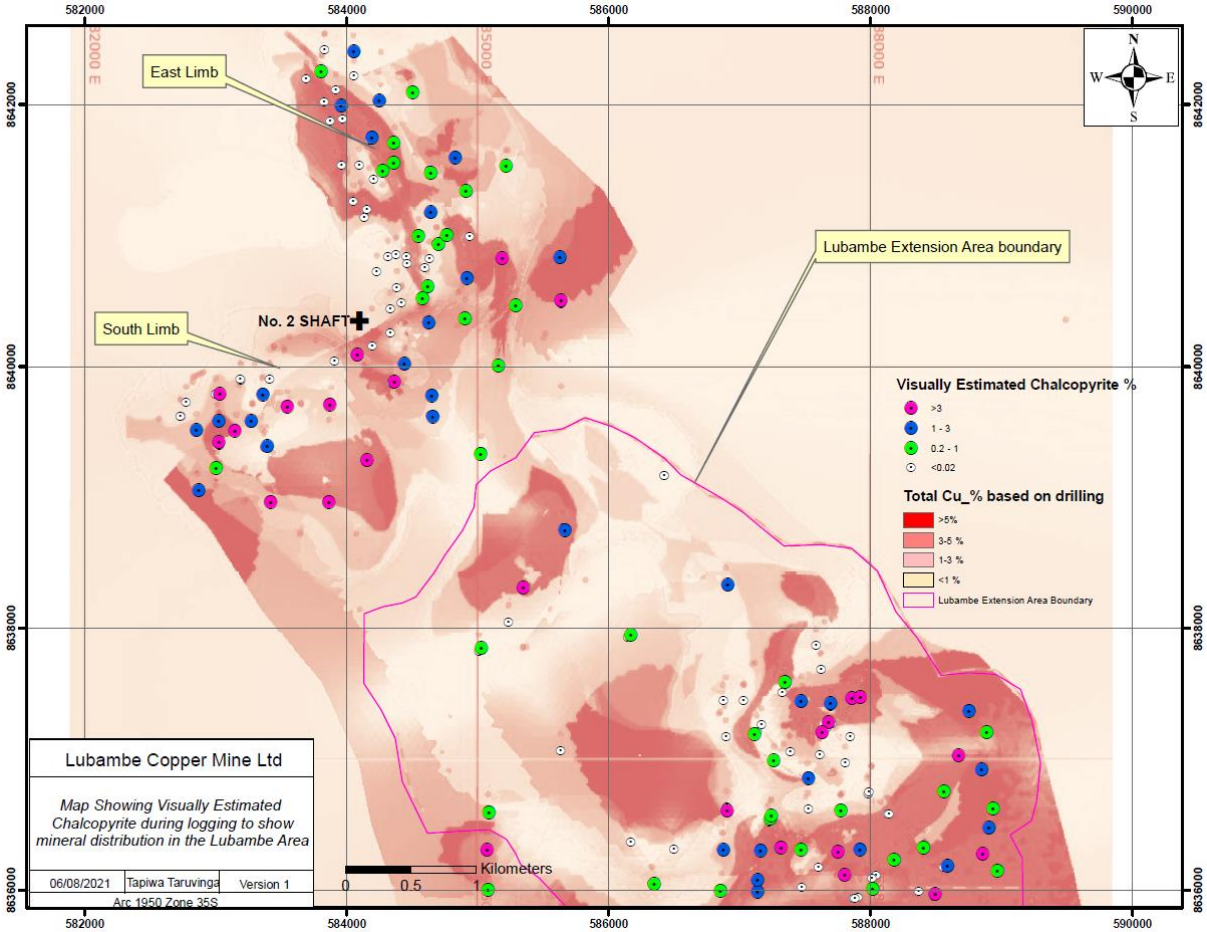

Figure 4-58: Plan showing chalcopyrite distribution in the Lubambe Area as visually estimated in drill core.

4.6.1.2 Chalcocite

The plot for chalcocite shows significant percentages in the holes that intersected the OS1 Member nearer surface on the East Limb (Figure 4-59). On the South Limb, chalcocite is moderate at deeper levels further down-dip of the orebody. The Southeastern part of the Extension Area has high percentages of chalcocite resulting in high total copper overall percentages. Indications are that the near-surface chalcocite is due to supergene enrichment whereas that in the deeper levels down-dip especially on the East Limb and Southeast of the Extension Area is probably hypogene in origin.

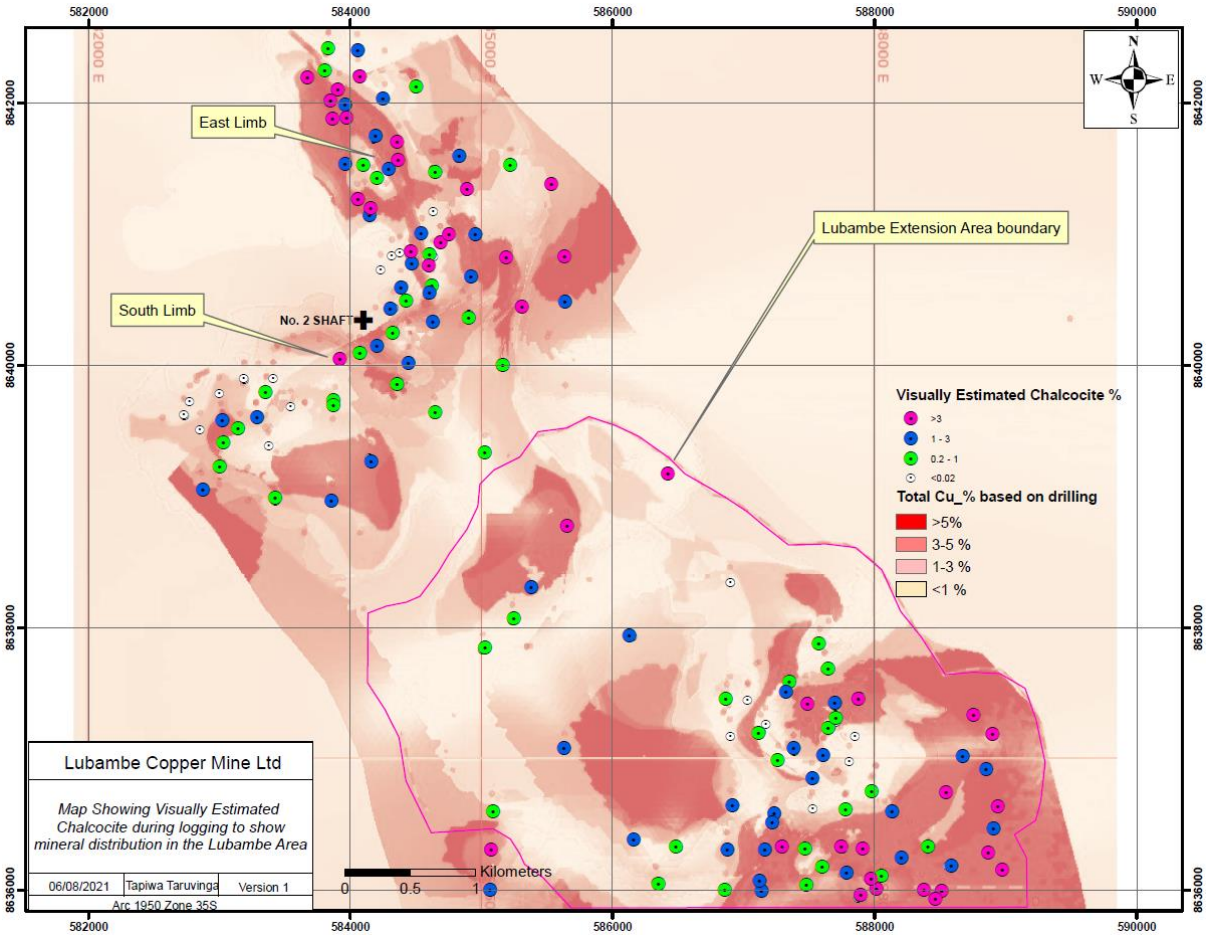

Figure 4-59: Plan showing chalcocite distribution in the Lubambe Area as visually estimated in drill core.

4.6.1.3 Bornite

The plot for bornite shows a marked area of enrichment at depth in the East Limb (Figure 4-60). Lesser amounts of bornite with moderate percentages of between 1 - 3% are recorded in the South Limb and the Extension Area. The absence of significant bornite mineralisation in the South Limb provides evidence of a lack of distinct copper mineral zonation in some areas. However, it is a different case in the East Limb where strong chalcocite and bornite presence down-dip was observed, indicating evidence of copper mineral zonation at depth. Bornite mineralisation intersected is interpreted as a hypogene pattern.

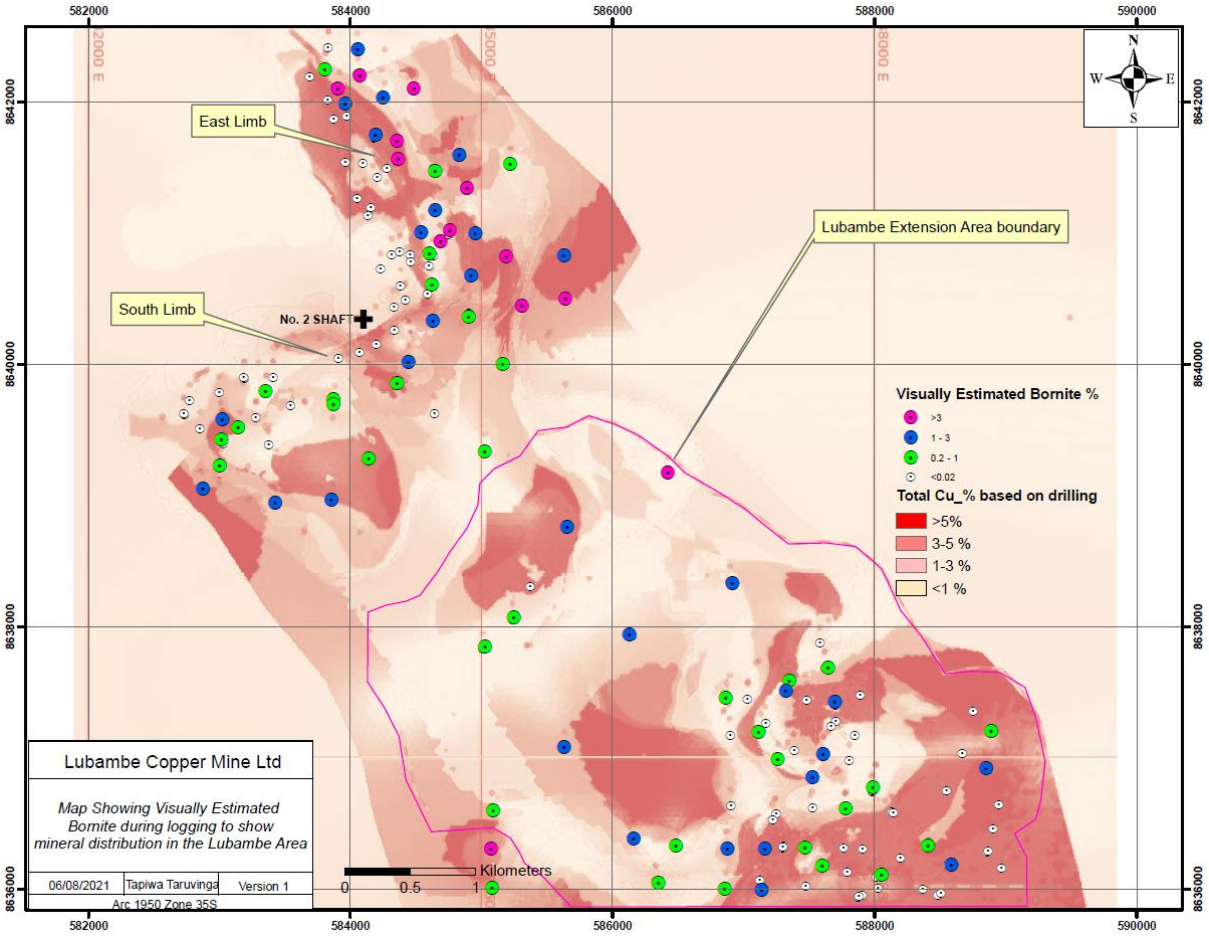

Figure 4-60: Plan showing bornite distribution in the Lubambe Area as visually estimated in drill core.

4.6.1.4 Pyrite

The plot for pyrite shows relatively few pyrite-rich holes in all the deposits (Figure 4-61). Most pyrite was observed in the Mwashia (shales and dolomites) and the Lower Kundelungu Groups. In holes where pyrite was found in higher percentages above and below the OS1 Member, the copper mineralisation and composite grades obtained were poor.

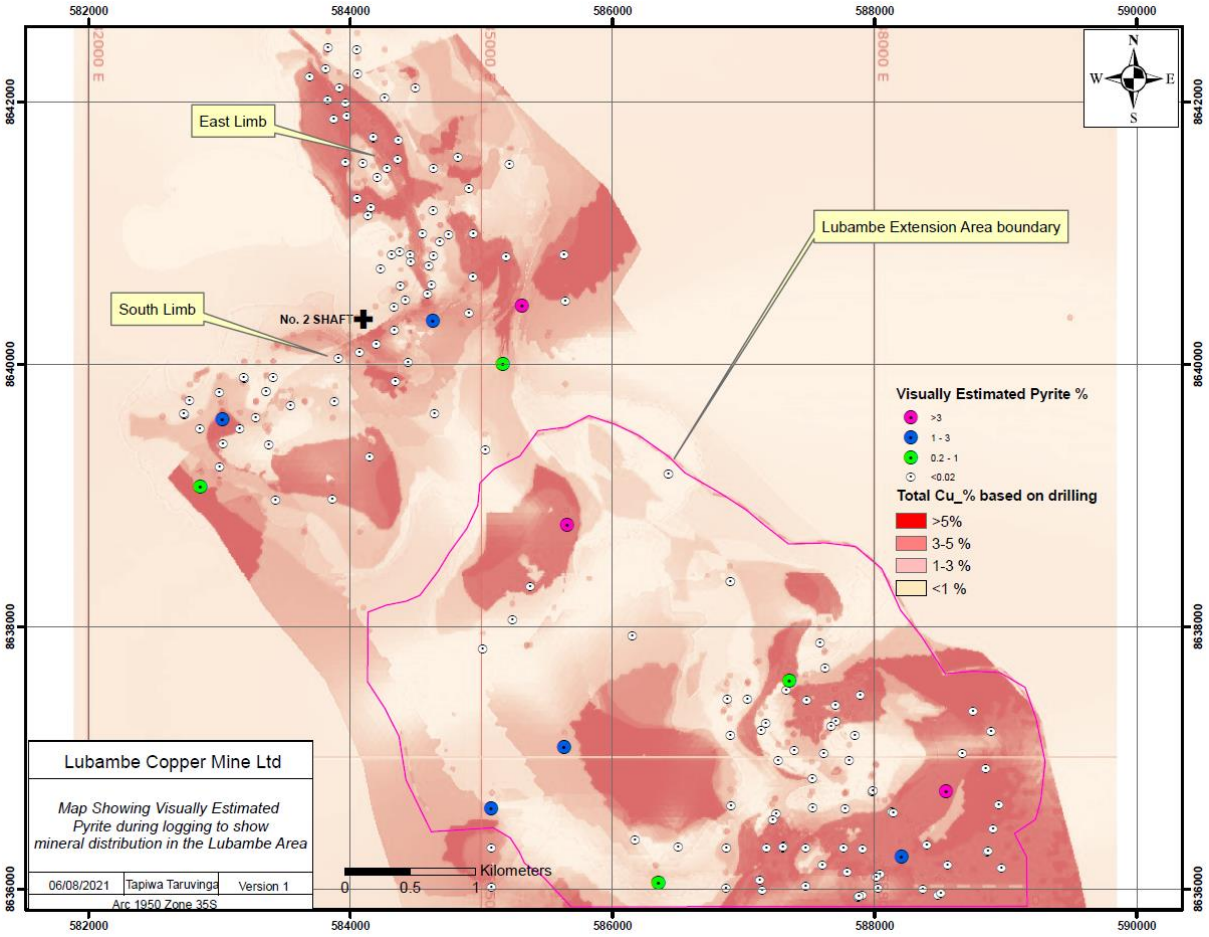

Figure 4-61: Plan showing pyrite distribution in the Lubambe Area as visually estimated in drill core.

4.6.1.5 Limonite

Limonite was mainly observed near surface, with more recorded in the South Limb than other orebodies (Figure 4-62). This was attributed to higher proportions of chalcopyrite in the original hypogene ore (Sutton and Maynard, 2005). The East Limb and Extension Area have some scattered holes with high proportions of limonite at depth. This is attributed to increased porosity through fracture links and joints connected to surface which enable groundwater to percolate through (Simposya and Hart, 2008).

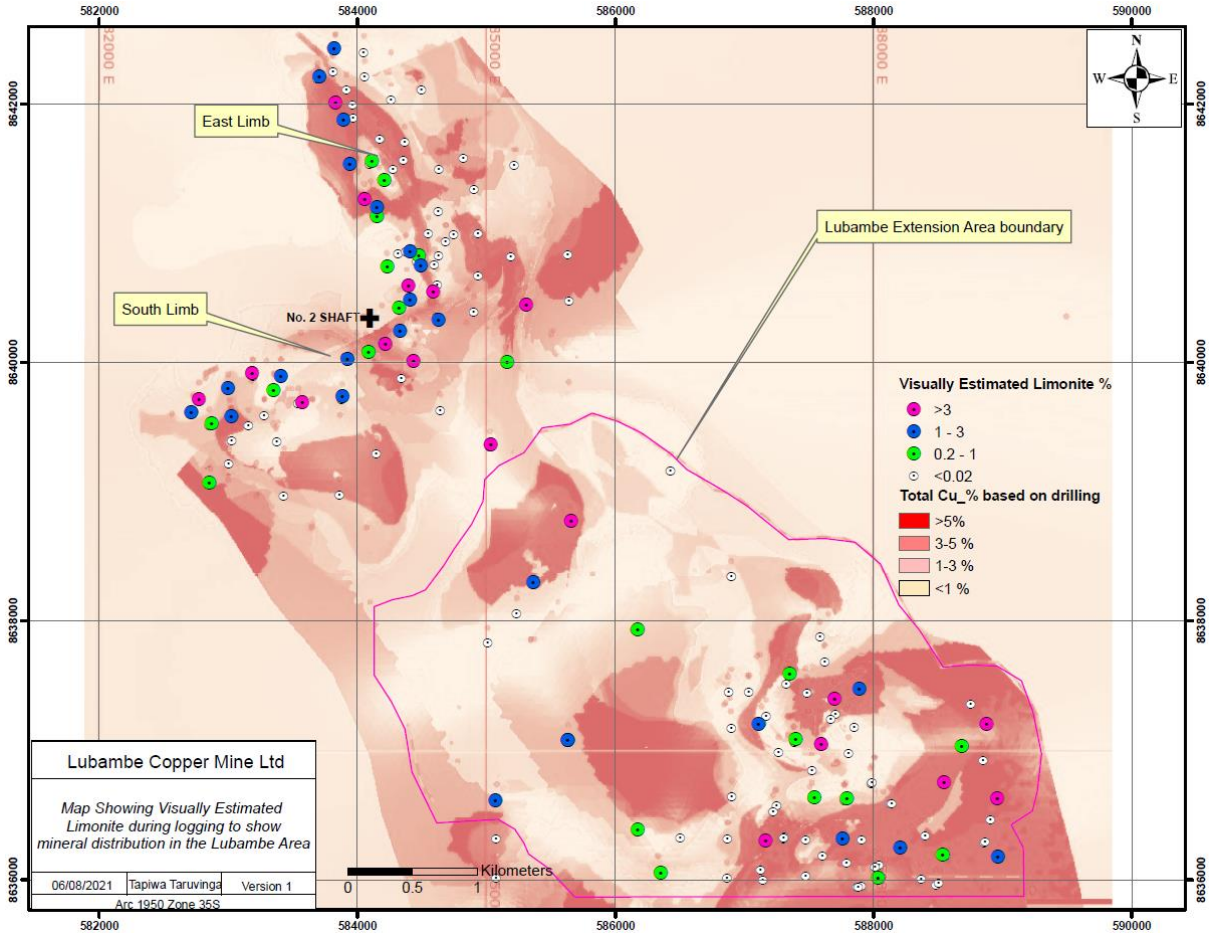

Figure 4-62: Plan showing limonite distribution in the Lubambe Area as visually estimated in drill core.

4.6.2 TOTAL COPPER DISTRIBUTION IN THE LUBAMBE AREA

The results of the Lubambe drilling program show continuous mineralisation over an area of approximately 30 km² encompassing the Musoshi orebody in the north, Lubambe orebodies at the centre of the basin, and the Konkola orebody in the south. A geological resource of nearly 300 Mt of copper at an average grade of 2.5% TCu is defined (AMEC, 2014; Reid, 2020). Copper distribution within the Lubambe area has been shown to vary as a result of supergene processes to certain surficial depths then become more structurally controlled at deeper levels (Subramani, 2018). Major structural features affecting both primary and secondary copper distribution laterally and at depth include joints, folds, faults and fractures. Replacement of primary ore minerals by secondary minerals is very common especially where supergene processes are prominent. In the Lubambe area, evidence of remnant signatures of hypogene primary mineralisation still exist especially in the East Limb and Extension Area together with zoning patterns related to hypogene mineralisation (Simposya and Hart, 2008).

Figure 4-63 shows a TCu distribution map plotted using geochemical assay results from the project area. Despite some of the results being constrained by widely separated data points (boreholes) in some sections, mineralisation and copper distribution trends can be picked from the map. An elongated roughly north-south, 200 m to 1200 m wide weakly mineralised or barren zone occupies the area between the fold nose (between the East and South Limb) and the Extension Area. Mineralisation is richest in the southeastern part of Extension Area where it increases to grades of approximately 12% TCu (Figure 4-63). The mineralisation is correlated with increasing thickness of the Ore Shale Member (Figure 4-65). The other major formations also thicken consistently to the southeast.

The most striking features from the TCu distribution map are the two small depocentres, one on either side of the Konkola Anticline (Figure 4-63). The rich zone on the East Limb, with >3% TCu, laps around the plunging crest of the Konkola Anticline. It is separated from the higher-grade ores on the South Limb, about 4% TCu, by a lower grade zone, about 1% to 2% TCu, trending northeast (Figure 4-63). The high-grade zone appears to cross the crest of the Konkola anticline nose and extend to the southeastern side. However, drilling density is much lower in this area and so the structure and ore distribution is not well-constrained.

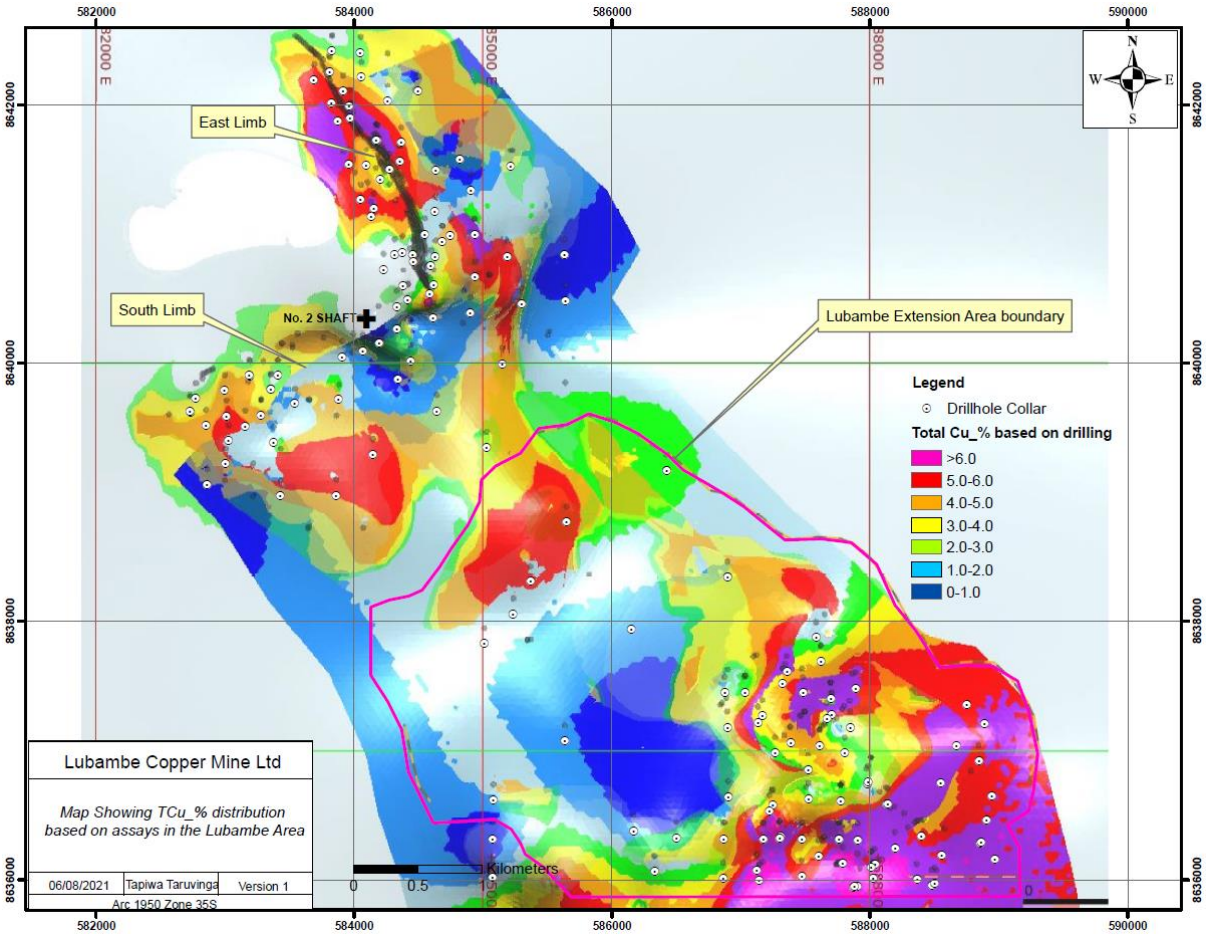

Figure 4-63: Plan showing Total Copper distribution in the Lubambe Area.

The distribution of TCu grades in the drill holes is generally lower at the upper and lower limits of the orebody, whilst the higher grades are at the centre. This is due to the application of assay grade contacts during grade and thickness compositing. The upper orebody normally has weak copper mineral disseminations as mineralisation diminishes towards the OS2 Member whilst the lower is dominated by oxide mineralisation and weak sulphide mineralisation in the footwall. Figure 4-64, is an illustration of drill hole traces KN114 and KN120 showing the grade distribution in the boreholes.

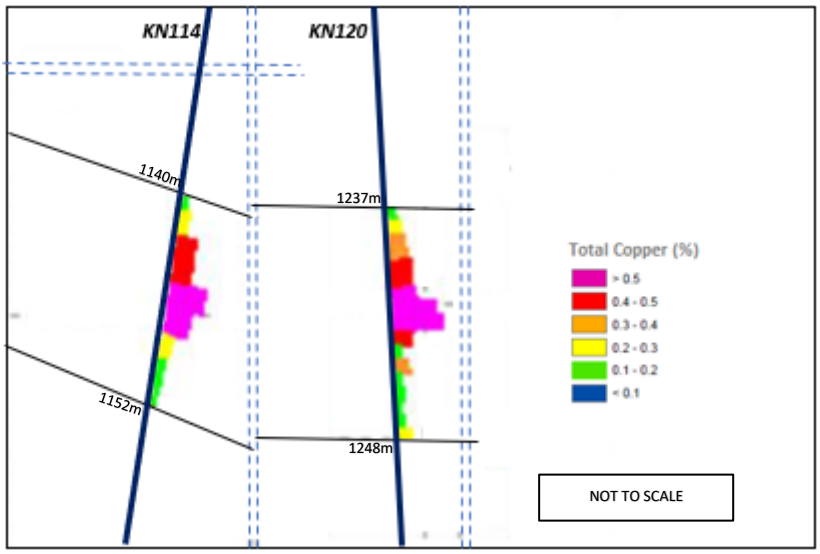

Figure 4-64: Illustration showing total copper distribution of drill hole traces KN114 and KN120.

4.6.3 TRUE THICKNESS MODEL

The Veining Tool in Leapfrog creates hanging wall and footwall contacts of the mineralised zone. The software is able to use this data to calculate the true thickness of every corresponding footwall and hanging wall triangle. This information was exported as points and used to estimate true thickness into the block model using the Estima process in Datamine. Thickness ranges from less than 2 m (colored in dark blue) to over 16 m (pink) (Figure 4-65). The thickest intersections are located on the southeastern portion of the project area where thicknesses exceed 10 m. East of this area, the plan shows intersections below 2m (Figure 4-65).

The orebody true thickness model at 1% TCu cutoff is shown in Figure 4-65. A low-grade block exists between the East and South Limbs and coincides with thin orebody thickness ranging between 2 to 4 m. Comparison of Figure 4-63 and Figure 4-65 shows a positive correlation between grade and thickness throughout the entire area. Steepest orebody dips are observed along the E-W trending South Limb orebody, whilst thin OS1 units are prominent at the edges of the Konkola Dome in both limbs (East and South Limbs) although this is attributed to some of the holes being collared within the outcrop of the formation. Thin orebody thicknesses are also observed on the northern part of the Extension Area (Figure 4-65).

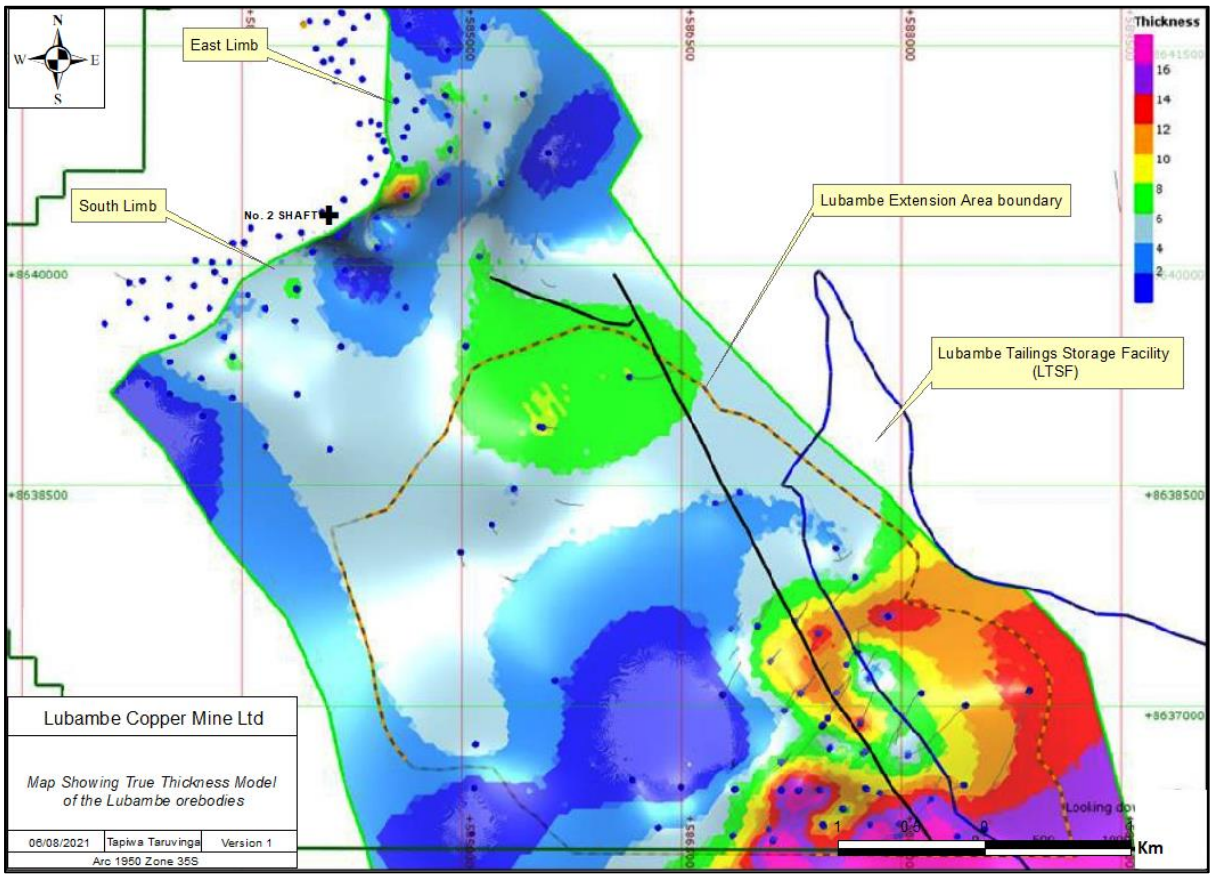

Figure 4-65: Plan showing the OS1 true thickness distribution plot of mineralised envelopes in the Lubambe Area.

The East and South Limb ore zones have average thicknesses of 5 - 6 m and are clearly differentiated from the lower grade fold nose zone and surrounding areas, which show thicknesses of 2 - 3 m. The southeastern margin of the project area has ore zone thicknesses greater than 10 m (Figure 4-65). Thicknesses of over 5 m have been observed in the centre of the project area, which corresponds with the centre of the structural basin. The areas surrounding the central part of the Extension Area have thicknesses of approximately 4 m (Figure 4-65).

4.6.4 ACID-SOLUBLE COPPER OXIDES

Acid-Soluble Copper (ASCu) is described as the fraction of Total Copper (TCu) recoverable in oxide copper deposits. ASCu assays are achieved by subjecting a sample of pulverized core material to sulphuric acid leach. Sulphuric acid will dissolve malachite and azurite completely, but only partially (~50%) dissolve the cuprite and tenorite minerals in the sample. Chrysocolla will not dissolve readily in sulphuric acid. ASCu assay values therefore reflect an incomplete dissolution of the minerals that are generally termed 'copper oxides'. Considering that the TCu assays represent total dissolution and hence all copper in the sample (including acid-soluble copper etc.), the difference between TCu and ASCu may approximate the copper associated with sulphide phases in the sample (Subramani, 2018). This is termed the Acid Insoluble Copper (AICu) where AICu = TCu – ASCu. However, it is important to note that this calculation does not represent an absolute measure of sulphide copper (Subramani, 2018).

In this study, the Oxidation ratio (OX_RAT) is calculated based on the ASCu and TCu assay results as received from the laboratory, and expressed as a ratio ASCu to TCu. In theory, this ratio should always be equal to or less than 1. During modelling, the OX_RAT was estimated using the Estima process in Datamine and the ASCu content was calculated and plotted from the estimated OX_RAT and TCu values (Figure 4-66).

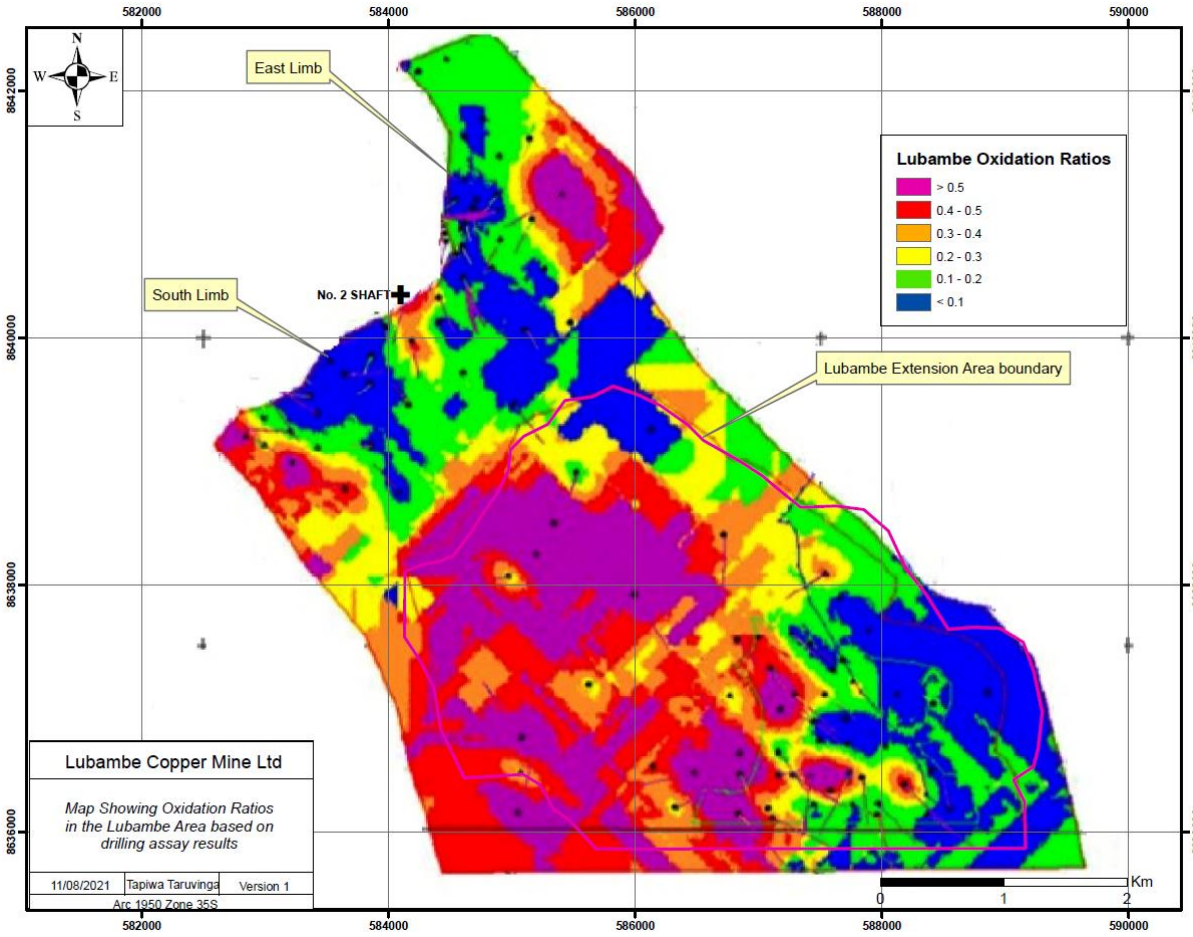

Figure 4-66: Plan showing oxidation ratios (OX_RAT) within the Lubambe Area.

The OS1 Member is closer to surface and more oxidised on the eastern part of the East Limb, northwestern and southwestern parts of the Extension Area, with oxidation ratios exceeding 0.5. This elevated acid-soluble copper content is related to near surface weathering processes operating to

depths of 300 – 400 m. The area to the southeast has a deeper OS1 and lowest oxidation ratios of less than 0.2. Below this depth, the acid-soluble content reduces to 15% and 13% on the East and South Limbs respectively (AMEC, 2014). Below a depth of ˜400 m, acid-soluble content and distribution thereof are related to structure throughout the area (AMEC, 2014).

It is critical to map in detail the distribution and proportion of ASCu as it strongly influences metallurgical process options and metal recoveries. The oxidation of sulphide copper in the Lubambe ore bodies is interpreted to reflect oxidation (weathering) along weak zones in the rocks, i.e., joints, faults, coarse-grained units, rock unit contacts, etc. Although drilling data shows highest values in holes near surface, copper oxides are very widely scattered throughout the entire project area suggesting considerable groundwater flow at depth. Oxidation at these depths does not reflect a progressive profile, but its severity entirely depends on circumstances in the rock units.

CHAPTER 5

DISCUSSION

5.1 INTRODUCTION

This chapter discusses the combined findings of this study to give an indication on whether the study achieved the set objectives or not. Data from literature review, interpretations by other scholars and studies in similar geological environments are given reference to as a way to compare and make sense of the findings. Based on the study findings, targets for further exploration are suggested to practically test the logic and concepts obtained from this study.

5.2 RELATIONSHIP BETWEEN STRUCTURES AND MINERALISATION WITHIN THE PROJECT AREA

The aeromagnetics data from surveys carried out in the Lubambe license area were downloaded from the database. The datasets were largely dominated by shallow responses but there were also some distinctive responses from several units defining the lithologies and structures. Geophysical structural interpretation was carried out by Jon Woodhead in 2006. In his interpretation, Woodhead (2006) notes several major and intermediate structures forming lineation trends from the regional high resolution airborne aeromagnetics (Figure 5-1). Woodhead (2006) interpreted lineation/trends as having been caused by major structures then inferred and extrapolated fault structures and signatures. These can be seen in the structures of the three basins on the eastern side of the Extension Area (Figure 5-1).

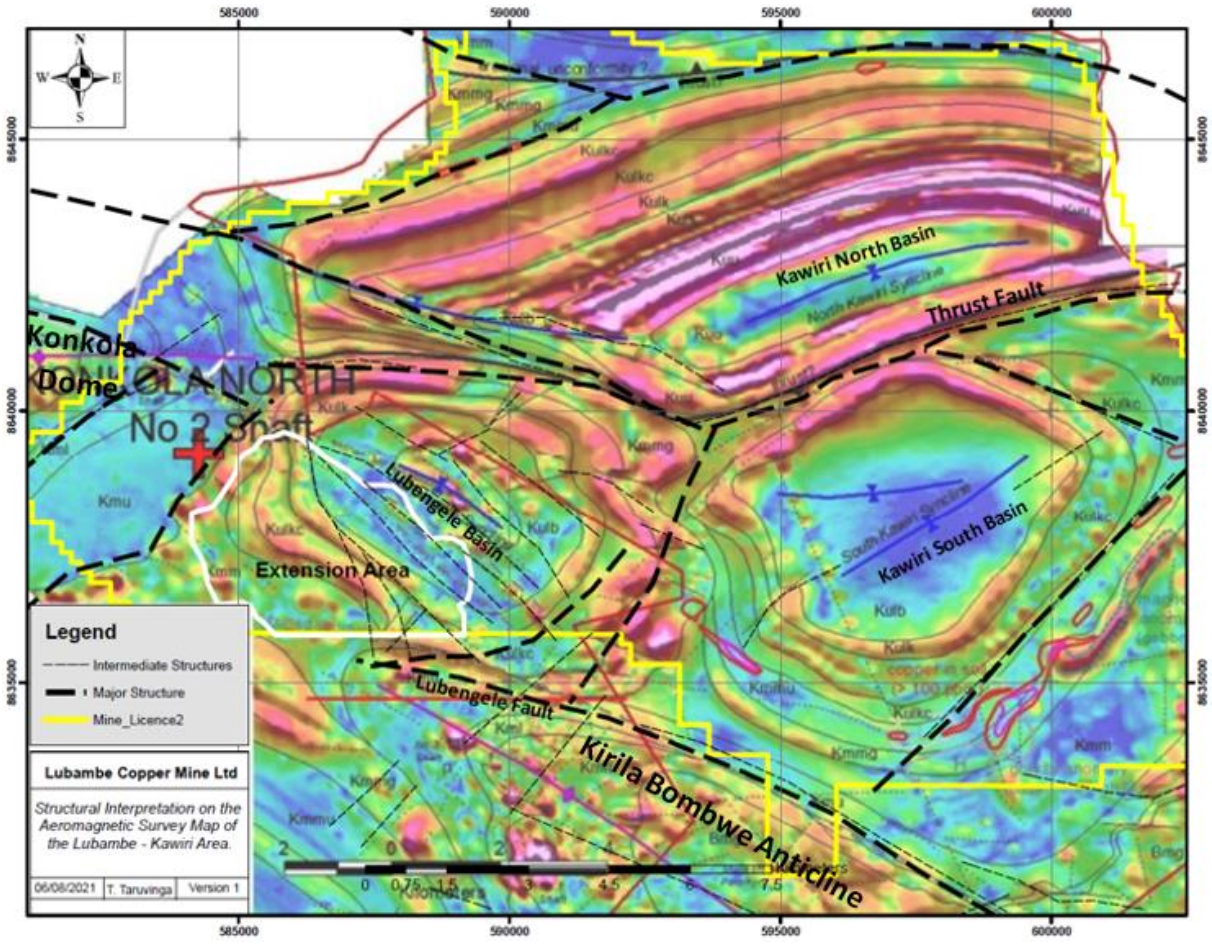

Figure 5-1: Map showing structural interpretation of the Lubambe aeromagnetic data. (after Woodhead, 2006).

Within the Extension Area there is a set of major faults trending NE-SW crossing the intermediate faults trending NW-SE (Figure 5-1). Generally, these faults are most easily identified by displacement in the Kundelungu Group rocks, but they probably extend into the Mwashia Formation as well. This trend is the Lufilian trend and is parallel to several other features such as the Kirila Bombwe anticline. The magnetic map shows a discontinuity and an area of disrupted magnetic patterns to the south of the Lubambe license boundary. This could be the trace of what has been called the Lubengele Fault, which is based on the sharp differences in elevation of strata seen in the ZCCM historic drill holes (Knupp, 2006).

Soft-sediment deformation structures and abrupt changes in bedding angles in cores seen in the drill cores suggests prevalence of faulting at micro- and macro-scale. This is also supported by the presence of slump structures. This can also be taken as evidence of contemporaneous seismic activity along nearby faults. The prevalence of strong mineralisation in highly faulted areas suggests a strong relationship between structures and mineralisation (Figure 5-1). This favors the proposed mineralisation model (Figure 1-6) where mineralising fluids were channeled through growth faults at the margins of Lower Roan basins. Ore was then deposited from the pregnant copper-bearing fluids at the first redox boundary represented by the OS1 in the Lubambe project area. The fluid is assumed to have "ponded", resulting in continuous precipitation and deposition of copper. High-grade chalcocite and bornite became more concentrated closer to the faults, whilst chalcopyrite showed concentration further away from the faults due to mineral zoning (Sutton and Maynard, 2005). It has been further postulated that these extensional faults were later re-activated during the Mwashia event and much later, with basin inversion, they were reversed as thrusts during the Lufilian Orogeny (Daly, 1986).

Figure 5-2 is a schematic illustration based on the interpretation of the aeromagnetic data in the study area. Findings are that there are two basement features attributed to mineralisation within the Lubambe mining area and the Lubambe Extension Area. The first is the Konkola Dome with an easterly extension which plunges to the east under the Kawiri Basin, at the Central Hinge Zone. The second feature is the deep-seated Kirila Bombwe dome just southeast of the Lubambe No. 2 Shaft. The Kirila Bombwe basement has an ESE trend and to the NE it is overlain by the Lubengele Basin. The interaction of the basin and the basement high has resulted in deformation of the Lower Kundelungu Group units defining the basin. Katangan sedimentary rocks are folded and faulted whilst draping around these basement highs. The geometry of the Lubengele Basin is asymmetrical, it is shallower to the SW and the Kundelungu Group units dip shallowly to the NE and on the opposite side of the basin the same unit's dip to the SSW.

Major regional structures transecting the project area are predominantly NW-SE and E-W trending sinistral faults, thrust faults, anticlines, major synclinal basins, and basement domes (Figure 5-2). The synclines in the southern project area are characterised by relatively open asymmetrical shapes and consistent stratigraphy while the Kawiri North Syncline is slightly tighter and elongated in shape (Figure 5-2). The North Kawiri Syncline has also been largely affected by sinistral translation and the southern margin is bound by a major east-west trending, south dipping thrust fault (Knupp, 2006).

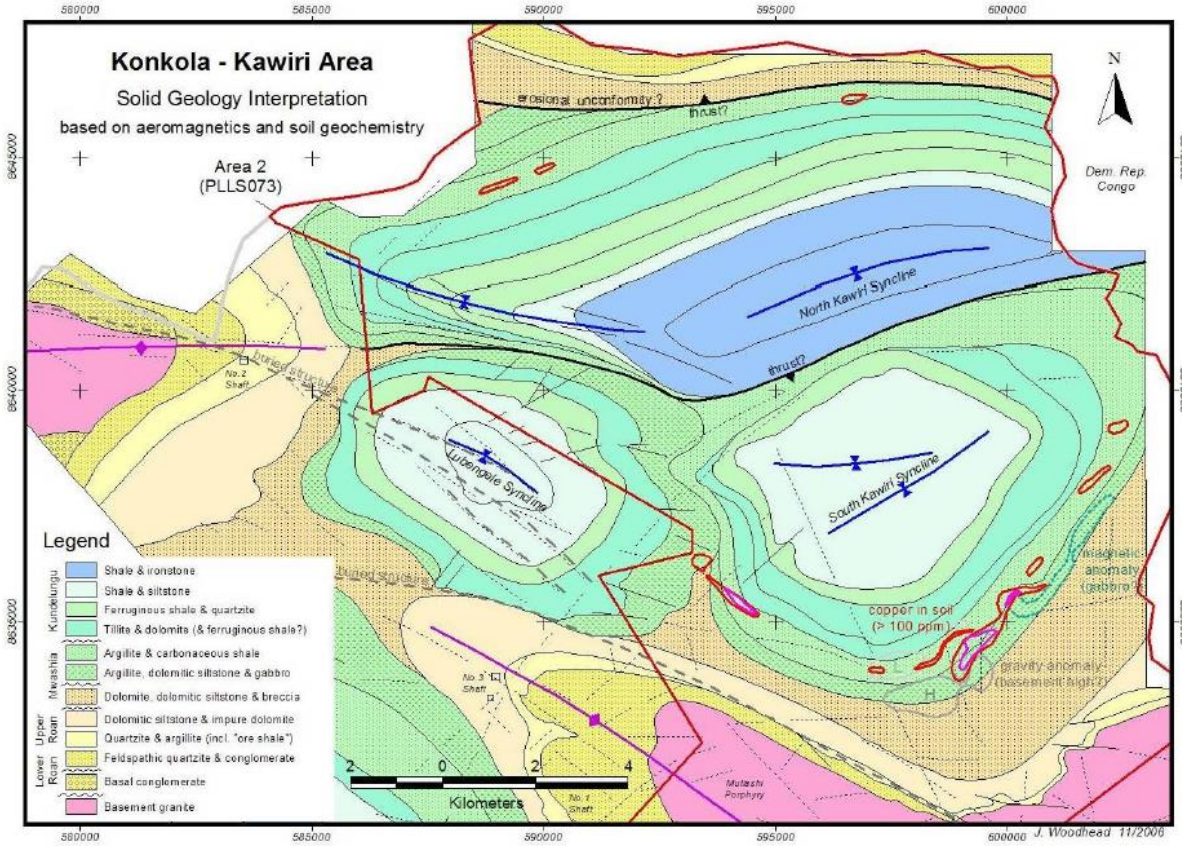

Figure 5-2: Map showing the Konkola-Lubambe geology and the interpreted structural framework of the Lubambe License Area (based on interpretation by Woodhead, 2006).

A thrust fault (Kawiri Fault) separates the North and South Kawiri Synclines and the stratigraphy within the fold nose of the Northern Syncline is internally folded (Figure 5-2). Anticlinal features are interpreted to have formed over thrust ramps in the basement horst block within the Lubambe license area and these features can also be identified within the eastern domain and south-central region of the project area (Carey and Cevallos, 2012).

Drilling results from the East Limb, South Limb and Extension Area show variations in grades, orebody thicknesses and continuity of the orebody in the Lubambe mining area. The drilling results were superimposed over the interpreted structural map to ascertain the influence of structures on copper mineralisation, distribution and spatial occurrence. Figure 5-3 is an illustration showing the variation in ore zone grades and thickness (TCu_% x Total Thickness) in relation to interpreted structures from aeromagnetic structural data.

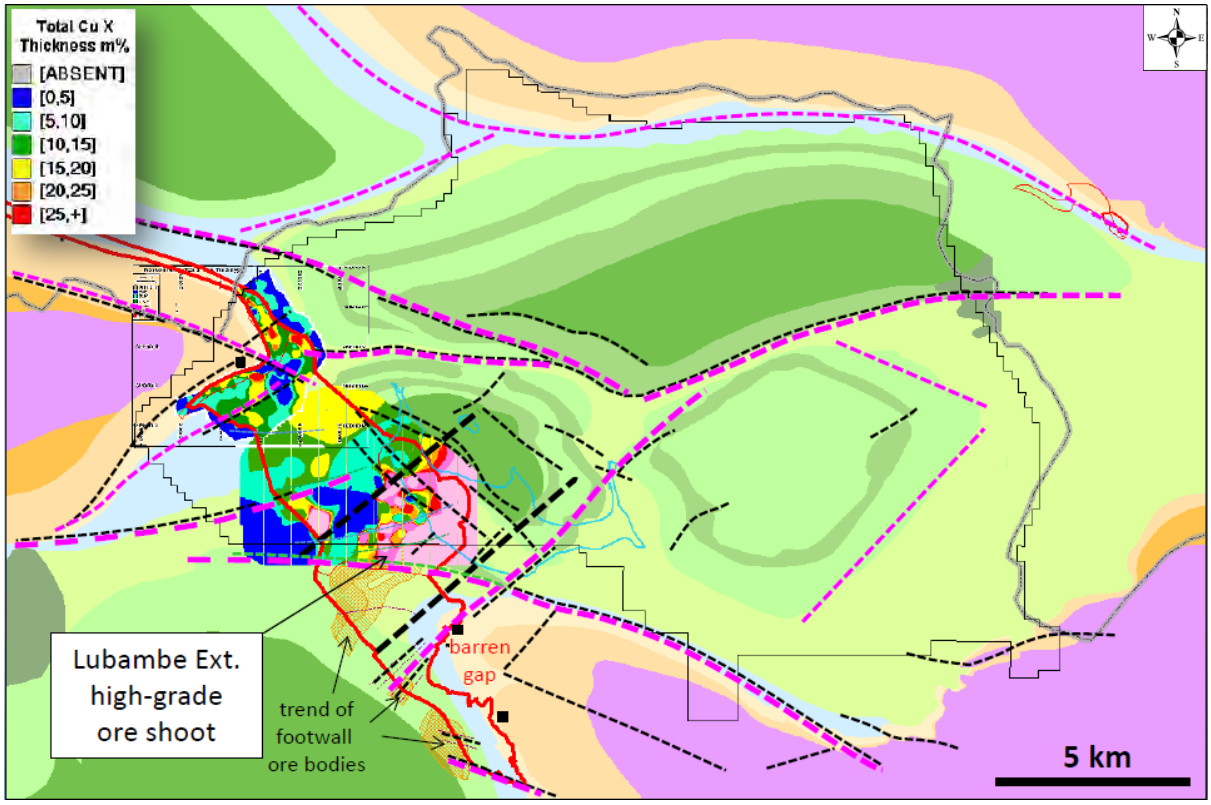

Figure 5-3: Illustration showing the Total Cu x Thickness spatial distribution in the Lubambe project area (sketch is based on interpretation by Woodhead, 2006).

Two higher grade zones are defined on the East Limb, that is, a major NW-trending zone that defines the major orebody trend and a weaker E-W trending zone. To the east, the orebody is abruptly cutoff at depth (based on drilling data) by a zone of intense fracturing and brecciation associated with K-Fe alteration (Anglovaal Mining, 1999a). Interpreted geophysical data show an intersection of NW-SE trending faults and a major E-W discontinuity. This event imposed itself onto the existing mineralisation, whilst associated with a K-Fe alteration, which later replaced sulphide mineralisation. Based on the drilling data, the alteration event is deemed responsible for the termination of mineralisation in the extreme north of the project area. Despite failure by several holes to reach the intended OS1 target there is evidence to suggest that the East Limb deposit probably links up with the Extension Area deposit at depth. Copper grade distribution near surface is unpredictable and inconsistent due to surficial weathering processes (Torremans et al., 2013).

The South Limb deposit has structures trending NW-SE interpreted to have contributed to re-mobilisation of secondary copper mineralisation, which resulted in mineralisation overprints (Sutton and Maynard, 2005). These structures control supergene enrichment processes and copper distribution as they allow copper-carrying fluids through veins, joints and fractures, thereby determining the concentration of high-grade and low-grade secondary minerals through their intensities.

In the Extension Area, sub-parallel NW-trending intermediate structures are responsible for higher grade zones, as is evident in Figure 5-3, separated by a lower grade block. Where the NW-trending intermediate structures intersect the NE-trending major structures in the southeastern part of the Extension Area, elevated grades and greater orebody thicknesses were obtained. Structural trends observed from interpreted geophysical data and structural logging coincide with regional lineaments determined through regional aeromagnetic and gravity surveys. Figure 5-3 indicates that the distribution of mineralisation is closely controlled by regional and local structures. Structural evidence

from drilling shows that they post-date initial mineralisation and were responsible for localising supergene and leaching processes.

5.2.1 Field Mapping

Despite the absence of outcrop over the greater part of the property, some major structural features and key stratigraphic contacts as defined in the geophysical data could be confirmed through field mapping. The portion mapped during field traversing correlates well with the detailed structures as observed in the aeromagnetic images and regional structural trends. Similar major lineament trends such as the prominent NW-trending and the E-W-trending lineaments were observed.

Field mapping findings were integrated to aid descriptions of geology, geophysical and stratigraphical interpretations. Although no direct orebody signatures can be seen on surface, results allow for extrapolations to be made regarding OS1 Member depths and potential controls on copper ore distribution.

5.2.2 Petrography

A variety of primary and secondary copper minerals were identified in the drill core samples analysed using a microscope. Of these, the most abundant are chalcopyrite, chalcocite, bornite and malachite +/- chrysocolla. However, what may have been identified as chalcocite in polished thin sections may probably be a combination of chalcocite and digenite as these two normally co-exist together and are difficult to distinguish (Darnley, 1960; Robb, 2005). Haematite and goethite are the most dominant iron oxides and normally occur in association with secondary copper minerals.

Hand specimens cut were ppredominantly moderately metamorphosed with clastic sedimentary textures and lamination bands. Weak to moderate foliation fabric could also be observed. The general appearance of the polished sections under the microscope was dominated by poorly phased phyllosilicates (mostly K-feldspar and quartz).

The Cu sulphides are mostly finely disseminated in silicate gangue minerals. The primary sulphides comprise chalcopyrite and bornite. Chalcopyrite is associated with pyrite. Alteration of these primary sulphides to chalcocite (digenite?) is evident in the form of rims surrounding the primary sulphides, cross-cutting of primary sulphides by secondary sulphides, and also inclusions of primary sulphides within secondary sulphides. Chalcocite and malachite were observed occurring in association with iron oxides (haematite or goethite). Oxide minerals generally showed larger average grain sizes than sulphide minerals. Where present, chrysocolla was always associated with malachite.

Petrography and copper element spatial distribution analysis show that the majority of copper minerals are fine grained, and mostly disseminated with secondary copper mainly occurring as fillings in joints, fractures and veins. Vertical zonation of copper minerals is noted particularly in the East Limb, Extension Area and the eastern side of the project area. Lubambe resource figures show more chalcopyrite related copper resource in the South Limb as compared to the East Limb and the Extension Area and this was confirmed by petrography (Figure 4-34 to 57) and copper element distribution analysis (Figure 4-58 to 66).

5.2.3 Copper-bearing Mineral Elements Distribution

Figure 4-58 to Figure 4-62 show evidence of lateral copper mineral zonation from chalcocite-bornite-chalcopyrite on the East Limb to the Extension Area. Zonation is not so clear in the South Limb (which is chalcopyrite dominated) but remains a possibility. The South Limb is chalcopyrite-dominated and shows evidence of a bornite hinge at depth (Figure 4-60). Shallow boreholes close to the Konkola dome have shown high limonite content (Figure 4-62) and a large spread of copper values which is an indication of copper mobility due to weathering and leaching processes. Vertical zonation of copper minerals (from chalcocite-bornite-chalcopyrite) is observed associated with an increase in copper content with depth and a decrease in iron and sulphur content. An idealised copper mineralisation profile has chalcocite enrichment at the base of the OS1 Member resulting in high-grade copper values diminishing upwards and gradually replaced by bornite which, in turn is replaced by chalcopyrite towards the top of the OS1 Member. The acid-soluble minerals are generally concentrated around the base of the OS1 Member, extending into the Footwall Conglomerate. This zone marks the zone of most intense leaching and represents a high permeability channel way for copper-bearing fluids.

Figure 4-58 to Figure 4-62 show evidence of primary sulphide mineralisation being originally more extensive in both the lateral and vertical sense but distinct patterns were disrupted by supergene processes (weathering, oxidation and leaching). Weathering, oxidation and leaching processes have been attributed to vertical distribution of copper at shallow levels whilst syn-deformational fluids along structures like faults, joints and fractures is attributed to copper re-distribution at depth. This resulted in depletion and enrichment of different areas thereby causing a spatial difference in copper distribution resulting in barren, low-grade pockets and high-grade pockets (Figure 4-63).

5.2.4 Oxide Copper Mineral Distribution

Through the OX_RAT analysis and modelling, this study managed to map out the distribution of leachable copper minerals and distinguish such zones from sulphide-rich floatable ore. The variability of the ore mineral distribution, and in particular, the relative proportion of acid-soluble oxide material, strongly influences mine production scheduling and metallurgical process route options.

In terms of ASCu, the East Limb and the southeastern part of the Extension Area have higher percentages as compared to the South Limb and the eastern drill holes. Oxidation of the upper zones of the deposit is evident from the presence of malachite, pseudo-malachite and chrysocolla. ASCu is mostly contained in carbonates, silicates and phosphates. Considering areas currently being actively mined (that is East Limb and South Limb), ore from the East Limb should be treated using the acid leaching extraction process whilst that for the South Limb should be treated using sulphide concentration extraction processes. The results of this study are consistent with chemical analysis performed on the samples and with the trends revealed by metallurgical testwork.

5.3 PROSPECTIVITY POTENTIAL OF THE PROJECT AREA

The potential to discover new copper deposits in the project area is considerable based on the prospective geology and structures, and similarities in the area to well-studied deposits elsewhere in the Copper Belt within the Katangan Supergroup. Several authors have suggested that in the Copper Belt mineralising fluids were focused along growth faults along the basin margins and that these faults may have been reactivated during subsequent orogeny or deformation (Unrug, 1988). Similar basin margin faults can be identified along the edges of the survey area in association with basement domes, as well as complex faults and fold structures surrounding the large synclines in the southern project area that may also be related to fault re-activations within the basin (Roberts et al, 2005).

The prospectivity of the Lubambe License Area is increased by the presence of previously unidentified small folded structures that may be related to thrust propagation folds or basement highs placing Lower Katangan sequences closer to surface. The strong link between ore formation and the development of structures during basin inversion and the Lufilian Orogeny supports the need to complete further exploration in the eastern domain of the Lubambe License Area to identify potential stratiform and/or vein copper mineralisation along the southeastern unconformable contact of the South Kawiri Syncline and within antiformal structures in the Mwashia Formation (McGowan et al., 2005).

A revised solid-geology (2D) interpretation map was compiled using the geophysical data in combination with geological data. Outcomes were used in conjunction with the 3D Lubambe model to identify residual exploration opportunities in the larger Lubambe License Area. The project area contains several prospective target areas for copper which were identified from the HELITEM data, in conjunction with magnetic data, radiometrics, and a detailed analysis of the geophysical responses of both lithologies and structures combined with geochemical data in the project area. These target areas require follow up work and possibly ground geophysical modelling to help constrain the minor structural and stratigraphic controls on potential copper mineralisation in the area. Anomalous features can generally be separated from the relatively flat-lying near-surface layer that also contains moderately anomalous values associated with weathering.

The project area is dominated by clusters of linear anomalies zoned into target areas (Figure 5-4), that align with interpreted and inferred structural and lithological boundaries including faults, fault splays/shears, geological contacts and unconformities. Immediate outcomes of the regional-scale exploration within the property include the identification of three priority exploration targets. These targets are located in the eastern side of the Lubambe License Area and are supported by orebody trends and structural features favorable to the hosting of copper mineralisation. All targets are conceptual in nature and require drill testing as a primary follow-up method. However, drill hole positioning may be aided by additional gravity or (CS)AMT surveys. Pitting may locally yield structural (dip) information. Anticlinal areas interpreted as having the potential to host mineralisation at relatively shallow depths (<1200 m) are prioritized. Figure 5-4 shows targets A and B whilst Figure 5-5 shows target C where further work has been recommended in the Lubambe License Area.

Targets A and B (Figure 5-4), are prioritised on the basis of structural features (interpreted growth faults) and the extrapolation of regional ore trends. Both anomalous zones lie where there is a strong electromagnetic profile shape and a coincident magnetic anomaly (Figure 5-1). Both localities take the shapes of structural embayment between major basins/synclines, which can be good fluid focal points for mineralised fluids to be channeled. They are also associated with folded structures at depth which could relate to structural and stratiform controlled copper mineralisation. The targeted areas contain several east-west trending linear discrete and bedrock anomaly clusters (red dots) that are proximal to major thrust faults separating the Lubengele basin and the North and South Kawiri Synclines (Figure

5-4). Bedrock and discrete anomaly clusters along the margins between major basins may reflect stratiform targets for base metals.

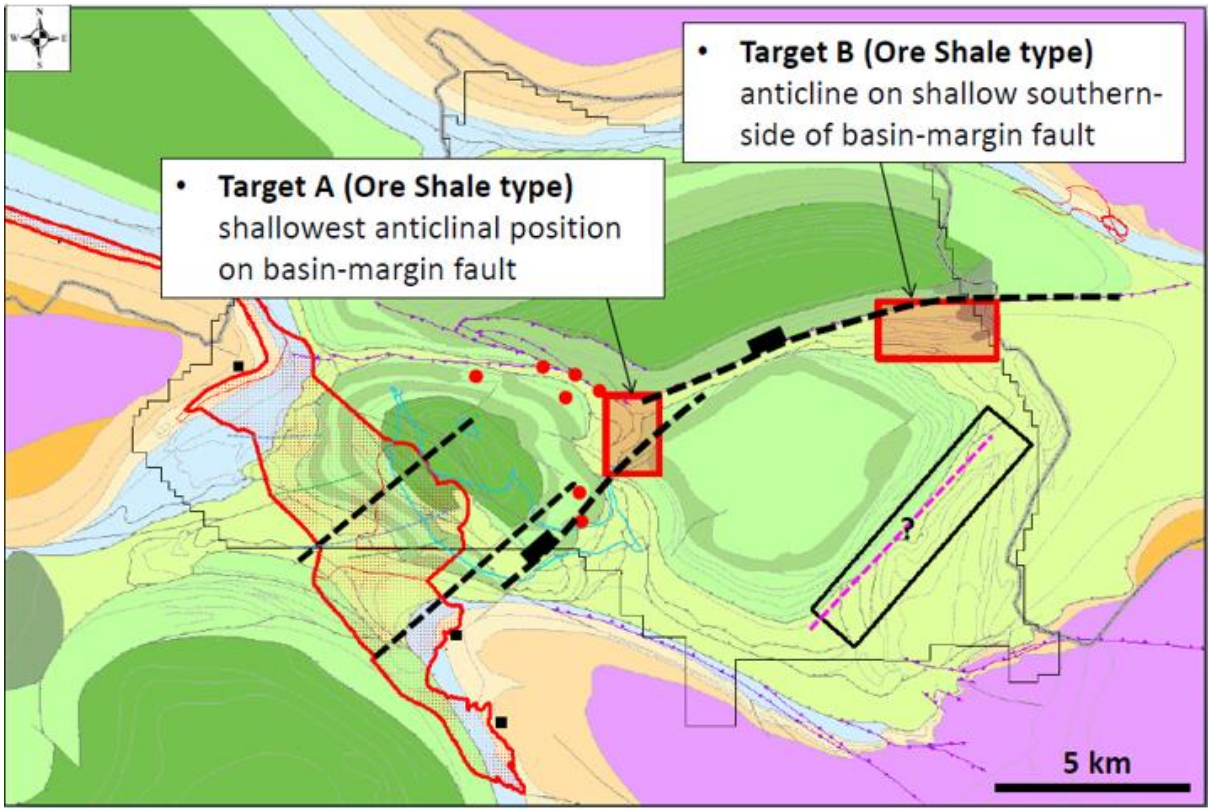

Figure 5-4: Illustration showing targets A and B recommended for further exploration in the Lubambe License Area.

Target C (Figure 5-5), represents an untested geochemical anomaly in a shallower Upper Roan/Mwashia Formation position. Soil sampling was done historically at 400 m x 400 m grid (Mwelwa, 2020). Linear features in the Mwashia Formation along the southern margin of the Kawiri South Syncline may reflect deeper mineralisation associated with known copper anomalies in soil geochemistry.

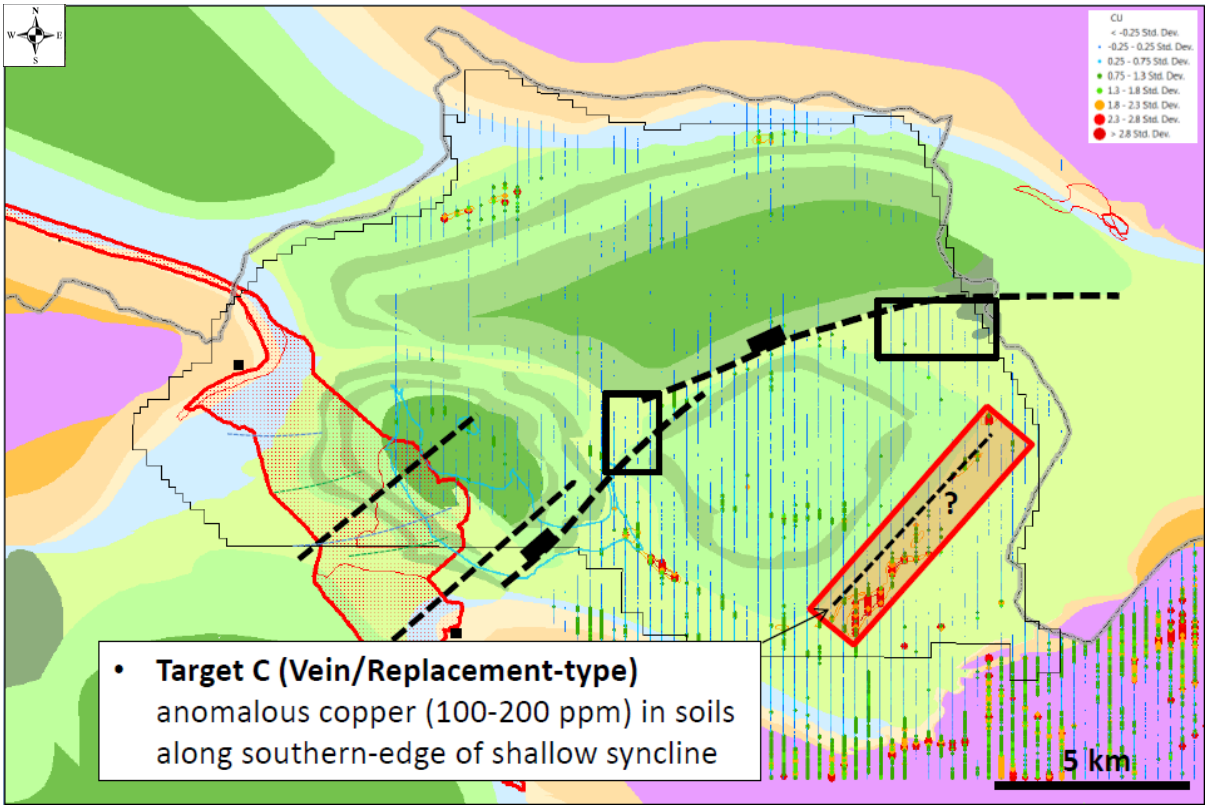

Figure 5-5: Illustration showing target C recommended for further exploration in the Lubambe License area.

Target C requires infill geochemical confirmation. Although existing geophysical data has not provided significant sub-surface information to date, further review of the data at the scale of each target is recommended. Specifically, geologically-constrained forward models of the gravity and magnetic data may help to elucidate target depths and dip orientations. Three principal sections through the Kawiri Basin should initially be modelled.

CHAPTER 6

CONCLUSIONS AND RECOMMENDATIONS

6.1 CONCLUSIONS

An integration and re-interpretation of geophysical and geological data in the Lubambe mining area and Lubambe East / Kawiri area has resulted in a significantly improved understanding of the geology of the area and potential controls on ore distribution. Despite limited subsurface information from the geophysical datasets, the exercise has provided significant confidence to detailed mapping of poorly exposed parts of the area. Interpretation outcomes from this mapping and geophysical surveys (aeromagnetic and gravity) suggest that the distribution of major folds reflects an early extensional, basement architecture which is thought to be key to ore deposit formation in the Zambian Copperbelt. Additionally, geophysical interpretation and geological modelling of the Lubambe-Konkola area has shown that a relationship potentially exists between ore distribution, fold axes and stratigraphic thickness trends. Specifically, the model suggests that both copper grades and Ore Shale thickness trends are controlled by NE-trending growth faults which can be traced to the eastern side of the property. Such relationships require further evaluation at a detailed scale for the purpose of grade prediction and improved drill hole targeting in the Lubambe Extension Area and also to provide direct support for exploration elsewhere in the basin.

The interpretation that best fits the data is the classic Copperbelt shale-hosted ore deposit model. The faults in the East and South Limbs were extension faults on the margins of sub-basins. A major basin margin fault lies to the south of the Extension Area. Ore fluids moved along the faults and deposited copper in the OS1 Member. The fluids were copper-rich nearest to the focus of fluid flux becoming progressively more iron-rich away from the focus. The ore fluids were also responsible for sericitisation, pyritisation and, perhaps silicification in the footwall and hanging-wall. It may be possible to use these early alteration patterns as ore guides. The presence of slump structures indicates that the faults were active during sedimentation. The possible correlation with mineralisation therefore suggests that the hypogene mineralisation is early, perhaps syn-diagenetic.

The generally higher copper grades and the increase in thickness of the ore zone (OS1 Member), in the southeast of the Extension Area shows that the southeast and eastern Lubambe are potentially richer than the East and South Limbs where current mining is taking place due to the high influence of crosscutting major and minor structures related to the Lufilian Orogeny and fault reactivation deformational events which opened up channel-ways for mineralised fluids to be focused through.

Gridding and contouring of the total copper grade reveal linear zones trending NW-SE and E-W. This trend is parallel to the dominant regional structural grain, as evidenced by the trend of structural features mapped from aeromagnetics, gravimetric, satellite imagery and aerial photography. Two of these zones define the East and South Limb deposits. The high-grade nature of the East Limb deposit is clearly evident. Of importance is the evidence presented in Figure 4-49 showing mineralisation distribution in the East Limb orebody as being contiguous with the southeast Extension Area orebody.

The investigation of ore mineralogy suggests that a supergene assemblage has been superimposed on an original hypogene pattern. The original hypogene pattern could have been zoned separately in three different centres. The East Limb probably had a core of bornite with an outer zone of chalcocite. The South Limb was slightly lower grade with less bornite and more chalcocite in the core but with richer chalcopyrite down dip. The southeastern part of the Extension Area also had a core of bornite, with an outer zone of chalcocite as noted from the increased chalcocite found at the northern margin

of the Extension Area and copper grades being richer in the extreme southeast suggesting that a zoning arrangement has been present. The outer chalcopyrite zones from all three centres merged to form a single hypogene deposit over virtually the whole project area.

The distribution of malachite, chrysocolla and limonite staining, together with much of the chalcocite, represents supergene enrichment in the shallower parts of the East and South Limbs and perhaps also associated with deep circulating groundwater in fractures elsewhere in the centre of the deposit. The effect of the elevated, and often variable, component of ASCu content on TCu is important for the assessment of the impacts on metallurgical processing and metal recoveries for the Lubambe ore bodies.

6.2 RECOMMENDATIONS

The main objective of this study is to provide a fundamental interpretation of the data available as a way to understand the controls of mineralisation, major lithological and structural features, spatial distribution and factors that influence copper distribution in the project area. Such interpretation enables identification of target areas for potential base metal mineralisation. This objective can be easily and better achieved if recommendations below are incorporated by Lubambe Copper Mine.

Lubambe Copper Mine can highly benefit from the integration of geochemical, geophysical, geological and drilling results to identify major and minor structures and stratigraphic features that control copper mineralisation and spatial distribution. Based on the prospective results and features identified, it is recommended that detailed follow-up ground geophysical data acquisition over target areas is done to delineate prospective copper mineralisation. The delineation of potential mineralisation and more detailed explanations of discrete anomalies could be achieved by additional geophysical modelling over the selected discrete anomalies indicated as target areas for further exploration.

The use of seismics to delineate the OS1 Member and deeper structures within the Lubambe License Area should be re-considered and executed properly. Seismic surveys can give vital information on deeper structural horizons, resolve some geological features that are of interest to the Lubambe drilling program and can also provide sufficient data to estimate thickness of the Kafufya Formation and basement contact. Other objectives of the seismic surveys should be to check if there are any lithological contacts within the Lower Roan succession which might be seismic reflectors and be used to delineate faults and other structures would have a direct effect on the location (depth) and continuity of the ore-bearing unit. If the seismic method could resolve one or more reflectors that could be used to locate the ore bearing unit, then the method could be used to reduce some of the drilling costs, that is, seismics could basically fill in the gaps between wider spaced boreholes. Furthermore, seismics can assist in the mapping of faults and other structures which is critical not only for locating the ore-bearing unit, but also to establish continuity of the ore zone for future mine planning. It is also recommended that seismics be done with some of the survey lines positioned over existing boreholes to provide geological control on the data.

Structure is a significant control on the distribution of mineralisation in the area. Therefore, core orientation should be carried out where possible in order to enable collection and interpretation of structural data from drilled holes. Currently, only five holes (drilled between 2018 to 2020) have structural data recorded whilst the rest of the holes have no structural data. Structural data collection should also include identification of fold hinges and fold intersections. Folding within the project area is characterised by zones of brecciation, contortion and a highly variable mineral content. Fold intersections are commonly sites of oxidation, leaching and brecciation of ore which directly affect

the quality of mineralisation. Fold hinge zones are sites of potential dilatancy and jointing which act as permeability channel-ways to groundwater movement.

It is recommended that a study be carried out to evaluate the mineralisation and resource lying underneath and east of the LTSF, where very high-grades and wide orebody thicknesses were intersected (Figure 6-1). This will clarify whether mining underneath the dam is feasible from a geotechnical and techno-economic perspective.

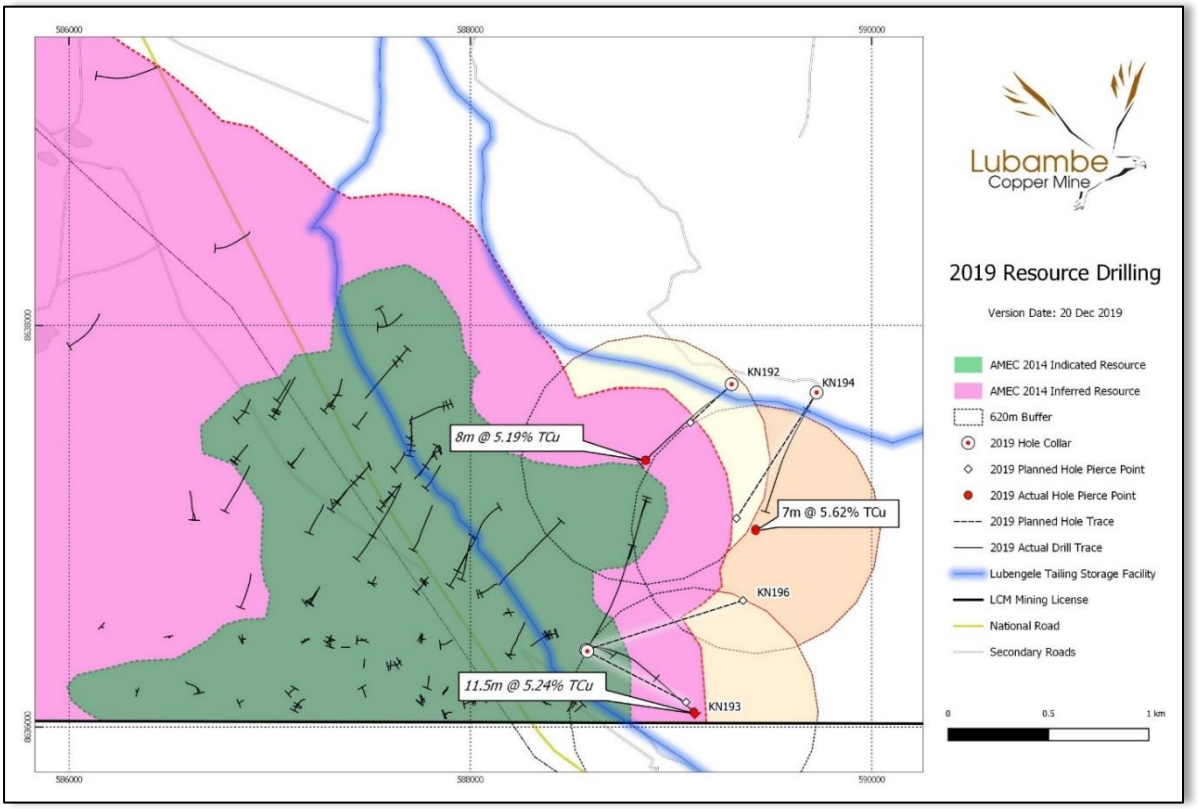

Figure 6-1: Plan showing intersections underneath the Lubengele Tailings Storage Facility (boundary shaded in blue) from the Lubambe 2019 – 2020 drilling (Stacey, 2020).

Further exploration on the eastern side of the Extension Area across the Lubengele Tailings Storage Facility should include the OS5 Member as a secondary orebody during ore resource evaluation. Results from the 2019 – 2020 drilling have proven that it has economic grades significantly above the current mining cutoff grades and sizeable thicknesses (>5 m) that can be exploited in future. Core logging in boreholes KN192 and KN194 (Figure 6-1) show thick OS5 zones with disseminations and strong mineralisation of chalcopyrite, bornite and chalcocite. Figure 6-2 and Figure 6-3 summarise the results from KN192 and KN194 intersections.

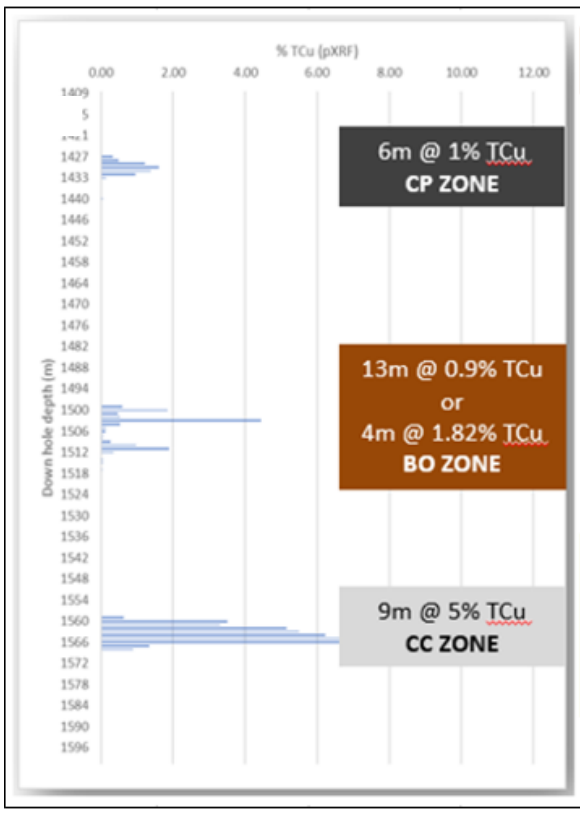

From (m)	To (m)	Interval (m)	Description
1,422	1,428	6	Chalcopyrite mineralization in OS5 as disseminations and veins demonstrating carbonate replacement. Moderate grades.
1,559	1,569	10	Chalcocite mineralization in OS1 as fine disseminations, blebs, and veins. Associated with cobaltoan carbonate on fractures and vein fills. Copper oxides present within footwall arkoses. High grade.

Figure 6-2: Showing plotted assay results for OS5 and OS1 Member intersections from borehole KN192 (Stacey, 2020).

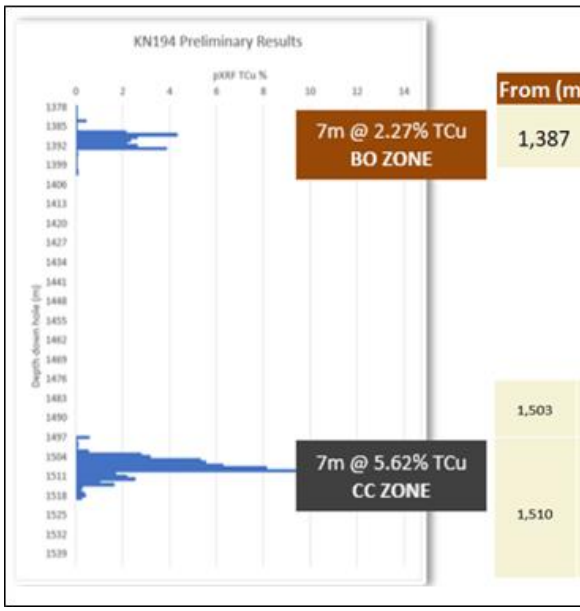

From (m)	To (m)	Interval (m)	Description
1,387	1,394	7	Bornite with chalcocite replacement occurring in the OS5 shales/siltstones and dolomitic shales.
1,503	1,510	7	Argillite-hosted (OS1) high grade disseminated chalcocite mineralization (up to 12% TCu).
1,510	1,515	5	Arkose and conglomerate-hosted (Kafufya Fm) copper mineralization as chalcocite, copper-oxides and native copper. Grade decreases with increasing depth into footwall.

Figure 6-3: Showing plotted assay results for OS5 and OS1 Member intersections from borehole KN194 (Stacey, 2020).

Zones of relatively high oxidation should be delineated and used when estimating the oxidation ratios into the block model. Oxidation domains may represent a proxy for major structural discontinuities. The variability of the ore mineral distribution and, in particular, the relative proportion of acid-soluble oxide material, strongly influences mine production scheduling and metallurgical process route options. Therefore, it is critical to map out the distribution of leachable copper minerals and distinguish such zones from chalcopyrite-rich floatable ore.

The drilling density in the project area needs to be increased in order to have an increased sample population for analysis and better constraint some of the mineralisation distribution trends. Having closely spaced holes will also enable a better understanding of the spatial continuity and variation of mineralisation at closer spacing. Wedges and hole deflections can also be used during drilling to increase the number of mineralisation intersections. The data generated can also be used in production planning prior to the extraction by mining.

REFERENCES

AMEC, E. S., 2014. Konkola North Resource Update, Chililabombwe, Zambia. Unpublished report, p. 1-69.

Anglovaal Mining., 1999a. Konkola North Project Prefeasibility Study – Detailed Technical Work – Report. Konnoco (Zambia) Limited, October 1999, v. 1, p. 1-36.

Annels, A.E., 1974. Some aspects of the stratiform ore deposits of the Zambian Copperbelt and their genetic significance, *in* Bartholome, P., ed., Gisements stratiformes et provinces cuprifères [Copper-bearing provinces and stratiform deposits]: Liège, Belgium, Société Géologique de Belgique, p. 235–254.

Arthurs, J.W., Mwelwa, E., Vila, S., 2009. A review of the geology of Area A Konkola North Project. Internal Report, Unpublished, p. 1-22.

Barra, F., Broughton, D., Ruiz, J, and Hitzman, M., 2004, Multi-stage mineralization in the Zambian Copperbelt based on Re-Os constraints: Geological Society of America Abstracts with Programs, v. 36, p. 5-516.

Bhattacharrya, B. K., 1978. Computer Modelling in Gravity and Magnetic Interpretation, Geophysics, v. 43, p. 912-929.

Binda, P.L., and Porada, H., 1995. Observations on the Katangan breccias of Zambia, *in* Wendorff, M., and Tack, Luc, eds., Structure and metallogeny of Central African Neoproterozoic belts: Tervuren, Belgium, Musée royal de l'Afrique centrale, Annales en Sciences Géologiques, Vol. 101, p. 49–62.

Binda, P.L., Van Eden, J.G., 1972. Sedimentological evidence for the origin of the Precambrian Great Conglomerate (Kundelungu Tillite), Zambia. Palaeo-geography, Palaeo-climatology, Palaeo-ecology, v. 12, p. 151-168.

Broughton, D., 2014. Geology and ore deposits of the central African copper belt. Unpublished PhD. Thesis, Colorado School of Mines, 189 pp.

Bull, S., Selley, D., Broughton, D., Hitzman, M., Cailteux, J., Large, R., and McGoldrick, P., 2011. Sequence and carbon isotopic stratigraphy of the Neoproterozoic Roan Group strata of the Zambian copperbelt. Precambrian Research 190 (2011) p. 70– 89.

Cailteux, J.L.H. and Kampunzu, H.A.B. 1995. The Katangan Tectonic Breccias in the Katanga Province (Zaire) and their genetic significance. Annals of Geological Sciences., v. 101, p. 63-76.

Carey, H and Cevallos, C. 2012. Fundamental geological interpretation of helicopter electromagnetic and radiometry data north of Chililabombwe, Zambia. Konkola North, Zambia, Geophysical Interpretation Report. v. 3, p. 1-37.

Chilekwa, M., 2015. Petrography, metamorphism, deformation and P-T conditions in the western arm of the Lufilian arc, Zambezi, Northwestern Zambia. Unpublished MSc thesis, Rhodes University, p. 168.

Condor Consulting., 2014. Stratigraphy of the Lubambe Area, Chililabombwe, Zambia. Final Geological Report. Konnoco (Zambia) Ltd, Unpublished Report, v. 2, p. 3-91.

Cosi, M., De Bonis, A., Gosso, G., Hunziker, J., Martinotti, G., Moratto, S., Robert, J. P., and Ruhlman, F., 1992. Late Proterozoic thrust tectonics, high-pressure metamorphism and uranium mineralization in the Domes area, Lufilian arc, Northwestern Zambia. Precambrian Research, v. 58, p. 215–240.

Cox, D.P., 2003. Descriptive model of Revett Cu 30b.4, in Cox, D.P., Lindsey, D.A., Singer, D.A., Moring, Barry, and Diggles, M.F., Sediment-hosted copper deposits of the world—Deposit models and database: U.S. Geological Survey Open-File Report 03–107, v. 1, p. 3-50. (Also available at http://pubs.usgs.gov/of/2003/of03- 107/.

Cox, D.P., Lindsey, D.A., Singer, D.P., Moring, B.C., and Diggles, M.F., 2007. Sediment-hosted copper deposits of the world: Deposit models and database: U.S. Geological Survey Open File Report 03-107, p. 53.

Daly, M. C., Chakraborty, S. K., Kasolo, P., Musiwa, M., Mumba, P., Naidu, B., Nameteba, C., Ngambi, O., and Coward, M. P., 1984. The Lufilian arc and Irumide belt of Zambia: Results of a geotraverse across their intersection: Journal of African Earth Sciences, v. 2, p. 311–318.

Daly, M., 1986. Crustal shear zones and thrust belts: Their geometry and continuity in Central Africa. Royal Society of London Philosophical Transactions Series A, v. 317, p. 111–127.

Darnley, A.G., 1960. Petrology of some Rhodesian Copperbelt orebodies and associated rocks: Institute of Mining and Metallurgy Transactions, v. 69, p. 137–173.

Hanson, R. E., Wardlaw, M. S., Wilson, T. J., and Mwale, G. 1993. U-Pb zircon ages from the hook granite massif and Mwembeshi dislocation: Constraints on Pan-African deformation, plutonism, and transcurrent shearing in central Zambia. Precambrian Research, v. 63, p. 189–209.

Hanson, R. E., Wilson, T. J., and Munyanyiwa, H., 1994. Geologic evolution of the Neoproterozoic Zambezi orogenic belt in Zambia: Journal of African Earth Sciences, v. 18, p. 135–150.

Hitzman, M. W., Broughton, D. W., Selley, D., Woodhead, J., Wood, D. and Bull, S., 2012. The Central African Copperbelt: Diverse Stratigraphic, Structural and Temporal Settings in the World's Largest Sedimentary Copper District. Society of Economic Geologists, Inc, Special Publications 16, p. 487–514.

Jackson, M. P. A., Warin, O. N., Woad, G. M., Hudec, M. R., 2003. Neoproterozoic allochthonous salt tectonics during the Lufilian orogeny in the Katangan Copperbelt, central Africa. Geological Society of America Bulletin, v. 115, p. 314-330.

Kampunzu, A. B., and Cailteux, J. L. H., 1999. Tectonic evolution of the Lufilian arc (Central Africa Copper Belt) during Neoproterozoic Pan African orogenesis: Gondwana Research, v. 2, no. 3, p. 401–421.

Kampunzu, A. B., Cailteux, J. L. H., Kamona, A. F., 2009. Sediment-hosted Zn–Pb–Cu deposits in the Central African Copperbelt. Ore Geology Reviews 35, 263–297.

Key, R. M., Liyungu, A. K., Njamu, F. M., Somwe, V., Banda, J., Mosley, P. N., and Armstrong, R. A., 2001. The western arm of the Lufilian arc in NW Zambia and its potential for copper mineralization: Journal of African Earth Sciences, v. 33, p. 503–528.

Kirkham, R.V., 1989. Sediment-hosted Stratiform Copper Deposits. Geological Association of Canada, Special Paper 36, p. 499–518.

Knupp, K. P., 2006. Copperbelt JV Geophysical Interpretation, Report for ARM Exploration (Zambia) Ltd, Earth Maps Consulting, p. 1-51.

Lydall, M.I. and Auchterlonie, A., 2011. The Democratic Republic of Congo and Zambia: Growing global 'hotspot' for copper-cobalt mineral investment and exploitation: 6th Southern African Base Metals Conference 2011, South African Institute of Mining and Metallurgy, p. 25–37

Master, S., and Wendorff, M., 2011. Neoproterozoic glaciogenic diamictites of the Katanga Supergroup, Central Africa. Geological Society, London, Memoirs 2011; v. 36; p. 173–184.

McGowan, R., S. Roberts, and A. J. Boyce, 2005. Origin of the Nchanga copper-cobalt deposits of the Zambian Copper Belt, Mineralium Deposita, v. 40, no. 6-7, p. 617-638.

Mendelsohn, F., 1961. The geology of the Northern Rhodesian Copperbelt: London, MacDonald. xvi, p. 523.

Mendelsohn, F., 1989. Central/southern African ore shale deposits, *in* Boyle, R.W., Brown, A.C., Jefferson, C.W., Jowett, E.C., and Kirkham, R.V., eds., Sediment-hosted stratiform copper deposits: Geological Association of Canada Special Paper 36, p. 453–469.

Mwelwa, E., 2020. Lubambe Copper Mine annual exploration report for 2020. Internal Report. Lubambe Copper Mine. P. 1-86.

Ngoyu, K., Liegeois, J.P., Demaiffe, D. and Dumont, P. 1991. Age tarti-ubendien (Proterozoique inferieur) des domes granitiques de l'arc cuprifere zaire-zambien. C.R. Academic Science Paris, Serie II v. 313, p. 83-89.

Nyoni, M. M., 1999. Geophysical Interpretation - Memorandum - Area 2, mn\mem99\zam\02, p. 1-11.

Porada, H., 1989. Pan-African rifting and orogenesis in Southern to Equatorial Africa and Eastern Brazil, Precambrian Research. p. 103–136.

Porada, H., and Berhorst, V., 2000. Towards a new understanding of the Neoproterozoic-early Palaeozoic Lufilian and northern Zambezi belts in Zambia and the Democratic Republic of Congo, Journal of African Earth Sciences, v. 30, p. 727–771.

Rainaud, C., Master, S., Armstrong, R. A., and Robb, L. J., 2005. Geochronology and nature of the Palaeoproterozoic basement in the Central African Copperbelt (Zambia and the Democratic Republic of Congo), with regional implications. Journal of African Earth Sciences, v. 42, p. 1–31.

Reid, D., 2020. Wood: Report on Mineral Resource Estimate, Lubambe Extension Copper Project, February 2020 Resource Statement update, by Wood Group USA, Inc. (Wood). p. 1- 35.

Robb, L., 2005. Introduction to ore-forming processes. Blackwell Science Ltd, Oxford, p. 373.

Roberts, S., McGowan, R., and Boyce, A., 2005. Origin of the Nchanga copper-cobalt deposits of the Zambian Copperbelt, Mineral Deposit Research, v. 2, p. 171-173.

Saintilan, N. J., Selby, D., Creaser, R. A., Dewaele, S., 2018. Sulphide Re-Os geochronology links orogenesis, salt and Cu-Co ores in the Central African Copperbelt. Nature Scientific Reports 8:14946 DOI:10.1038/s41598-018-33399-7

Selley, D., Broughton, D., Scott, R., Hitzman, M., Bull, S., Large, R., McGoldrick, P., Croaker, M., Pollington, N., and Barra, F. 2005. A New Look at the Geology of the Zambian Copperbelt. Economic Geology, v. 100, p. 965–1000.

Sillitoe, R. H., Perello, J., Creaser, R. A., Wilton, J., Wilson, A. J., Dawborn. T., 2017. Age of the Zambian Copperbelt. Mineralium Deposita 52, 1245–1268.

Simposya, V.M., and Hart, P.C.L, 2008. Technical report on the mineral resources for the Konkola North Copper project, Chililabombwe, Zambia: SRK Consulting Project Number 384408, prepared for TEAL Exploration and Mining Co., March 2008, p. 78.

Stacey, J., 2020. A report on the Lubambe Extension Area drilling, statistical analysis of assay data and resource classification. Lubambe Copper Mine, Unpublished report, v. 4, p. 1 – 132.

Subramani, D., 2018. Lubambe Extension Project, Interim Mineral Resource Estimate, Reference: C8375-TRPT-001, Revision 1, 2018. p. 1 – 81.

Sutton, S. J., and Maynard, J. B., 2005. A fluid mixing model for copper mineralisation at Konkola North, Zambian Copperbelt. Journal of African Earth Science, v. 42, p. 95-118.

Sweeney, M., Binda, P. L., 1989. The role of diagenesis in the formation of the Konkola Cu–Co orebody of the Zambian Copperbelt. Geological Association of Canada Special Paper, v. 36, p. 499–518.

Tembo, F., Kampunzu, A. B., Porada, H., 1999. Tholeiitic magmatism associated with continental rifting in the Lufilian Fold Belt of Zambia. Journal of African Earth Sciences, v. 28, p. 403–425.

Theron, S. J., 2013. The origin of the Central African Copperbelt - in a nutshell. The Southern African Institute of Mining and Metallurgy Base Metals Conference, 21-36.

Torremans, K., Gauquie, J., Boyce, A.J., Barrie, C.D., Dewaele, S., Sikazwe, O., Muchez, P.H., 2013. Remobilisation features and structural control on ore grade distribution at the Konkola stratiform Cu–Co ore deposit, Zambia, v. 2, p. 3–22.

Unrug, R., 1988. Mineralization controls and source of metals in the Lufilian fold belt, Shaba (Zaire), Zambia, and Angola. Economic Geology, v. 83, p. 1247–1258.

Wendorff, M., 2005. Sedimentary genesis and litho-stratigraphy of Neoproterozoic mega-breccia from Mufulira, Copperbelt of Zambia. Journal of African Earth Sciences, v. 42. p. 61–81.

Wendorff, M., and Key, R. M., 2009. The relevance of the sedimentary history of the Grand Conglomerate Formation (Central Africa) to the interpretation of the climate during a major Cryogenian glacial event. Precambrian Research, 172 (1–2), 127-142.

Woodhead, J. A., 2006. The African Copperbelt, Republic of Zambia and Democratic Republic of Congo – Copper and Cobalt Production. Colorado School of Mines, v. 24, p. 71–90.

APPENDIX 1

HOLEID	Northing	Easting	Elevation	Azimuth	DIP	EOH	Thickness_Grade
KN02D1	8636970	587526	557	216	-69	454.50	7.63m@3.08%
KN03A	8641118	584939	1353	0	-90	794.85	5.89m@3.91%
KN05	8641704	584822	1352	0	-90	775.00	1.96m@3.07%
KN11D1	8640565	584855	704	328	-73	33.60	0.39m@3.06%
KN16D1	8636364	588201	81	228	-81	86.50	13.91m@4.28%
KN24	8641295	584631	1359	0	-90	514.50	3.16m@3.14%
KN28	8640793	584938	1354	0	-90	611.00	6.32m@3.03%
KN29	8640944	585192	1351	0	-90	1048.90	4.41m@2.87%
KN32	8640118	585152	1349	0	-90	1303.00	5.89m@2.51%
KN36	8639523	583029	1355	0	-90	405.00	4.33m@2.94%
KN37	8640580	585301	1351	0	-90	1081.00	3.13m@3.08%
KN40D1	8636436	587177	1055	59	-90	706.00	12.38m@4.17%
KN41D1	8636437	587764	739	318	-90	414.50	7.87m@3.54%
KN44	8636132	588027	416	262	-80	383.70	16.50m@7.16%
KN46D2	8636118	587144	550	227	-83	334.00	19.04m@3.21%
KN54	8636124	588370	1311	0	-90	1402.00	13.2m@4.61%
KN55	8640982	584378	1369	0	-90	380.50	7.65m@2.99%
KN63	8639093	583431	1343	0	-90	630.00	3.92m@2.99%
KN64	8639222	583218	1347	0	-90	497.00	4.27m@2.60%
KN66	8642318	583692	1375	0	-90	248.20	2.56m@2.59%
KN67	8642115	583965	1371	0	-90	480.00	3.30m@2.57%
KN69	8639101	583863	1348	0	-90	725.50	4.59m@2.81%
KN73	8641950	583994	1372	0	-90	395.00	5.41m@3.20%
KN75	8641812	584051	1372	0	-90	330.00	5.93m@3.25%
KN76	8641708	584187	1369	0	-90	374.60	5.56m@3.39%
KN79	8641266	584323	1367	0	-90	280.00	8.64m@3.09%
KN80	8641016	584899	1354	0	-90	614.50	3.76m@3.23%
KN101B	8637403	587706	280	189	-75	196.00	6.25m@4.92%
KN110	8637185	587390	565	218	-73	453.50	10.80m@3.59%
KN114	8636431	587909	1322	0	-90	1181.50	11.39m@3.50%
KN116	8636218	588014	579	252	-87	493.00	10.75m@6.03%
KN118	8638177	585238	1340	0	-90	1179.30	5.17m@2.51%
KN120	8636253	587793	1322	0	-90	1281.50	18.30m@4.72%
KN121B	8636094	588507	1310	357	-75	1508.20	15.59m@4.94%
KN123	8641479	584008	1378	0	-90	204.00	7.30m@2.54%
KN126	8637106	587268	1325	0	-90	1119.50	4.05m@2.59%
KN127	8641259	584135	1368	0	-90	215.00	6.42m@3.41%
KN129	8641320	584156	1367	0	-90	242.36	6.03m@2.82%
KN130	8641406	584108	1364	0	-89	248.50	5.10m@2.78%
KN131	8637367	587670	1313	75	-90	1159.00	9.90m@2.81%
KN133	8641639	583920	1375	0	-90	220.10	3.87m@3.60%
KN134	8641662	583963	1375	0	-90	238.00	6.04m@3.03%

HOLEID	Northing	Easting	Elevation	Azimuth	DIP	EOH	Thickness_Grade
KN136	8637567	587485	1314	0	-90	1297.00	10.38m@4.66%
KN137D5	8636460	588402	275	45	-67	342.00	7.09m@7.40%
KN138D1	8637336	587135	382	220	-81	259.78	11.00m@4.79%
KN139AD3	8637163	587614	676	218	-80	585.00	11.15m@3.95%
KN141D3	8637640	587328	427	219	-78	452.00	9.04m@3.51%
KN144	8640961	584317	1366	286	-84	232.00	6.53m@2.82%
KN149	8639887	582826	1338	307	-85	195.50	5.36m@4.49%
KN155	8641656	584097	1375	276	-84	295.50	3.64m@3.48%
KN156	8641996	583876	1374	297	-86	269.50	8.33m@3.07%
KN157	8642140	583827	1386	177	-85	276.50	4.03m@3.43%
KN160	8636708	588144	1314	38	-63	1338.00	10.89m@2.93%
KN166D2	8637044	588850	208	17	-66	251.00	8.88m@6.20%
KN167D2	8637606	587893	196	69	-87	303.00	16.85m@3.43%
KN169D1	8636441	587302	590	169	-88	465.90	16.19m@2.79%
KN171D1	8640140	583522	1180	0	-90	284.60	4.35m@3.02%
KN173	8639742	582736	1350	0	-90	344.50	2.98m@2.60%
KN174D1	8639715	583280	1162	223	-88	283.00	2.77m@3.51%
KN176D2	8642016	583971	1069	318	-87	123.00	4.85m@2.77%
KN177D4	8641853	584176	1013	0	-90	193.00	3.88m@2.78%
KN178	8641685	584360	1370	0	-90	650.50	5.49m@2.91%
KN179	8641620	584279	1372	0	-90	433.00	6.56m@3.00%
KN183	8641112	584749	1361	0	-90	605.50	2.95m@3.17%
KN184D1	8641062	584686	1016	0	-90	131.00	6.95m@3.09%
KN190	8638893	585651	1332	0	-90	1178.00	7.50m@2.74%
KN191A	8636074	587907	1316	0	-90	1283.50	10.05m@6.59%
KN191AD1	8636065	587874	154	0	-90	78.90	8.01m@3.13%
KN191AD3	8636069	587882	370	0	-90	310.57	10.77m@7.8%
KN192	8637712	589310	1307	227	-75	1649.80	7.68m@5.02%
KN193AD1	8636252	588919	587	0	-90	750.55	19.74m@4.26%
KN194D1	8637613	589698	1159	212	-63	1367.80	6.58m@5.82%